MOLTEN-SALT CATALYTIC PYROLYSIS (MSCP):

A SINGLE-POT PROCESS FOR FUELS FROM BIOMASS

by

Xiangyu Gu

A Thesis

Submitted to the Faculty

of the

WORCESTER POLYTECHNIC INSTITUTE

in partial fulfillment of the requirements for the

Degree of Master of Science

in

Chemical Engineering

May 2015

APPROVED:

_____

Prof. Ravindra Datta, Advisor

_____

Prof. David DiBiasio, Department Head

Abstract

A novel process for single-pot conversion of biomass to biofuels was developed called the molten salt catalytic pyrolysis (MSCP) method. The proposed single-pot MSCP process proved to be an inherently more efficient and cost-effective methodology for converting lignocellulosic biomass. In this study, several parameters that affect yield of bio-oil were investigated including carrier gas flow rate; pyrolysis temperature; feed particle size; varying types of molten salt and catalysts. Use of molten salt as the reaction medium offered higher liquid yield and experiments containing $ZnCl_2$ showed higher yield than other chloride salts. The highest yield of bio-oil was up to 66% obtained in a $ZnCl_2$-KCl-LiCl ternary molten salt system compared with 32.2% at the same condition without molten salts. In addition, the effect of molten salt on the composition of bio-oil was also studied. It was observed that molten salt narrowed the product distribution of bio-oil with furfural and acetic acid as the only two main components in the liquid with the exception of water. Finally, a thermogravimetric kinetic study on the pyrolysis of biomass in MSCP was conducted.

Acknowledgements

I would take this opportunity to thank everyone who provided consistent assistance to me throughout the whole project at WPI. It has been my most enriching experience and one of the best memories in my life.

First, I would express my sincere gratitude to my advisor Professor Ravindra Datta and co-advisor Professor James Dittami and Professor Michael Timko for their guidance and encouragement. Without their feedback and ideas, this work would not have been possible. A special thank to Prof. Datta for his consistent resources and solutions when I encountered problems; to Prof. Timko for his constructive suggestions for my project.

I also appreciate the technical support from Andrew Butler in GC/MS analysis and TGA experiments. His tutoring and devotion was a significant partof the success of the project. Besides, I would like to thank Felicia Vidito and Tiffany Royal for their help with ordering materials used in experiment. Furthermore, I feel very fortunate to meet a group of talented colleagues in Prof. Datta's group and I appreciate their support, especially by Pei-Shan Yen, Drew Martino, Patrick O'Malley and Yan Dong.

Table of Contents

Table of Figures

List of Tables

Chapter 1. Introduction

1.1 Introduction

Human beings began burning fossil fuels extensively at a rough time scale in the mid-to-late 1800s when the First Industrial Revolution broke out. More and more fossil fuels, especially coal and crude oil were exploited from that moment on. The acceleration of consumption of coal, crude oil and natural gas occurred since 1985 due to the growing demand for huge quantity and high quality industrial products as a result of developing economics. Currently, approximately one-third of the Earth's technically and economically recoverable stocks of fossil fuels have been exploited. Based on prediction of resource experts shown in Figure 1, the world is approaching peak consumption for coal and oil in view of the condition that though plenty of coal exists, much of it now looks too costly to recover.

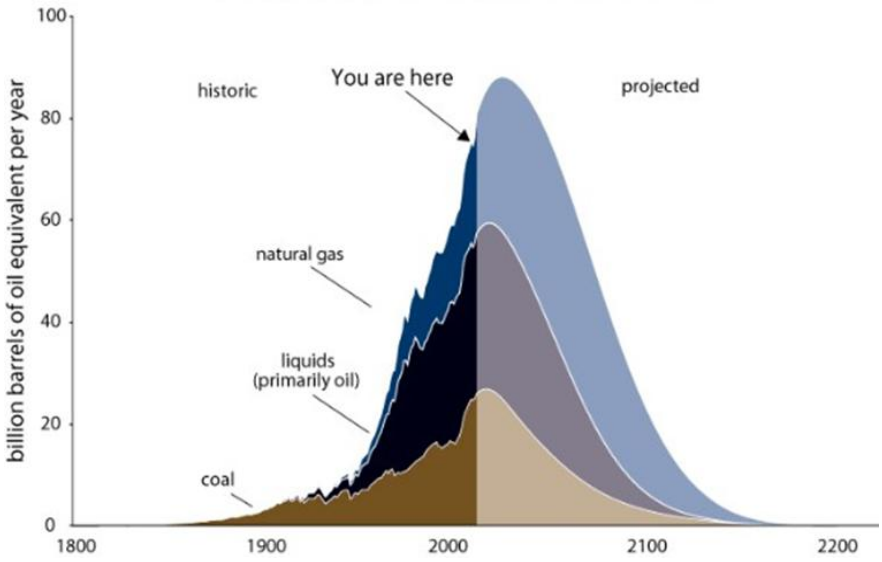

Figure 1: Fossil fuels: global production, 1800–2200.
(http://www.rmi.org/RFGraph-Fossil_fuels_global_production)

Due to the overuse of fossil fuel, pollution resulting from fuel combustion and green house effect has led to some serious effects on people's health and environment. The emissions of greenhouse gases such as CO_2, and pollutants such as N_2O and SO_2 have changed the climate step by step and caused severe natural disasters. So the corresponding environmental issues have gained great attention. One approach to address these concerns is to improve the current techniques for fossil fuel utilizations,

such as using novel catalysts to decrease toxic substances in exhaust emissions. The second approach is to explore new green technologies, such as hydro-power, wind, solar, geothermal and biomass, to gain energy, other than just improve existing techniques and equipments. Figure 2 produced by U.S. Energy Information Administration (EIA) indicates that the energy consumption pattern of the United States has altered significantly over the last fifty years and grown in diversity after 1970s, as new energy sources have been developed and as uses of energy has changed. However, the three major fossil fuels—petroleum, natural gas, and coal, which make up nearly 90% of total usage, still dominate the U.S. fuel consumption. Nonetheless, the increasing rate of other renewable resources is promising in the new century, especially biomass energy. The 21st Century promises a significant shift to alternate industrial feedstock and green processes to produce power and chemicals [1].

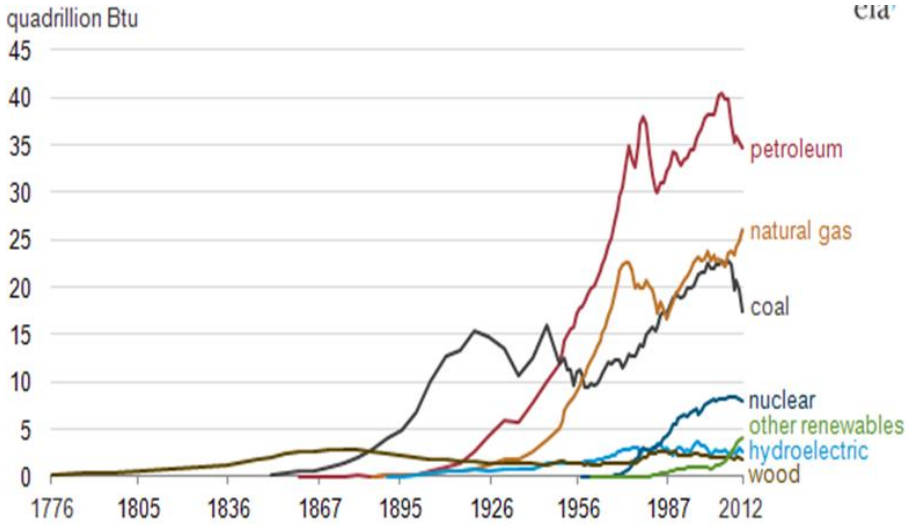

Figure 2: History of energy sources consumption in United States.
(http://www.eia.gov/todayinenergy/detail.cfm?id=11951&src=Total-b1)

Among many alternatives sources that have the potentials to replace the role of fossil fuels, biomass energy could be one of the most promising ways to realize this goal. Firstly, biomass contributes less or no net CO_2 than conventional fossil fuel in the atmosphere, since use of biomass releases the same amount of CO_2 as it absorbed in its growth, and the cycle time is much shorter than for fossil fuels [2]. Secondly, biomass is clean for its negligible content of nitrogen, sulphur and ash, which produces significantly less emission of nitric oxide, SO_2 and soot. In this way,

biomass-based fuels and products could mitigate the global warming as well as air pollution to some extent. Thirdly, biomass is the only resouce that has the ability to provide three main sources of renewable energy: liquid, gaseous and solid fuels. It can not only power turbine to generate electricity by burning, but also offers a source o for a variety of industrial raw materials or commercial products directly [3]. Finally, the liquid product called 'bio-oil' or 'bio-crude' could be refined or upgraded in existing petroleum refineries to produce transportation fuels and other chemicals by undergoing conventional reactions such as steam reforming, hydrocracking, hydrotreating, isomerization and catalytic cracking [4,5].

The process of biomass conversion has been investigated quite intensively in recent decades. Compared with gaseous and bio-solid products, research on bio-oil received the most attention. However, the complexity of biomass feedstock and conversion chemistry involving hundreds of reactions during the process, instability and complex composition of bio-oil, unknown reaction mechanisms, and lack of well-established industrial production techniques, provides a huge challenge to the advancement of this technology. Nonetheless, because of decreasing stocks of fossil fuels and the growing environmental problems, it is quite evident that the development of a method which could eliminate or reduce the adverse factors mentioned above is of great interest. Consequently, there is currently a great deal of research on the development of a high efficiency, selective, cost-effective, and environment-friendly production of bio-oil as well as its upgrading chemicals such as transportation fuel.

1.2 Problem Identification and Research Objective

Thermo-chemical decomposition of biomass has attracted great interests as it can convert raw feedstocks directly into bio-liquid [6]. Both lab-scale research and industrial applications have been investigated for several decades. However, current production processes of bio-liquid are deficient in three ways: (1) poor efficiency in biomass heat treatment; (2) presence of hundreds of compounds in bio-oil; (3) unclear biomass conversion reaction kinetics and mechanism. So research on how to improve bio-liquid production is still ongoing intensively and so far no effective method has

been proposed to overcome the drawbacks mentioned above.

Recently, molten salt catalytic pyrolysis (MSCP) process was proposed by researchers at the Department of Chemical Engineering, Worcester Polytechnic Institute (WPI). The former proposed single-pot reactor with MSCP process had proved to be an inherently more efficient and cost-effective methodology for converting cellulosic biomass feedstock [7-9]. However, the effect of molten salts on more general patterns of biomass- lignocellulosic biomass hasn't been investigated yet. Moreover, pyrolysis reaction kinetics and mechanism in molten salt bath haven't been illustrated systematically.

The aim of this project is to provide a novel and systematic process for single-pot conversion of biomass (sawdust, newspaper and recycled print paper) to liquid fuels and chemicals derived from and improving previous work. Due to the difference in composition between laboratory cellulose studied previously and more complicated natural lignocellulosic biomass, the reaction conditions for best yield of liquid and the product distributions and properties were investigated. Also, the relationship between composition of bio-oils and corresponding reaction condition was established. Furthermore, thermogravimetric decomposition of biomass with molten salt was investigated for the first time. Pyrolysis kinetics models and potential mechanisms could be achieved with the analytical experiments. This project is more promising because, unlike pure cellulose, lignocellolose is the cheapest and most abundant source of biomass, which can be gathered directly from farmland or forest. If lignocellolose could be used as feed to produce biofuel in an economical way, it will definitely have a great impact on the energy domain.

1.3 Dissertation Overview

This dissertation is organized into 5 chapters. Chapter 1 gives a general background on current energy sources utilization and accompanying energy crisis, as well as environmental issues. Also, the motivation of this project is briefly presented at the end of this Chapter. Comprehensive and state-of-the-art literature review is presented in Chapter 2. Chapter 3 deals with the experimental procedures utilized. Chapter 4 is

dedicated to a discussion of the experimental results in detail, which contains three parts: optimizing bio-oil yields, compositions of bio-oil analysis, and pyrolysis kinetics models and decomposition mechanisms. General conclusions and directions for future work are presented in Chapter 5.

Chapter 2. Literature Review

This review starts with a systematic description on biomass chemistry including composition of biomass and characteristics of each component, followed by general information about current development of bio-products technology, which is mainly focused on bio-oil and bio-char. Next, a comprehensive introduction to some common processes that produce fuel from biomass is presented. Further, the state-of-the-art fast pyrolysis technology is described thoroughly, coupled with catalysis, molten salts media, process enhancement, etc. Finally, several potential mechanisms and pyrolysis reaction kinetics models of thermo-decomposition of particular biomass proposed by researchers are described in detail.

2.1 Biomass Chemistry

Biomass is defined as the biological material of recent living origin [10]. Plant-based biomass, are those which are derived from plant matter, containing a few basic monomer units such as, celluloses, hemicelluloses, extractives (starches, terpenes), lignins, uronic acid, proteins, as well as ash. Typically, there are several classes of plants: lignocellulosic plants, starch-based plants, triglyceride-producing plants and rubber-producing plants [11]. In this project, only lignocellulosic plants biomass is under investigation for its wide-distribution in the U.S. (also due to its lower cost than starch or sucrose based materials) and its intensive-use in research.

2.1.1 Composition of Biomass

Lignocellulose is the most abundant plant material that makes up the cell walls of woody plants such as grasses, trees and some crops. Most Lignocellulosic biomass contains three major components: cellulose, hemicellulose and lignin [12]. The relative content of each part is: cellulose (35-50%), hemicellulose (20-40%) and lignin (5-30%), together with infinitesimal amounts of minerals [13].

Cellulose, as shown in Figure 3, is a biological linear polymer with β-1, 4 linkages of D-glucopyranose monomers [14]. Due to the existence of hydroxyl groups and bonded hydrogen atoms, the cellulose chains can form intra- and inter-hydrogen

bonds to form a crystalline configuration [15]. In this configuration, both top and bottom layers are completely hydrophobic, while the sides of chains are essentially hydrophilic with formation of hydrogen bonds, as aliphatic hydrogen atoms are all located in axial positions, whereas polar hydroxyl are assigned in horizontal positions [11]. Groups of chains twist and twine together in narrow space to form ribbon-like microfiber, which is the element to build up more complicated fibers. Cellulose fibers, the main component in the cell wall, give wood 'strength' and minimize flexibility [16]. Reactions that involve cellulose fibers are mostly allowed to take place on the surface of bio-polymer. Moreover, the intramolecular and intermolecular hydrogen bond network in the bio-polymer makes its dissolution process more difficult. Cellulose is insoluble in water, but is capable of depolymerization with acid or base hydrolysis, to form cellotetrose (glucose tetramer), cellotriose (glucose trimer) and cellobiose (glucose dimer). When undergoing a complete acid hydrolysis process, cellulose has a tendency to be broken down into glucose [17]. As for the polymerization, the degree of polymer depends on the types of plants, usually about 500-15000 [18].

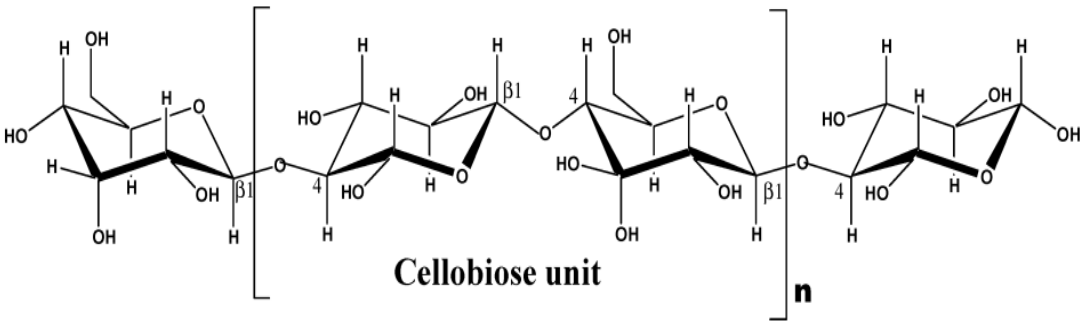

Figure 3: Chemical structure of cellulose [14].

Hemicellulose is the second major ingredient in wood, which comprises six main basic unit components: glucose, galactose, manose, xylose, arabinose and glucuronic acid, as shown in Figure 4 [14]. In contrast to cellulose, which is in good order of assembly of single glucose, hemicellulose is a polysaccharide complex, consisting five carbon sugars (xylose and arabinose), six carbon sugars (glucose, galactose and manose) and carbonyl acid (glucuroic acid). Besides, it is claimed that not only

glucose, but also the other four unit sugars which their alcoholic group could be substituted with acid [11]. The major hemicellulose sugar in softwood is mannose, while xylose is the most common hemicellulose sugar in hardwood [19]. The molecular weight of hemicelluloses is much lower than that of cellulose, since the repeating unit number of hemicellulose is only around 150. For the macro-structure, hemicellulose exhibits amorphous structure owing to the branched side chain and the difference of monomers [14].

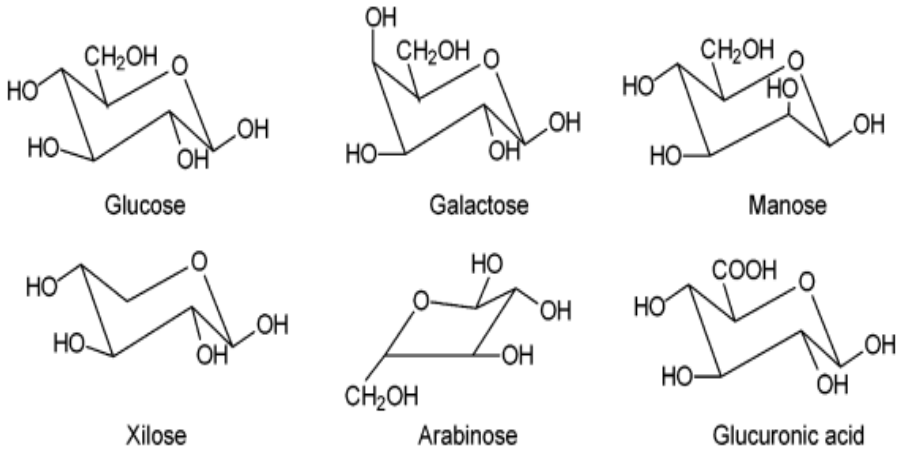

Figure 4: Main components of hemicelluloses [14].

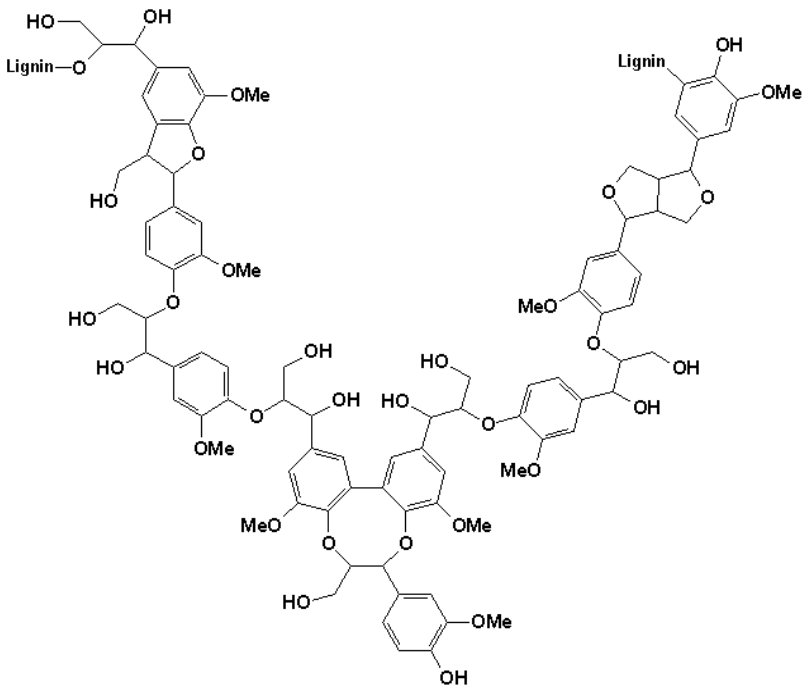

Figure 5: Part of lignin structure.
(http://en.wikipedia.org/wiki/Lignin#/media/File:LigninStructure.png)

The third common constituent, lignin, has the most amorphous cross-linked configuration without specific structure. As shown in Figure 5, lignin is a highly branched, water-insoluble and polyphenolic substance that comprised of an irregular array of diversely connected 'hydroxy-' and 'methoxy-' substituted phenylpropane units [20]. The three general phenylpropane units are p-coumaryl, coniferyl and sinapyl [21]. Lignin is always associated with cellulose and hemicellulose, to provide firm shield against destruction of lignocellulosic fibers. Lignin presents structure reinforcement and offers shields to protect cell walls from biological and physical attack, thus lignin is treated as the hardest obstacle for biomass deconstruction process [22]. Also, different types of plants give varied structures of lignin, and different extraction methods to separate lignin from lignocelluloses result from the diverse patterns of lignin [11, 14].

The composition and property of biofuel extracted from lignocelluloses don't only rely on the content of each component in raw feedstock, but also depend on the interaction of each component. It is the one reason of why biomass conversion is so complicated and this part will be illustrated in detail later

2.1.2 Characteristics of Biomass

Figure 6 shows how the three main components (cellulose, hemicelluloses and lignin) structured in wood fiber. Cellulose fibers act as the basic skeleton of cell walls. Hemicellulose is attached to the surface of cellulose non-covalently, regarded as an amorphous matrix material that is holding the cellulose fibers in positions. Hemicellulose also plays a role in connecting cellulose and lignin, as the hydrophobic groups in hemicellulose, for example, acetyl and methyl groups enhance the affinity of combinations [23]. More in-depth discussion about functionality of cellulose, hemicelluloses and lignin in cell walls and their biological behavior are out of scope of this work.

In order to derive biofuel from lignocellulosic biomass, the first step is to destruct solid biofibers before those decomposition reactions can occur. However, plants themselves have strategies to protect them from being digested. So it is necessary to

have a good knowledge in the characterization of lignocellulosic plant cell wall. Himmel *et al.* [24] and Chundawat *et al.* [25-27] have published some excellent papers in recent years to characterize the macro- and micro- structure of lignocellulosic plant cell wall by many characterization methods, such as, scanning electron microscopy (SEM), atomic force microscopy (AFM), transmission electron microscopy (TEM), immune-electron microscopy (IEM), nuclear magnetic resonance (NMR), nitrogen physisorption analysis, etc. The rigid plant cell must be broken down, especially for downstream process which involving fermentation reactions. Considering the recalcitrance of lignocellulosic fibers, pretreatment is always required to deal with raw feedstock and this part will be further elucidated later on.

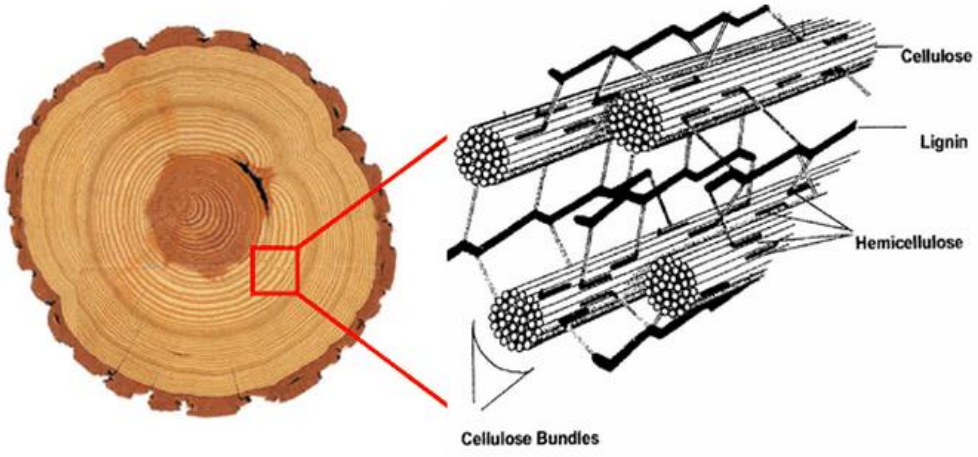

Figure 6: Internal structure of wood fiber.
(https://www.bnl.gov/newsroom/news.php?a=1928)

2.2 Bio-products

The development of human civilization cannot be separated from “fire”. In ancient times, people already knew how to make uses of energy from biomass. In the very beginning, humans learnt to burn wood by chance to get warm, cook food, etc. Coal, petroleum and natural gas, which are all considered to be derived from decomposed biomass over millions of years, were exploited by humans as recently as only two centuries ago. However, these types of fuels are nonrenewable and they will all be used up someday in the future. Consequently, a potential method proposed in mid-20th century was to use raw biomass directly. Biomass after thermal-decomposition

process can be converted into three types of energy resources- biochar, bio-oil and bio-gas, which has similar role as coal, petroleum and natural gas, respectively. Below, a detailed review of current utilization of biochar, bio-oil and bio-gas is given.

2.2.1 Biochar

Biochar is the solid carbonaceous product of thermal degradation of waste organic feedstock by controlled pyrolysis (carbonization) process [28]. Biochar mainly comprises of three major components, i.e., stable carbon, labile carbon and ash. The most dominant feature of biochar is the larger proportion of the aromatic carbon it contains. The carbon patterns and structures contribute to the stability of biochar [29]. Biochar chemical stability is governed by the fraction of labile carbon, which could be leached readily and utilized by microorganisms as an energy source. The ash in biochar is comprised of some essential inorganic elements and its presence also plays an important role in biochar stability. Depending on different types of biochar, the surface properties and sorption capacities vary greatly. Table 1 shows the physical and chemical properties of different biochars [30].

Table 13. Physical and chemical properties of selected feedstcoks [30].

Feedstock	Temperature (°C)	pH (KCl)	pH (H_2O)	CEC[a] (mmolc kg^{-1})	CEC[a] (molc m^{-2})	C (%)	C/N ratio	Total P (mg kg^{-1})	Ash[b] (%)	Volatiles[b] (%)	Fixed C[b] (%)	H/C ratio[c]	O/C ratio[c]	Aromatic C[d] (% of total)	Aromatic clusters	SSA[e] (m^2 g^{-1})
Oak wood	60	3.16	3.73	182.1	ND[f]	47.1	444	5	0.3	88.6	11.1	1.48	0.72	ND	ND	ND
	350	5.18	4.80	294.2	0.65	74.9	455	12	1.1	60.8	38.1	0.55	0.20	82.8	18	450
	600	7.90	6.38	75.7	0.12	87.5	489	29	1.3	27.5	71.2	0.33	0.07	86.6	37	642
Corn stover	60	6.33	6.70	269.4	ND	42.6	83	526	8.8	85.2	6.0	1.56	0.74	2.0	6	ND
	350	9.39	9.39	419.3	1.43	60.4	51	1889	11.4	48.8	39.8	0.75	0.29	76.9	19	293
	600	9.42	9.42	252.1	0.48	70.6	66	2114	16.7	23.5	59.8	0.39	0.10	88.2	40	527
Poultry litter	60	7.53	7.53	363.0	ND	24.6	13	16,685	36.4	60.5	3.1	1.51	1.03	ND	ND	ND
	350	9.65	9.65	121.3	2.58	29.3	15	21,256	51.2	47.2	1.6	0.57	0.41	ND	ND	47
	600	10.33	10.33	58.7	0.63	23.6	25	23,596	55.8	44.1	0.1	0.18	0.62	ND	ND	94

[a] Cation exchange capacity, determined at pH 7 using buffered ammonium acetate (Nguyen and Lehmann, 2009).
[b] Mass % w/w analyzed using ASTM D1762-84.
[c] Molar ratios.
[d] In rings, determined by direct polarization ^{13}C nuclear magnetic resonance spectroscopy.
[e] Specific surface area, CO_2 as sorbent (courtesy A. Zimmerman).
[f] Not determined.

In consideration of different feedstock and production conditions, biochar has a variety of applications in soil amendment [30], wastewater treatment [31], gas

purification [32] and catalysis [33]. Ashwoth *et al.* [34] studied the physical and chemical characteristics of biochar produced by pyrolysis of switchgrass both in a batch reactor and continuous auger reactor. The water-holding capacity of biochar mixed with soil and nutrients profile of biochar were also evaluated. They concluded that additions of chars in soil could increase gravity-drained water content. Thermal decomposition processed affected biochar nutrients profile in different ways: NO_3^- concentrations were almost independent of pyrolysis temperature; Higher pH values could be gained at higher temperatures and longer residence times. Biochar derived from papermill showed high surface area and calcium mineral agglomeration when mixing with soil [35]. Biochar used as an adsorbent in organic and inorganic contaminants removal was reviewed in water treatment domain [36]. Removal capacities of organic groups (dye, phenols, benzene and selected pesticides) and inorganic groups (metal ion and some anions) in water with different types of biochars were determined.

Besides these studies, some other characteristics of biochar have also been explored. Meiluweit *et al.* [37] conducted an in-depth research on a molecular- level assessment of biochar properties by analytical methods such as Brunauer- Emmett- Teller (BET), X-ray diffraction (XRD), synchrotron-based near-edge X-ray absorption fine structure (NEXAFS) and Fourier transform infrared (FT-IR). They indicated that four distinct categories of biochar could be obtained at an elevated pyrolysis temperature from 100 ℃ to 700 ℃. More recently, Lehmann *et al.* started to investigate combustion and flammability properties of biochar [38], as well as ecotoxicological characterization of biochars [39].

Given that biochar can present different properties depending on production process, experimental research on how biochar is produced and how different kinds of biomass from is crucial. Morphological characteristics of biochar derived from pyrolysis of hemicelluloses were determined at 400 ℃, 550 ℃ and 900 ℃. As temperature increased, more pores structures formed in biochar and less irregular agglomeration presented [40]. In Demirbas's work [41], influence of pyrolysis temperature and feed particle size on biochar yield with three different feedstocks were discussed. Results showed that biochar yields increased with a decrease in

temperature and an increase in particle size. High lignin content in feedstock led to a higher biochar yield and high ash content in feedstock made biochar more reactive. Liu *et al.* [42] investigated pyrolysis kinetics regarding biochar production. 16 mechanisms were tested to fit the experimental data, in which reaction order and nucleation mechanisms correlated data well. Experiments about properties of biochar were also carried out in $ZnCl_2$-KCl molten salt system [43]. Existence of molten salts and increasing temperature in molten salts bath could both result in an increase of biochar yields.

2.2.2 Biofuel

2.2.2.1 Biofuel Economics

In 2013, the United States energy consumption was 97.53 quadrillion Btu, of which 84% of the total energy was domestic production. Natural gas took the first place for the largest domestically produced energy resource for the past three years, and together with other types of fossil fuels, made up more than 75% of total energy production. At the same time, renewable energy only accounted for less than 10% with biomass energy far less [44].

The U.S. Department of Agriculture and Oak Ridge National Laboratory predicted that approximatly 1.3×10^9 metric tons of dry biomass from agricultural and forest resources could be produced every year in the U.S. [25]. Based on Klass's estimation, this amount of biomass provides energy equivalent of 3.8×10^9 barrels of oil/year. If assuming all the biomass belongs to lignocellulosic biomass, thus 1 barrel of oil derived from biomass has 5.904 GJ [46]. Clearly, 21.3 quadrillion Btu could be produced by biomass resource, which is nearly 25% of the U.S. total energy consumption in 2013. Current estimated cost of lignocellulosic biomass ranges from \$5 to \$15 for 1 barrel of oil, while the recent price of West Texas Intermediate (WTI) crude oil is around \$100/bbl on average [47].

2.2.2.2 Biofuel Classification

As the consequence of biofuel evolution, at least four generations of biofuels have

been emerged so far. These four different types of biofuels are classified by their feedstocks, production methods, etc.

The production of first-generation biofuels mainly comes from food crops such as oil seeds, cereals and some high-sugar-content crops [48]. The three main categories of first generation biofuels used commercially are biodiesel (bio-esters), ethanol and biogas, and the production of these three kinds of chemicals is considered a well-understood industrial technology [49]. Though first-generation biofuel plays a role in minimizing fossil fuel burning and CO_2 emissions, some disadvantages are: (1) Food versus fuel competition- the potential stress that first-generation biofuel puts on soil, water and nutrients used for food [50]; (2) Relatively high process operation cost in need of government subsidies to maintain its production in order to compete with fossil fuels. (3) Changing the assessment of net greenhouse gas reductions if land-use alters [51].

In view of these drawbacks, the second-generation biofuel has evoloved. Second-generation biofuels are mainly produced from lignocellulosic biomass, involving bagasse, rice straw, grass, forest residues, etc., which are abundant and cheap resources. Many of the disadvantages of first-generation biofuels can thus be overcome by the second-generation biofuels, since there are less economic and environmental implications. However, industrial large-scale production of second-generation biofuels is still under development and appropriate technology needs to be developed [50].

In order to further decrease the demand for farmland needed to cultivate feedstocks for the first and second generation biofuels, nature algae based third generation biofuel has been proposed [52]. Algae can be produced using natural recourses as nutrients and propagated extensively in most aqueous environment. Compared with former two kinds of biofuels, algae stands out for its high-efficiency photosynthesis, which can fix the CO_2 into sugars in presence of photon energy and further convert to lipids via microalgae cells. Algae could contain up to 70% of lipid on a dry weight basis. Another advantage of algae is its high reproduction rate [53]. Maity *et al.* recently published a good review of current utilization of algae in third generation

biofuels [54]. Similar to third generation biofuels, the fourth generation biofuels introduces genetic modification and metabolic engineering in algae production [55]. Its purpose is to improve the lipids contents in algae and make the whole biofuel production process more cost-effective.

The production processes for these four generations biofuels are different from each other. In the first generation, biodiesel production involves steps including sugar extraction, transesterification and two step distillations, while bioethanol production contains liquefaction, saccharification, fermentation and distillation. In the second generation, two common methods exist: the first separates different components in lignocelluloses and then using fermentation process to produce ethanol or butanol; the second method uses thermal treatment directly to produce biofuel. The third and fourth generation biofuel production processes are divided into three types: direct oil extraction, biochemical process, and thermochemical process. As for the economical concerns, the first and second generation biofuels price is equal to or lower than gasoline, while biofuel price from third and fourth generation can be as much as three to ten times higher than gasoline, based on different production processes. Moreover, only first generation biofuels have been commercialized at industrial level, while the other three are still at research level [52].

2.2.2.3 Biofuel Chemistry

As biofuel can be produced via many different processes and feedstocks, the compositions and properties of biofuel vary tremendously. Here, only second generation biofuels are reviewed. Second generation biofuel is usually a dark brown liquid with a distinctive odor. More than 400 different organic compounds are present in biofuels and the concentrations can vary by several magnitudes [56]. Normally biofuels contain acids (formic acid, acetic acid and propanoic acid), esters (methyl formate and butyrolactone), alcohols (methanol, ethanol and ethylene glycol), ketones, aldehydes (formaldehyde and acetaldehyde), furans (furfural and HMF), phenols, sugars (anhydroglucose, cellobiose, fructose and glucose), guaiacols, and miscellaneous oxygenates. All chemicals involved in biofuels are formed through a

huge numbers of reactions such as, hydrolysis, isomerization, dehydrogenation, dehydration, aromatization, coking, etc [11]. The composition of biofuel depends on many factors, such as feedstocks, reaction temperature and time, pretreatment method, storage time, etc [57]. As a result of the complexity of components, high oxygen content, and instability of biofuel, the direct utilization of raw bio-oils is impractical. Thus, biofuel upgrading process is necessary, but the discussion of the upgrading technology is beyond the scope of this work.

2.2.2.4 Biofuel Production

At present, though a number of technical barriers impede the development of second generation biofuel, utilization of lignocelluloisc biomass- the most abundant natural source in the world, is now attracting more and more attention and research. Our society has made use of lignocelluloisc biomass for a long time, to generate heat and even electricity. However, the production of biofuel from lignocelluloisc biomass seems to have a great potential. Figure 7 introduces an overall roadmap of biomass conversion processes [49].

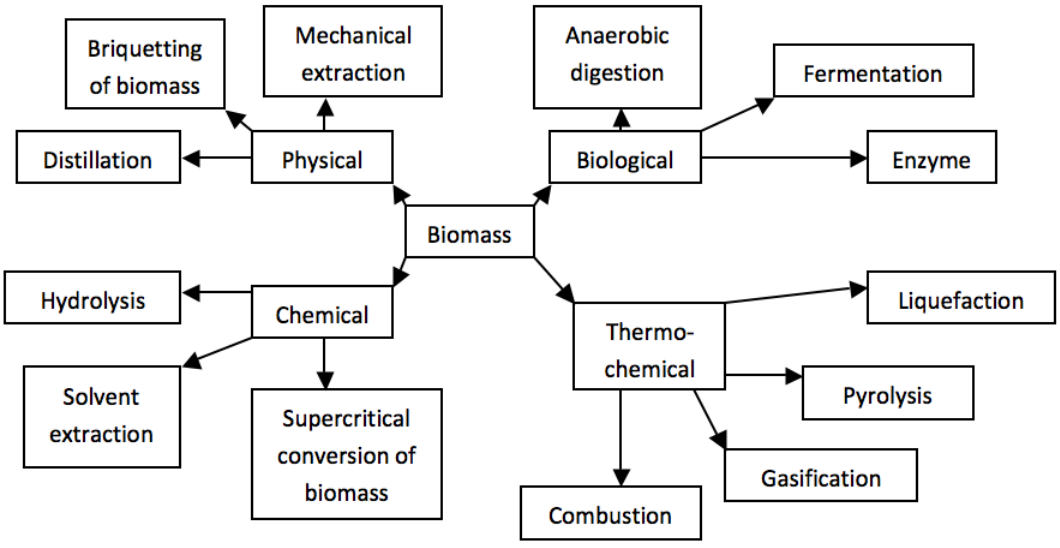

Figure 7: Overview of biomass conversion processes [49].

Conventional physical conversion requires high energy input and makes the biofuel production less cost-effective. Also, taking into account limited mechanical extraction

ability and phase equilibrium in distillation process, bio-oil yield derived from physical conversion is not as high as other methods. When utilizing pure chemical conversion, the operation and environment problems are always the issues. So the most attractive production of biofuels from lignocelluloisc biomass can be achieved by two preferable routes: biochemical and thermo-chemical conversion. Biochemcial conversion, namely biomass feedstocks are converted to biofuels by the effect of micro-organisms added into the reaction system. The common step is undergoing chemical hydrolysis first, followed by biological treatment or the two steps are carried out simultaneously. However, research on high-efficiency and low-cost micro-organisms is the bottleneck of this method. In this case, the fourth route seems to be the most promising. Thermo-chemical conversion is a process that involves thermo-decomposition and chemical reformation of raw materials, to produce a wide-range products distribution [58]. The thermo-chemical method can convert all the organic contents of lignocelluloisc biomass and directly produce bio-oil compared with biochemcial conversion. Since combustion is just to burn the biomass to generate heat and get black carbon as the final products, only three other processes (liquefaction, gasification and pyrolysis) involved in thermo-chemical method will be discussed in the following, and full description of other processes can be obtained in some good publications [1, 59-62].

Liquefaction of biomass usually takes place at high pressure (50-200 atm) and relatively moderate temperature (250-450 ℃), to produce water insoluble oils with solvents, reducing gases (CO or H_2) and catalysts present as media [63]. Alkalis, glycerin, propanol, butanol and water are the common solvents and have been investigated [64]. A liquefaction process was developed and tested by Shell. However, the biggest disadvantage of this process is the high viscosity of the biocrude [65]. In contrast, gasification of biomass is conducted at very high temperatures, which can be as high as 1300 ℃ where no catalyst is present. Reaction temperature is expected to decrease to 900 ℃ with advanced catalysts [66]. The main steps involved are the biomass reacting with air, oxygen or steam to produce a gaseous mixture of CO, CO_2, H_2 and CH_4. Meanwhile, water gas shift (WGS) and methanation reactions occur

during gasification [63]. The gaseous product can be utilized in Fischer-Tropsch (F-T) or methanol synthesis followed by other downstream reactions to produce liquid fuels [67]. Bio-oil produced by pyrolysis is the most promising method among the three ways mentioned above. Pyrolysis of biomass is thermo-degradation of biomass material at elevated temperatures, typically ranging from 300 to 900 ℃ in the absence of oxygen, which produces char (solid), bio-oil (liquid) and non-condensable vapor (gas) [64]. Compared with conventional pyrolysis, which occurs at a slow heating rate (0.1-1 ℃ /s) and long residence time (45-550 s), the state-of-the-art fast pyrolysis process occurs at a rapid heating rate (10-200 ℃ /s) and short residence time (0.5-10 s) with relatively fine biomass particles (<1 mm) typically [68]. More detailed information about pyrolysis is provided later on.

2.2.3 Bio-gas

Bio-gas is the non-condensable gaseous product in biomass conversion process. The components of bio-gas are highly dependent on the production method adopted in conversion process. In biochemical process, the bio-gas mainly comprises of CH_4 (50-75%) and CO_2 (25-50%), as microorganisms are used to conduct anaerobic digestion in the biomass conversion process [69]. In thermo-chemical process, the main components of bio-gas are H_2, CH_4, CO, and CO_2 together with a small quantity of C_2H_4 and C_2H_6 [70]. Cheng *et al.* [71] investigated bio-gas produced by pyrolysis of ramie residue. They concluded that when increasing reaction temperature from 657 ℃ to 928 ℃, the yields of H_2 and CO went up first and then dropped down after passing through a maximum. In contrast, the yield of CH_4 decreased monotonously and the yield of CO_2 increased monotonously as the temperature rose. Wijayantia *et al.* [72] studied on in-situ gas products of woody biomass pyrolysis. They found that as the reaction proceeded, the highest generated gas product flow rate occurred at round 80 min when reaction temperature was at 600 ℃ and 800 ℃. Whereas, the highest flow rate at 400 ℃ occurred at 60 min. Another conclusion they obtained was that within the 50 min reaction time, the only gas product was CO_2. CH_4 and CO began to emerge after 70 min and then H_2 come out after 90 min.

In view of the presence of CO_2 in the bio-gas, directl use of bio-gas is challenging. One possible method is to decrease CO_2 content by adding CO_2 absorbent like CaO in reaction system [73]. Another promising mrthod is to improve H_2 content by a series of reforming reactions [74]. Figure 8 shows the potential ways for bio-gas utilization in industry [75].

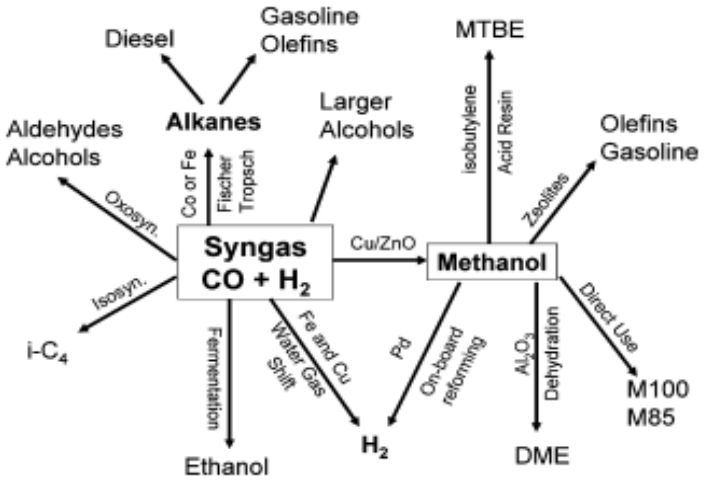

Figure 8: Bio-gas conversion processes [75].

2.3 Pretreatment Methods

The objective of pretreatment of lignocellulosic biomass is to enhance the performance of biomass hydrolysis for conversion to fuels. Specifically, pretreatment aims to remove hemicelluloses and lignin portions in lignocelluloses, break down crystalline structure of cellulose, and increase accessibility to biomass. Besides, some basic requirements should be met, such as, avoiding the degradation or loss of carbohydrate and avoiding the formation of some substances that may cause inhibitions of subsequent processes [76]. Pretreatment process plays an important role in achieving high biofuel yield, but is not limited to biochemical conversion methods. There are several pretreatment methods that have been proposed so far: physical (milling, grinding, microwave, and extrusion), chemical (acid, alkali, oxidizing agents, and organic solvents), physicochemical (steam explosion, ammonia fiber explosion, CO_2 explosion, and wet oxidation), biological, electrical, and their combination [77].

Table 14. Comparisons of common used pretreatment methods in lignocellulose biomass [76].

pretreatment process	advantages	limitations and disadvantages
mechanical comminution	reduces cellulose crystallinity	power consumption usually higher than inherent biomass energy
steam explosion	causes hemicellulose degradation and lignin transformation; cost-effective	destruction of a portion of the xylan fraction; incomplete disruption of the lignin−carbohydrate matrix; generation of compounds inhibitory to microorganisms
AFEX	increases accessible surface area, removes lignin and hemicellulose to an extent; does not produce inhibitors for downstream processes	not efficient for biomass with high lignin content
CO_2 explosion	increases accessible surface area; cost-effective; does not cause formation of inhibitory compounds	does not modify lignin or hemicelluloses
ozonolysis	reduces lignin content; does not produce toxic residues	large amount of ozone required; expensive
acid hydrolysis	hydrolyzes hemicellulose to xylose and other sugars; alters lignin structure	high cost; equipment corrosion; formation of toxic substances
alkaline hydrolysis	removes hemicelluloses and lignin; increases accessible surface area	long residence times required; irrecoverable salts formed and incorporated into biomass
organosolv	hydrolyzes lignin and hemicelluloses	solvents need to be drained from the reactor, evaporated, condensed, and recycled; high cost
pyrolysis	produces gas and liquid products	high temperature; ash production
pulsed electrical field	ambient conditions; disrupts plant cells; simple equipment	process needs more research
biological	degrades lignin and hemicelluloses; low energy requirements	rate of hydrolysis is very low

Several typical methods are briefly described below, and more detained information could be found in Mood's review paper for lignocellulosic biomass pretreatment [78]. Table 2 summarizes advantages and disadvantages of common pretreatment methods [76]. For acid pretreatment, concentrated H_2SO_4 and HCl are the most commonly employed agents. They aid hemicelluloses to be hydrolyzed to monosaccharides, thus improving accessibility to cellulose. Using high concentration acid is relatively economic since the process can be performed at lower temperature, while low concentration is attractive in industrial as this process generates less inhibitor [79]. The highest sugar yield of 83% was obtained by 1% (w/w) H_2SO_4 pretreatment at 160-180 ℃ for 1-5 min [80]. For alkaline method, lime and NaOH are commonly used. They can effectively remove lignin, acetyl groups and different uronic acid substitution which could inhibit sequence enzymatic saccharification [81]. Lime pretreatment achieved a polysaccharide conversion approaching 100% for corn stover [82].

Besides chemical pretreatment, explosion method is also a competitive pretreatment technique, which biomass is treated with a high pressure fluid for several seconds to a few minutes, and then the pressure is suddenly released to atmospheric pressure, as a result of which the degradation of biomass occurs [83]. The fluid could be water steam and liquid ammonia, which the latter one is more effective. Ammonia fiber xxplosion (AFEX) pretreatment can significantly enhance the fermentation rate of various herbaceous crops and grass with low lignin content (less than 20%) [84]. Chundawat *et al.* [85] used molecular dynamics simulations to test the effects of ammonia on changing the structure of cellulose fibrils. It proved that ammonia transformed cellulose crystalline allomorph by altering hydrogen bond network within cellulose fibrils. This rearrangement of hydrogen bond network increased the number of solvent-exposed glucan chain by 50%. Besides ammonia, supercritical water [86] and supercritical CO_2 [87] were also tested as potential fluids, as they have unique advantages of biomass pretreatment.

2.4 Pyrolysis of Biomass

2.4.1 General Information

Two publications in two consecutive years by Bridgewater, *et al.* [88, 89] reviewed the principles and practice of biomass fast pyrolysis technology until 2000. In the first paper, factors such as, feed drying, particle size, pretreatment method, reactor configuration, heating system, residence time, char separation and bio-oil collection system, which needed to be considered when designing a fast pyrolysis process were reviewed. The maximum liquid yield can be realized with high heating rate, temperature around 500 ℃, and short vapor residence time to minimize secondary reactions. Liquids for use as fuels can be produced with longer vapour residence times (up to 6 s) and over a wider temperature range although yields might be affected in two ways: secondary volatiles decomposition and repolymerization. In their second paper, the development of pyrolysis processes built at industrial scale in western counties was reviewed. The main difference between processes was the type of reactor utilized. Ablative and fluid bed reactors were used the most, especially fluid

bed reactors. Mohan, *et al.* [14] gave a comprehensive review og pyrolysis of woody materials; nearly 100 types of biomass were tested. The yield and property of bio-oil was largely dependent on the composition and structure of biomass, heating rate, residence time, etc. Recently, Isahak, *et al.* [90] reviewed current bio-oil production processes by using pyrolysis method. Both slow pyrolysis and fast pyrolysis (bubbling fluidized bed, circulating fluidized bed, rotating cone pyrolyzer, vacuum pyrolysis and auger reactor) were investigated. In general, fast pyrolysis can produce bio-oil yield at around 40-70% for different kinds of biomass, while slow pyrolysis process produces only at 20-30% at moderate temperature.

Even though the feedstocks and reactor maybe fixed, varying operating parameters also exert a great effect on the yield of bio-oil [91]. Temperature is the most important factor; intermediate temperatures (450-550 ℃) usually maximize the bio-oil yields. Lower or higher temperatures lead to the formation of char or gases. In terms of components of biomass, cellulose and hemicellulose tend to produce liquid products, while lignin is the major source contributing to char formation. Mineral matter content of biomass affect the bio-oil yield negatively. High heating rate and small particle size are preferable for high bio-oil yield. A rapid quenching of pyrolysis vapors coupled with short residence time produces maximum liquid yield. Also heat and mass transfer should be considered in order to obtain highest yield of bio-oil. Most papers published up to now mainly focus on yield rather than compositions of bio-oil. However, the composition is also important as to bio-oil utilization. Zhang *et al.* [92] made a comparison between biomass pyrolysis oil and heavy fuel oil in both physical and chemical properties. In their research, two biggest differences between pyrolysis oil and heavy fuel oil were the moisture content and the oxygen content. Pyrolysis oils have 150-300 times moisture and 35-40 times oxygen higher than that in heavy oil. More recently, Bridgwater [93] provided an updated review of fast pyrolysis of biomass and product upgrading. The potential of bio-oil is increasingly being recognized, with much more effort into improving bio-oil properties and biofuel production. However, much of the research is still at a fundamental scale even to the use of model compounds to represent whole bio-oil.

Catalytic pyrolysis is now of interest and requires intensive laboratory work to prove feasibility and viability.

2.4.2 Current Research on General Pyrolysis

With the increasing interest on pyrolysis biomass conversion, more and more research has been carried out to explore basic knowledge of pyrolysis of biomass. Thus, Luo *et al.* [94] built a fluidized bed reactor with continuous feeding rate at 3 kg/h, operated at atmospheric pressure, and reaction temperature at 500 ℃. Pterocarpus indicus, Cunninghamia lanceolata, Fraxinus mandshurica and rice straw were tested in the experiment. P. indicus gave the best results (bio-oil yield of 55.7%) when yield, heating value and water content were used as the evaluation criteria. Bio-oil from P. indicus was mainly comprised of levoglucosan, furfural and phenol. Zheng [95] investigated rice husk fast pyrolysis performance at temperatures between 420 ℃ and 540 ℃ in an enhanced fluidized bed reactor system. Results showed an optimal bio-oil yield of 56% at 465 ℃ with 25.2% water content, with main components being formic acid, toluene, β-Hydroxybutyric acid and 4H-Pyran-4-one, 2, 6-dimethyl-. Chen, *et al.* [96] researched pyrolysis of sucrose biomass in a tubular reactor with a slow heating rate (10 ℃/min) over a temperature range from room temperature to 1200 ℃. However, liquid formation could be ignored with more than 90% yield of gases when temperature was higher than 300 ℃, while the highest bio-oil yield was about 7% at 200 ℃. Low heating rate was the main reason that resulted in low liquid yield. They also investigated the performance of introduction of CaO into the reaction system. Results indicated that CaO could enhance conversion of sucrose to gases products and capture CO_2 produced. Kim *et al.* [97] studied prolysis of alga Saccharina japonica between 200 ℃ and 380 ℃ at a 10-20 ℃/min heating rate in a tubular reactor heated in salt bath. Results showed that highest yield of bio-oil was 28.78 % at 380 ℃ with dianhydromannitol and1-2(-Furanyl)-ethanone as the main components. Patwardhan *et al.* [98, 99] investigated primary and secondary bio-oil product distribution of fast pyrolysis of glucose-based carbohydrates with micro-pyrolyzer in which the heating rate could be greater than 2000 ℃/s. The

residence time was only 15-20 ms in micro-pyrolyzer to inhibit secondary products. In contrast, a fluidized bed reactor with a residence time of 1-2 s was used to make a comparison and explore secondary products. It suggested that levoglucosan and low molecular weight compounds, such as formic acid, furfural, and HMF, are formed through competitive paths in primary products. However, oligomerization of leglucosan and decomposition of primary products (mainly furfural and HMF) were the major reactions to produce secondary products. Li *et al.* [100] studied pyrolysis products from cellulose and levoglucosan. The product distribution was in great similarity, thus indicating the precursor conversion and formation mechanisms. Compared with extensive investigations on pyrolysis of lignocellulosic biomass and pure cellulose, pyrolysis chemistry of other two components (hemicellulose and lignin) has received less attention. Choi *et al.* [101] investigated kraft lignin pyrolysis in Tl-mini fast pyrolyzer system. The bio-oil yield was 29.95% at 450 ℃ and 38.09% at 500 ℃. The main products were acetic acid (2.70 wt. % dry basis), anhydro-sugars (1.70 wt. % dry basis), lignin derived phenols (0.92 wt. % dry basis), and guaiacols (25.64 wt. % dry basis). Wu *et al.* [40] studied on pyrolysis of corn stalk hemicelluolse in a tubular reactor. Large bio-oil yields occurred below 500 ℃ and the highest yield approaching 50% was at 450 ℃. The main liquid products were ketones (60.47 area percent), furans (19.02 area percent), acids (18.28 area percent), and alcohols (2.25 area percent). Four main individual chemicals were 1-hydroxy-2-propanone, acetic acid, furfural, and 1-hydroxy-2-butanone in sequence.

The effectiveness of heat transfer in pyrolysis process is a crucial factor. Poor heat transfer usually leads to a low yield of bio-oil. Therefore, improving thermal management is necessary especially in industrial scale production of bio-oil. Microwave-Assisted Pyrolysis (MAP) is a treatment process applied to thermal-decomposition of biomass. MAP is preferable for large-sized biomass particles due to the nature of fast and volumetric heating by microwave energy [102]. Moreover, microwave energy is easy to control and scale up. Some researchers have explored the temperature profile inside the feedstocks particles and its effect on pyrolysis process and final products [103, 104].

2.4.3 Pyrolysis with Additives

Natural biomass contains mineral matters which play important roles in pyrolysis chemistry. Different types of biomass contain different amounts of mineral matters. The main elements in minerals are Si, Ca, K, Na and Mg, together with slight amounts of S, P, Fe, Mn and Al. These elements are present as oxides, silicates, carbonates, sulfates, chlorides and phosphates [105]. Generally the inorganic salts contained in biomass inherently suppress the formation of char and favor char-forming reactions [106]. Raveendran *et al.* [105] investigated elements compositions of selected types of natural biomass and influence of minerals on the performance of biomass pyrolysis. They tested 13 kinds of biomass and demineralized biomass gave higher liquid yields than untreated, except coir pith, groundnut shell, and rice husk, which might be attributed to their high lignin, potassium, and zinc contents. Deashing process also increased biomass initial decomposition temperature and degree of pyrolysis. Salt ($ZnCl_2$ or KCl) impregnation of coir pith, groundnut shell, and rice husk increased bio-oil yields, which proved Zn and K catalytic role in bio-oil formation reactions. In thermal analysis, they observed $ZnCl_2$ impregnation of biomass increased the initial decomposition temperature while KCl reduced it. Shimada [107] studied the effects of NaCl, KCl, $MgCl_2$ and $CaCl_2$ on cellulose pyrolysis. They found both $MgCl_2$ and $CaCl_2$ can dramatically reduce pyrolysis temperature, and all kinds of salts changed the formation of low molecular weight products strongly. The effect of varying amounts of NaCl, KCl, $MgCl_2$ and $CaCl_2$ on 8 selected substances (furfural, HMF, formic acid, acetic acid, methanol, hydroxyl acetone glycol aldehyde, and levoglucosan) was tested. Their findings were reexamined in Patwardhan's work [108]. Nik-Azar *et al.* [109] investigated mineral effects on pyrolysis of beech wood. According to their study, acid washing wood samples reduced yields of char and gases; exchanging cations onto wood samples reduced yield of liquid. They also concluded that potassium and sodium cations offered stronger catalytic cracking reactions.

Recently, application of $ZnCl_2$ has drawn great interests in biomass pyrolysis

process, as $ZnCl_2$ performs effective catalysis in bio-oil production process. Lu *et al.* [110] studied the production of furfural from fast pyrolysis of biomass impregnated with $ZnCl_2$. It proved that increasing contents of $ZnCl_2$ (from 5% to 40 wt %) can improve the formation of furfural and reduced levoglucosan contents. Lu [111] found that $ZnCl_2$ proved to have two catalytic ways, one is for the formation of liquid at low temperature and the other is for formation of char at high temperature. Also, the by-product, activated carbon, derived from pyrolysis process was evaluated. Amarasekara *et al.* [112] studied effects of $ZnCl_2$ on thermal degradation of cellulose at 200 ℃. The highest yields of furfural and HMF were 8% and 9%, respectively, based on glucose unit of cellulose at $ZnCl_2$ concentration of 0.5 mol/ mol of glucose unit of cellulose. Yang *et al.* [113] conducted research on conversion of cellulose in zinc chloride solution under microwave irradiation. The microwave process not only significantly reduced the reaction time but also increased the yield of certain species.

2.4.4 Catalytic Pyrolysis

The usage of catalyst in biomass pyrolysis could decrease reaction temperature, increase reaction rate and conversion, as well as product selectivity. Alonso *et al.* [114] reviewed catalytic conversion of biomass in aqueous solution isolated after pretreatment and hydrolysis process. Hydrolysis- based compounds can be processed to certain products selectively. In their review, emphasis was placed mainly on selective transformations of platform chemical such as, furfural and HMF. Generally there are two ways to use catalysts in thermal treatment of biomass: one is catalytic upgrading bio-oil obtained from pyrolysis; the other is to catalyze pyrolysis reactions directly. The latter method is preferable as it can ameliorate costly condensation and reevaporation procedures in bio-oil upgrading process [115]. The current status of catalytic pyrolysis of biomass was reviewed by Hu and coworkers [116]. Nano-NiO and $ZnCl_2$ could effectively decrease cellulose pyrolysis temperature; K_2CO_3 could lower *M. Sinensis* and *A. Donax* pyrolysis temperature. NaY and HY could increase bio-oil yield from pyrolysis of several kinds of bamboo. Aluminium titanate, titanium silicate, aluminium oxide colombe and phosphoric acid could govern the formation of

anhydro-sugars. Zinc chloride and sulfated metal oxides could maximize yields of furan derivatives. NaOH, Na_2CO_3, Na_2SiO_3, and NaCl could favour acetol formation. Transition metals are supposed to catalyze phenols formation and zeolites catalyze aromatics formation.

However, research on catalytic pyrolysis is still limited, and the catalytic mechanisms are still unclear at present. Extensive researches on catalytic pyrolysis are of importance and development of new catalysts is of great significance. Thangalazhy-Gopakumar *et al.* [117] studied zeolite catalytic pyrolysis of pine wood with two different carrier gases: helium and hydrogen. Their results indicated that a high reduction in the yield of higher molecular weight oxygenated compounds in bio-oil occurred for non-catalytic pyrolysis in the presence of reducing hydrogen gas in contrast to inert helium gas. In their non-catalytic pyrolysis experiment, 15 compounds were quantified in bio-oil and the yields of these compounds under hydrogen environment were less than one thirds of those under helium. They also found that when zeolite catalyst was used, the yields of bio-oil increased in both cases and the ratio of biomass to catalyst affected the yield greatly in mixing bed method. Daniele Fabbri, et al [118] investigated effects of zeolites and nanopowder metal oxides on the formation of several anhydro-sugars from pyrolysis of cellulose, where the heating rate could be as high as 20 ℃/ms and the reaction lasted for only 60 s. Zeolite had the ability to change the anhydro-sugars product distribution and decreased the total yields of anhydro-sugars. The performance of nanopowder metal oxides depended on their nature: silicon oxide depressed total yields of anhydro-sugars while titanium oxides increased all yields especially in LGO and LAC. Their observations were confirmed by Torri *et al.* [119]'s research on pyrolysis of cellulose with MCM-41 as the catalyst. M. Zabeti, et al [120] used amorphous silica alumina (ASA) containing alkali metal or alkali earth metal as the catalyst to study on pine wood pyrolysis reactions. ASA had the effect of reducing the oxygen content in the bio-oil, improving bio-oil energy density, and altering the bio-oil and bio-gas product distribution. Ca, Cs, K, and Na were capable of decreasing oxygen content by 80% when associated with ASA. Wan *et al.* [121] studied microwave-assisted pyrolysis of corn stover and aspen

wood in present of metal oxides, salts, and acids including K_2CrO_7, Al_2O_3, KAc, H_3BO_3, Na_2HPO_4, $MgCl_2$, $AlCl_3$, $CoCl_2$, and $ZnCl_2$. K_2CrO_7, Al_2O_3, KAc, H_3BO_3, Na_2HPO_4, and $MgCl_2$ were tested and proved to increase yields of bio-oil. These catalysts might act as microwave absorbents to speed up heating or directly catalyze pyrolytic vapors. Furthermore, all chloride salts promoted furfural production and $ZnCl_2$ and $MgCl_2$ also suppressed the production of other components in bio-oil.

More recently, conversion of carbohydrates to HMF and furfural via Lewis and/or Brønsted acid catalysts in aqueous solutions have drawn much attention. The introduction of Lewis and/or Brønsted acid not only improves formation of HMF and furfural, but also gives an insight of biomass degradation mechanism. Yang *et al.* [122] used DFT theory to study the mechanism of Brønsted acid in conversion of glucose and fructose in water. Generally there are several elementary steps involved in Brønsted acid-catalyzed conversion: protonation, deprotonation, isomerization, dehydration, hydration, and intramolecular hydrogen transfer. Yang found that fructose dehydration by Brønsted acid was preferable by protonation of the O_2H group at the anomeric carbon atom, which further initiated formation of HMF. The followed rehydration reaction to levulinic acid was difficult, as it competed with formation reaction of humins. However, Brønsted acid-catalyzed mechanism of glucose conversion was quite different, and formation of HMF and levulinic acid (LA) was not preferable. Román-Leshkov and Davis [123] investigated functionality of Lewis acid in conversion of carbohydrates in aqueous media. They analyzed effects of Lewis acid on glucose isomerization, synthesis of lactate- derivatives from carbohydrates, and dehydration of C-6 and C-5 sugars. They found higher yields of fructose could be obtained from isomerization of glucose in presence of Lewis acid. Shi *et al.* [124] conducted research on conversion of cellulose to HMF in hot compressed water with salts ($NaHSO_4$, $KHSO_4$, NaH_2SO_4, and KH_2PO_4). It was concluded that higher relative humidity was preferred for HMF formation and the highest yield of HMF was 30.4 mol% with NaH_2PO_4 as the catalysts. Considering the resistance of high crystalline structure of cellulose, the research on biomass conversion to HMF and furfural are often limited to glucose [125]. Eranda Nikolla, et al

[126] reported that combination of Sn-Beta catalyst with acid catalyst in a biphasic reactor to produce HMF was an effective way to convert glucose, cellobiose, and starch. The highest selectivity of HMF was 79% for glucose using biphasic water/ tetrahydrofuran reactor with NaCl and HCl. They highlighted the performance of Sn-Beta catalyst in achieving the conversion of glucose to fructose. Furthermore, they found the yield of HMF decreased with time, which might have resulted from degradation and resinification of HMF over time at high temperature (> 160 ℃). Pagán-Torres *et al.* [127] conducted similar research giving the highest HMF yield of 68% using biphasic water/ 2-*sec*-butylphenol reactor with $AlCl_3$ and HCl. Yang *et al.* [128] studied one phase reaction system with mixed Lewis and Brønsted acid. In absence of HMF extraction process done by organic phase, the final major product was LA rather than HMF. The $CrCl_3$-H_3PO_4 system offered best performance of decomposition of glucose to LA. Besides liquid homogeneous catalysts, solid heterogeneous catalysts were also investigated. In Mazzotta *et al.* [129]'s work, nanoparticulates of porous sulfonated carbonaceous TiO_2 material that involve Lewis and Brønsted acid sites were proposed. This new kind of solid catalyst was effective in producing HMF and furfural from mono-and disaccharides, as well as xylose. Another notable feature of this catalyst was that it could be easily separated from the final products and be recycled to further uses, although the yields of HMF were usually lower than in liquid catalysts. The conversion of sugars to intermediate platforms is still facing challenges: lack of understanding of reactions in solvent-solute-catalyst system; poor performance on cellulose and lignocellulose; environmental issues and costs of organic solvent and homogeneous catalysts; separation considerations, etc [130]. Thus, further scientific and technological developments are still required.

2.4.5 Ionic Liquids (ILs) Pyrolysis

ILs are, by definition, organic salts that are in a liquid state at or below 100 ℃. Unlike inorganic salts which melt at higher temperatures, organic salts consist of larger and asymmetric organic cations with a delocalized positive charge, which offer

liquids exclusively composed of ions at relatively low temperatures. Recent studies have shown an increasing interest in the design of new ILs which have specific properties for varied applications including organic synthesis, electrochemistry, catalysis, separations and biomass treatment [131]. Some selected cations and anions used in modern ILs are shown in Figure 9 and Figure 10.

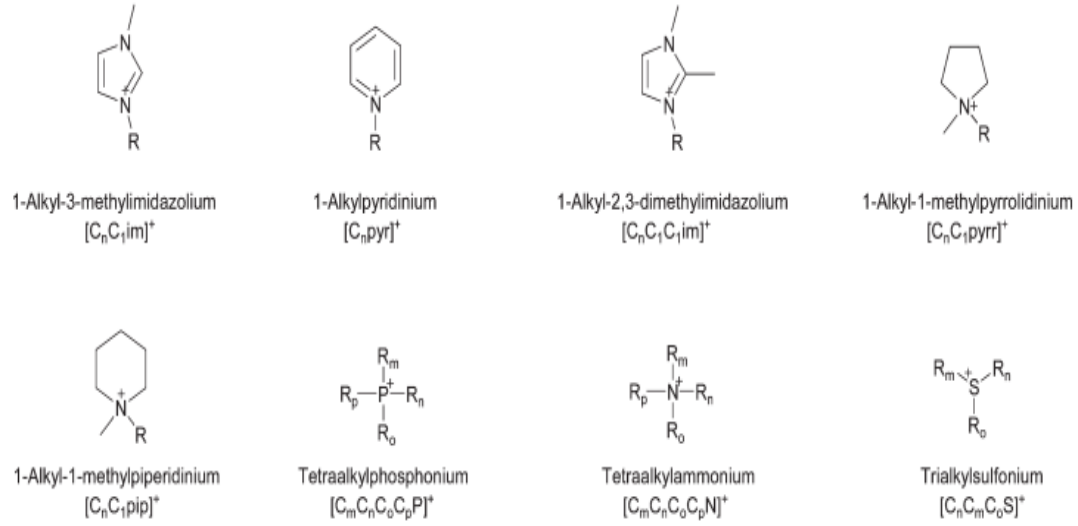

Figure 9: Common cations used in ILs [132].

The applications of ILs to biomass conversion are mainly divided into two types: biomass pretreatment and biomass pyrolysis. For the first application, ILs are considered to be able to destroy the hydrogen bond network existing between different polysaccharide chains and make the lignocellulosic biomass more susceptible to hydrolysis [133]. The use of acid-catalysts and metal-catalysts in combination with ILs in cellulosic biomass hydrolysis were recently reviewed by Tadesse and Luque [131], illustrating that catalyzed hydrolysis of cellulosic biomass in ILs proved to present higher yields of HMF or total reducing sugars under mild conditions. Another good review written by Brandt and coworkers [95] discussed the solubilities of cellulose, lignin and lignocellulose in certain ILs and further demonstrated biomass dissolution associated with depolymerization in ILs. More recently, Wen and coworkers [134] investigated the degradation chemistry of lignin in ILs and their findings give an insight on effects of ILs on biomass pretreatment.

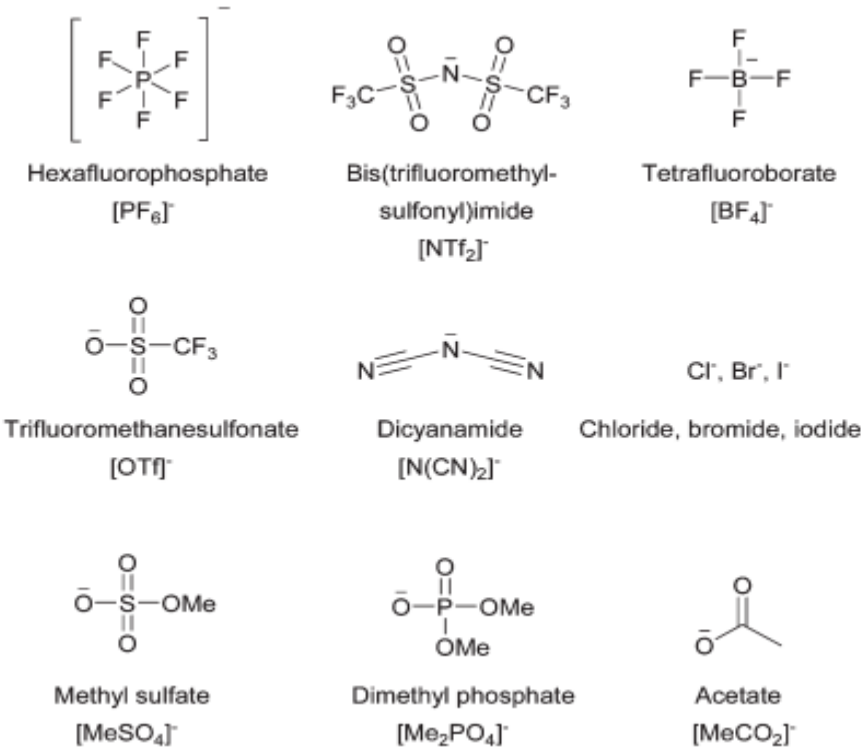

Figure 10: Common anions used in ILs [132].

The second application is biomass pyrolysis in the presence of ILs. ILs can be used as reaction media during the pyrolysis process. Compared to conventional pyrolysis, ILs pyrolysis can be carried out under milder conditions and overcome the biomass dissolution problem encountered in hydrolysis. Sheldrake and Schleck [135] first studied on controlled pyrolysis of cellulose to anhydrosugars in dicationic IL. They used molten diacationic imidazolium chloride and bromide salts as media to produce levoglucosenone by pyrolysis around 180 ℃. Their highest yield was 5% compared with 3% by conventional pyrolysis above 300 ℃. Du and coworkers [136] investigated on fast pyrolysis of biomass with ILs and microwave irradiation. The bio-oil yield reached 38% for rice straw and 34% for sawdust with 1-butyl-3-methylimidazolium tetrafluoroborate as IL for heating 20 mins at 640 W. The main components were acetic acid and furfural for both rice straw and sawdust. Due to the limited ILs pyrolysis data currently available, more research is required to determine the advantages of this process. Nevertheless, ILs pyrolysis shows a potential way in realizing thermochemical conversion of biomass at moderate temperatures.

However, applications of ILs are only promising if its advantages outweigh drawbacks. Crucial challenges still put a barrier for this technology. The major factor is the high cost of ILs. Currently used ILs are about 5-20 times more expensive than conventional solvents and it could cost more when applied at industrial scale [130]. Designing new kinds of ILs is a potential way to deal with the problem. Other factors such as recycling procedure and toxicity of ILs should also be further evaluated [137].

2.4.6 Molten Salt Pyrolysis

Inorganic molten salts pyrolysis technology has a lot of advantages: a) Molten salts serving as solvent can dissolve biomass material which facilitates decomposition reactions; b) selected eutectic combinations of salts can be melt at mild temperatures (150-450 ℃) to provide a good medium for pyrolysis reactions; c) molten salts have large heat capacity and thermal conductivity which favors effective heat transfer; d) good thermal and chemical stability, as well as low vapor pressure make molten salts media stable during pytolysis; e) some molten salts also have catalytic properties that can enhance the yields of certain productions; f) products yields and distributions can be adjusted be varying compositions and amount of molten salts [138]; and finally g) catalysts can be dispersed in molten salts.

However, research on the development of molten salts pyrolysis has been rather slow and there have been only a handful of publications about molten salts pyrolysis. Japanese researchers [139] firstly investigated the performance of pyrolysis of lignins (kraft and solvolysis) in $ZnCl_2$-KCl molten salts with molar ratios of 3/7 and 7/6 at temperatures from 500-800 ℃. The zinc halide could improve selectivity to produce single-ring aromatic compounds; the addition of KCl could act as a viscosity reducer, and could decrease the melting point of the salts. At a molar ratio of 3/7, phenol was the main liquid product for kraft and m-cresol was the main product for solvolysis. At molar ratio of 7/6, p-cresol was the main liquid product for kraft in most cases and m-cresol was the main product for solvolysis. Solvolysis gave higher liquid yields than kraft and this gap was narrowed when more zinc chloride was added. The maximum yield of cresols attained from solvolysis lignins was 4.6 wt % with a

mixture of $ZnCl_2$ –KCl (molar ratio was 7:6) at 600 ℃. In order to further improve the liquid yield, the same research group [140] later conducted research by adding tetralin vapor as a hydrogen donor. They found all the liquid products yields were increased by using tetralin vapor, especially the yields of cresols and total phenolic compounds were enhanced by 38 and 78%, respectively. In their third paper [141] the effects of three levels of salt-to-lignin ratio (SR), 1, 2, and 3 on liquid yields and product distribution were investigated. Both the yields of liquids and gases were dependent strongly on the amount of salts added. The highest yields of liquids and gases were both at SR of 3.Various kinds of components in liquid phase were tested at different SRs and reaction time. For example, the yield of phenol increased with SR; the yields of cresols increased slightly with SR.

A decade later, a Chinese research group [142] studied on the effects of the composition of molten salt, biomass materials and pyrolysis temperature on the performance of biomass pyrolysis. They pointed out that the highest liquid yield was 35% in pure $ZnCl_2$, in which the water content of the liquid was 46% at 450 ℃. Experiments with 53.8% $ZnCl_2$- KCl molten salt produced lowest liquid yield of 11.60% with water content of 50%. Experiments with 49.2% ZnCl2-39.8% KCl-CuCl gave 12.0% liquid yield, however the water content was only 21%. Nitrate molten salts in contrast gave 0% liquid yield. The liquid yield from cellulose was higher than that from rice straw in absence of molten salts and water content in cellulose derived bio-oil was lower than that of from rice straw. The components of bio-oil were extremely complex, while furan derivatives captured the major share. To expand knowledge of pyrolysis process with molten salts, the same research group [143] investigated pyrolysis of six kinds of biomass in five kinds of molten salts at temperature of 400-600 ℃. No significant improvement was founded. In their third paper [144], they studied effect of $FeCl_2$ added into $ZnCl_2$-KCl (7:6) molten salts on bio-oil yield produced by pyrolysis of rice straw. When adding 5 wt% of $FeCl_2$ into the system, the bio-oil yield was increased to 15% compared with 10% without $FeCl_2$ at 500 ℃. More recently, Ji *et al.* [145] reported a continuous production process of bio-oil from pyrolysis of sawdust in NaOH molten salts. Yield of char was increasing

with an increase of feeding rate, while yield of bio-oil increased first then decreased as feeding rate increased. The optimal yield of bio-oil was at feeding rate of 1.36 g/min. With a carrier gas flow rate from 50 to 200 L/h, the yield of bio-oil went down as gas flow rate went up. This might be due to the fact that higher gas flow rates led to shorter residence time of vapors in the condenser, thus vapors could not be condensed fully. Fir sawdust, brich sawdust, and their mixture were tested as the feedstocks. Results showed that the combinations gave the highest liquid yield at the same conditions. They also found that addition of $ZnCl_2$ into the system restrained the formation of bio-oil and char.

Jiang *et al.* [146] focused on hydrogen production from pyrolysis of biomass in molten alkali. Six kinds of biomass were tested at temperatures from 350-550 ℃. The biomass type had little influence on H_2 content percentage in pyrolysis gas, however, the total H_2 yield was significantly dependent on biomass type. Redwood sawdust gave the highest H_2 yield of 65.39 g/Kg biomass at 450 ℃. Both H_2 content percentage in pyrolysis gas and he total H_2 yield were independent of carrier gas flow rate, while H_2 yield favored at high temperature. They also found addition of 5% $NiCl_2$ increased H_2 yield from 46.33 g/Kg to 67.34 g/Kg. Nygård *et al.* [147] gave an important insight in a study on pyrolysis of wood particles with constant length of 30 mm and varying diameter of 1-8 mm in a FLiNaK melt. FLiNaK molten salt enhanced heat transfer significantly and improved the performance of pyrolysis especially for wood particles with diameter below 4 mm. For particles with diameter larger than 4 mm, the performance of heat transfer was mainly limited by the inner parts of wood particles. The presence of FLiNaK could provide a very high heat transfer value of around 218 ℃/s for beech wood. In short, the research on molten salts pyrolysis of biomass is still in its early stage, and needs extensive fundamental and careful investigations.

2.5 Biomass Conversion Kinetics and Mechanisms

Primary investigations on mechanism of biomass decomposition date back to the late 1970s. Both experiment-based and computer simulation-based methods have been

used to explore the mechanism. However, unlike other industrial chemical production processes, in which the mechanisms are relatively well-understood, mechanism of pyrolysis of biomass is still unclear for several reasons: (1) substantial functionality of biomass starting materials, intermediates and final products [148]; (2) short lifetime (less than 0.1 s) of condensed-phase intermediates [149]; (3) relatively slow heat transfer for biomass, leading to making isothermal pyrolysis challenging; (4) multi-parameters dependency of product distribution.

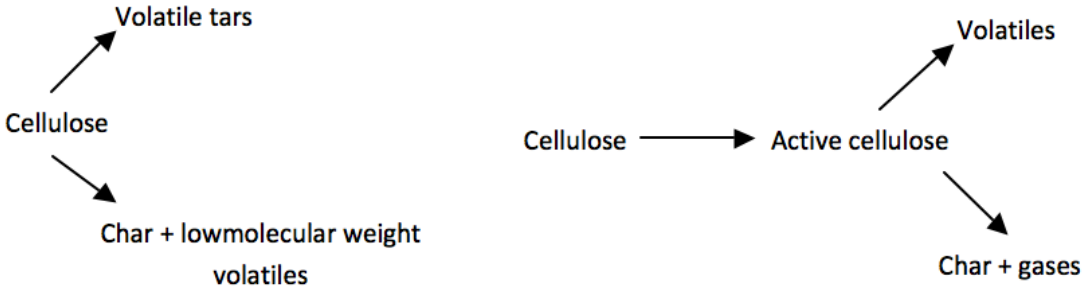

Figure 11: BN (left) and BSS (right) schemes for cellulose pyrolysis [152].

Thermogravimetric analysis (TGA) is a widely used method to investigate the thermal decomposition of polymers and obtain thermogravimetric data for determination of kinetics parameters and models. Thus, Flynn *et al.* [150] have given a comprehensive and insightful review of theoretical equations on thermal decomposition of polymers based on reaction order, activation energy, heating rate, and temperature dependence. Several kinetics models for cellulose were reviewed and compared in a comprehensive review published in 1995 [151]. Figure 11 lists some representative schemes based on the development of kinetics of biomass (pure cellulose only) pyrolysis, in the absence of any secondary, heterogeneous (vapor-sold) or homogenous (vapor phase) reactions. The first widely-accepted model was proposed by Broido and Nelson [152] in 1975. They developed a first order two-competitive-pathway mechanism in accord with their previous experiment results. In 1979, Bradbury *et al.* [153] proposed a scheme in which cellulose first decomposes to anhydro fragment, which is called ‘active cellulose’, then degrades into char, condensable volatiles and non-condensable gases. However, due to the large amount

of cellulose they used in the experiments (100 mg for Broido's and 250 mg for Bradbury's), char formation from vapor-solid interactions should occur, confirmed by abnormally high content of char. Mok and Antal [154] correlated gas flow rate and pressure with char formation and calorimetry of the process, indicating that high gas flow rate and low system pressure results in endothermic process with less char formation, while low gas flow rate and high pressure leads to exothermic process with high char formation. As shown in Figure 12, Banyasz *et al.* [155] proposed a gas evolution based mechanism of cellulose pyrolysis (whatman 41) from 400-800 ℃, which well-matched their mathematical model. Antal *et al.* [156] investigated pyrolysis kinetics of various pure cellulose samples. The pyrolytic weight loss of all the samples was well represented by a high activation energy (228 KJ/mole), first order rate law over a wide range of heating rates, which indicated that a global first order law could well represent thermal behavior of biomass decomposition.

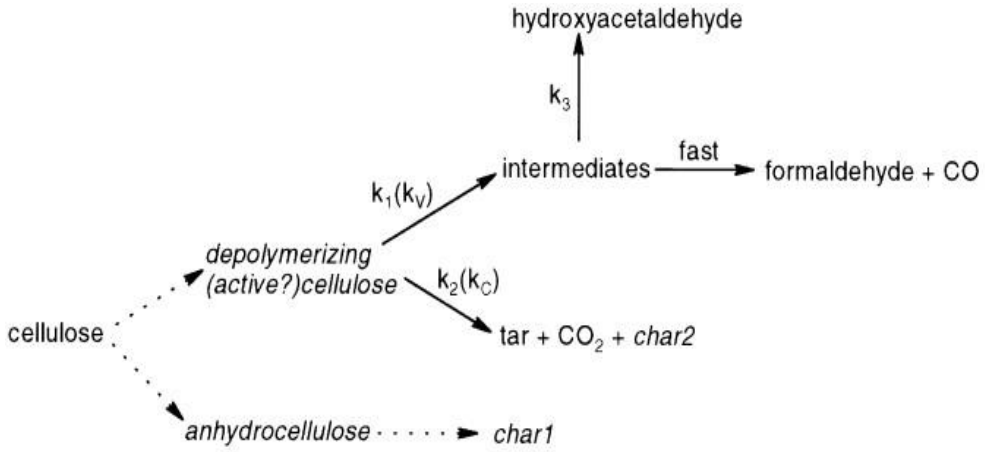

Figure 12: Gas evolution based mechanism of cellulose pyrolysis [155].

However, when considering mineral matter and existence of hemicelluose and lignin in lignocellulosic biomass, the single, first order model fails to represent the global behavior of biomass decomposition. For this case, Órfão *et al.* [157] proposed a three independent reactions model, which incorporated the effect of hemicelluose and lignin pyrolysis. The pyrolysis of three selected lignocellulosic biomass (pine, eucalyptus woods, and pine bark) was modeled with better approximation by the

proposed model than the first order model. The first reaction involved primary pyrolysis of cellulose; the second reaction represented primary pyrolysis of hemicellulose; and the third reaction contained pyrolysis of remaining amounts of non-primary components and lignin. Many à *et al.* [158] proposed a reformulated three-parallel-reactions model to simulate pyrolysis behavior. The main improvement was using a third-order reaction rate law to describe lignin pyrolysis. They also pointed that the three-parallel model could only be valid at low heating rate, for example, 5K/min. Because high heating rate would bring sever impact of heat transfer limitations on kinetic studies of endothermic reactions. Müller-Hagedorn *et al.* [159] reported a new method for the individual evaluation of kinetic parameters for the three main components of wood. It was found that coniferous lignin was more thermally stable than deciduous lignin. The different behaviors of thermal decomposition of wood species resulted from differences in lignin and hemicellulose portions in woody biomass. Hu *et al.* [160] compared three-pseudocomponent models to first-order model in modeling pyrolysis of six Chinese biomass feeds. Activation energies of three-pseudocomponent models with n^{th} (n>1) order were bigger than first-order model, and gave the best simulation results. Nevertheless, reaction order of one was preferable, as it had already been shown to be accurate enough and it is more convenient in chemical kinetic analysis. Sonobe *et al.* [161] used the distributed activation energy model to predict activation energy of pyrolysis reaction of biomass. The advantage of the distributed activation energy model was that no assumption and mathematical fitting was required. The calculated activation energy for rice straw, rice husk, corncob, and cellulose were 170, 174, 183, and 185 kJ/mol, respectively. Damartzis *et al.* [162] investigated pyrolysis kinetics of *Cynara cardunculus* with the independent parallel model, KAS, and OFW model. Slopiecka *et al.* [163] investigated pyrolysis kinetics of poplar wood with Kissinger, KAS, and FWO model, which the three models gaving similar activation energy values. Gao *et al.* [164] investigated effect of salts on pyrolysis kinetics of rice straw. It was found that alkaline CO_3^{2-} lowered the primary decomposition temperature and produced less solid residue than Cl^- and SO_4^{2-} with the same cation. Potassium salts had better ability to fix carbon

than that of sodium salts. Ioannidou *et al.* [165] used a predictive model to simulate pyrolysis or gasification of biomass in order to obtain yields of char and gas, as well as heating values of char and gas. The deviations ranged from 0 to 28% for pyrolysis process with agreement, however, this model failed to simulate gasification process with greater than 100% deviations.

Since biomass is comprised of three distinct components, it makes investigation of biomass decomposition mechanism quite challenging. Thus, research on cellulose, hemicellulose and lignin independently is a reasonable manner to get an in-depth knowledge of biomass decomposition mechanism. Yang *et al.* [166] investigated the pyrolysis characteristics of the three main components (cellulose, hemicelluloses, and lignin) of biomass by using a thermogravimetric analyzer with differential scanning calorimetry (DSC) detector. The main weight loss of hemicellulose occurred at 220–315 ℃ with a fair mass loss rate and that of cellulose occurred at 315–400 ℃ with a strong mass loss rate, while lignin started to decompose over a wide temperature range from 160 to 900 ℃ with the lowest mass loss rate. Also, lignin gave the highest content of residue left after thermal analysis and cellulose gave the lowest value. DSC curves showed that cellulose reaction is endothermic before 400 ℃ and exothermic after 400 ℃, while lignin and hemicellulose exhibited complex results. From gas analysis, hemicellulose had higher CO_2 and CO yield, while lignin showed higher H_2 and CH_4 yield. CO_2 generation was mainly caused by primary pyrolysis, while CO and CH_4 were the major gas products derived from secondary pyrolysis. In another paper of Yang *et al.* [167], they concluded that the overall biomass pyrolysis can be divided into 4 sequential ranges: <220 ℃, moisture evolution; 220-315 ℃, predominantly hemicellulose decomposition; 315-400 ℃, cellulose decomposition; >400 ℃, lignin decomposition. Two sets of predictive equations were set up to relate the amounts of the three main components and the weight loss in specified temperature ranges. Hosoya *et al.* [168] investigated the cellulose–hemicellulose and cellulose–lignin interactions in wood pyrolysis at 800 ℃. The former type was not significant, but lignin inhibited the thermal polymerization of levoglucosan formed form cellulose and enhanced the production of low molecular

weight products as well as less formation of char. On the other hand, cellulose decreased the secondary char formation from lignin and improved the formation of some lignin-derived products including guaiacol, 4-methyl-guaiacol and 4-vinyl-guaiacol.

Besides pyrolysis kinetics, pyrolysis mechanism is another important area of inquiry, which deals with pathways of how reactants convert to intermediates, and then to final products via various reactions. Most research regarding thermal degradation of biomass has been focused on reactions conducted in aqueous solution. Thus, Shi *et al.* [124] proposed putative mechanism for the proton-catalyzed isomerization of glucose to fructose. Yang *et al.* [128] proposed a mechanism of glucose isomerization to fructose in $CrCl_3$-H_3PO_4 catalysis system (Figure 13). Caratzoulas *et al.* [169] gave a detailed description on the fructose dehydration mechanism. Amarasekara *et al.* [112] provided a potential mechanism on $ZnCl_2$ mediated degradation of cellulose to glucose (Figure 14).

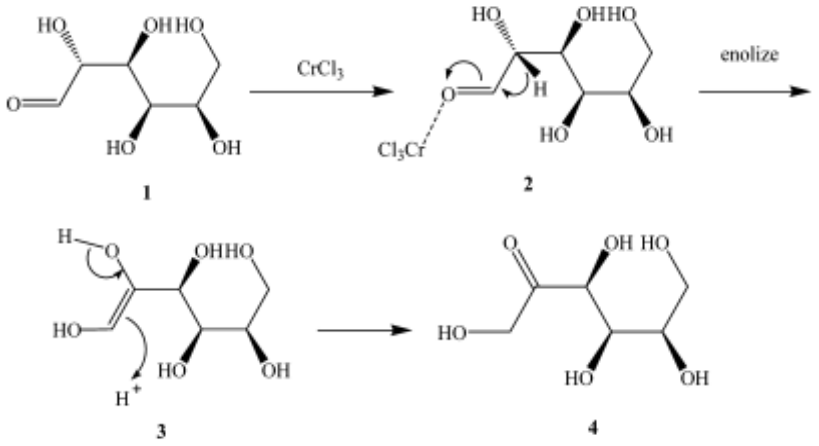

Figure 13 $CrCl_3$ aided catalytic conversion of glucose to fructose [128].

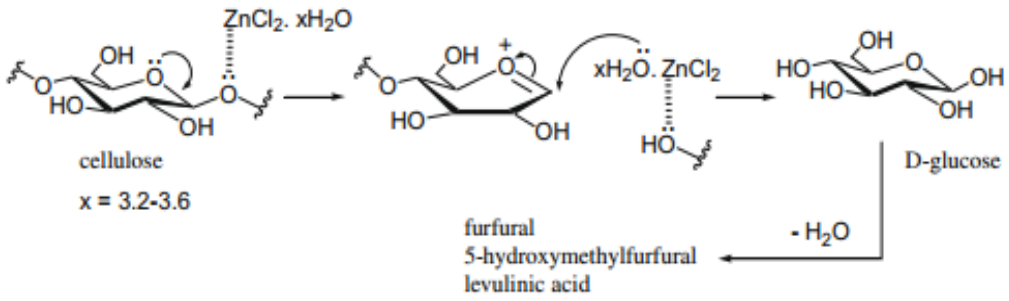

Figure 14: $ZnCl_2$ aided catalytic conversion of cellulose to glucose [112].

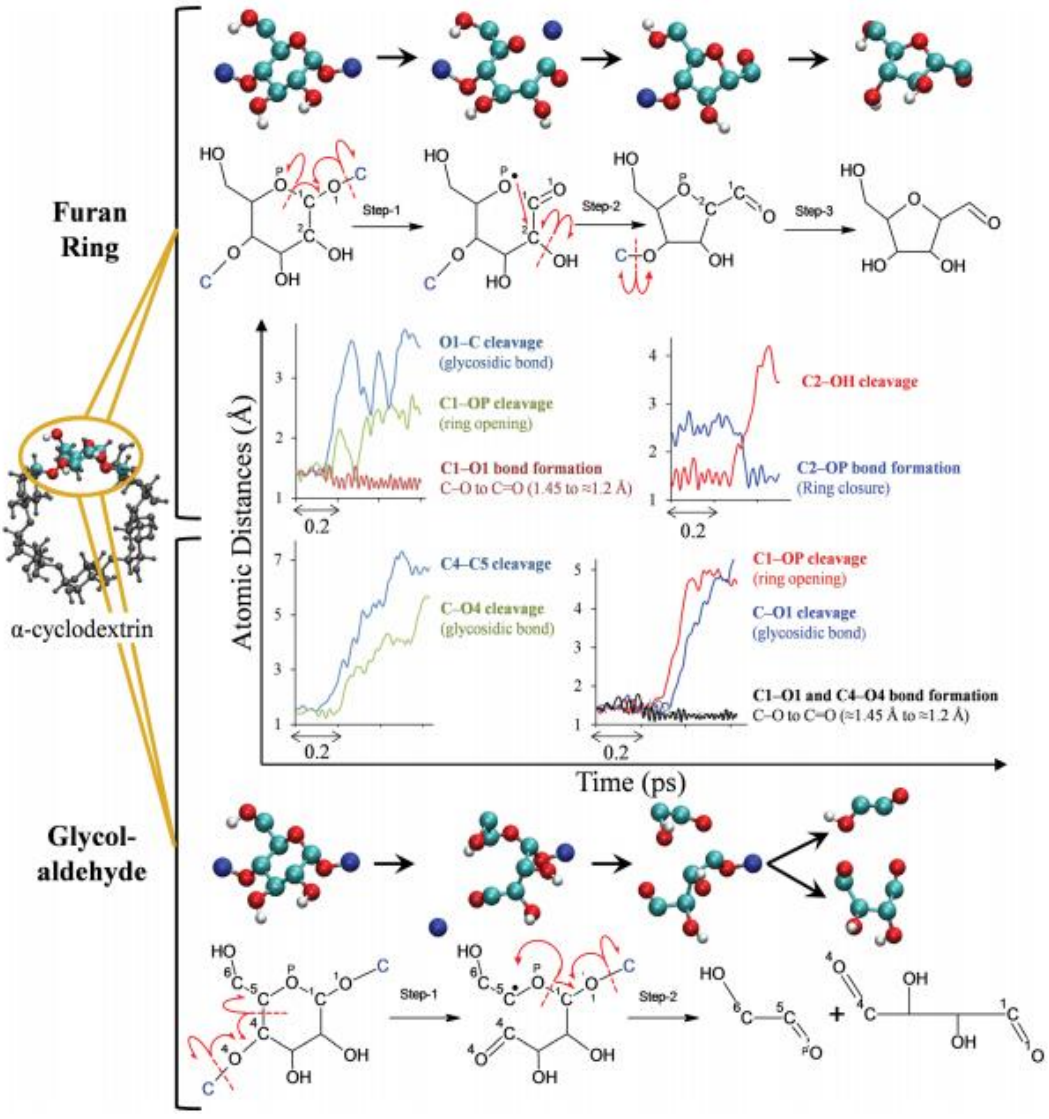

Figure 15: Reaction pathways of α-cyclodextrin (cellulose) pyrolysis [170].

Dauenhauer et al. [170] first revealed the pathways of condensed-phase pyrolysis chemistry via first-principles simulation method (Figure 15). For this purpose, they

identified α-cyclodextrin as an appropriate surrogate of cellulose to be investigated under pyrolysis condition. Several chemicals present in cellulose pyrolysis bio-oil can be formed directly without any small molecular intermediates such as glucose and levoglucosan. They showed that how furan rings, glycolaldehyde, 2, 5-dihydroxy-3-pentenal, 2, 3-hydroxy-4-pentenal, 4-hyroxy-2-butenal, formaldehyde, CO_2 and CO could be produced at molecular level. Additionally, both furan rings and glycolaldehyde formation are initiated by homolytic cleavage of glycosidic bonds, which mechanism is quite different from that in the aqueous phase. Similarly, Shen *et al.* [171] proposed possible routes for the formation of major products derived from pyrolysis conversion of cellulose (Figure 16 and 17).

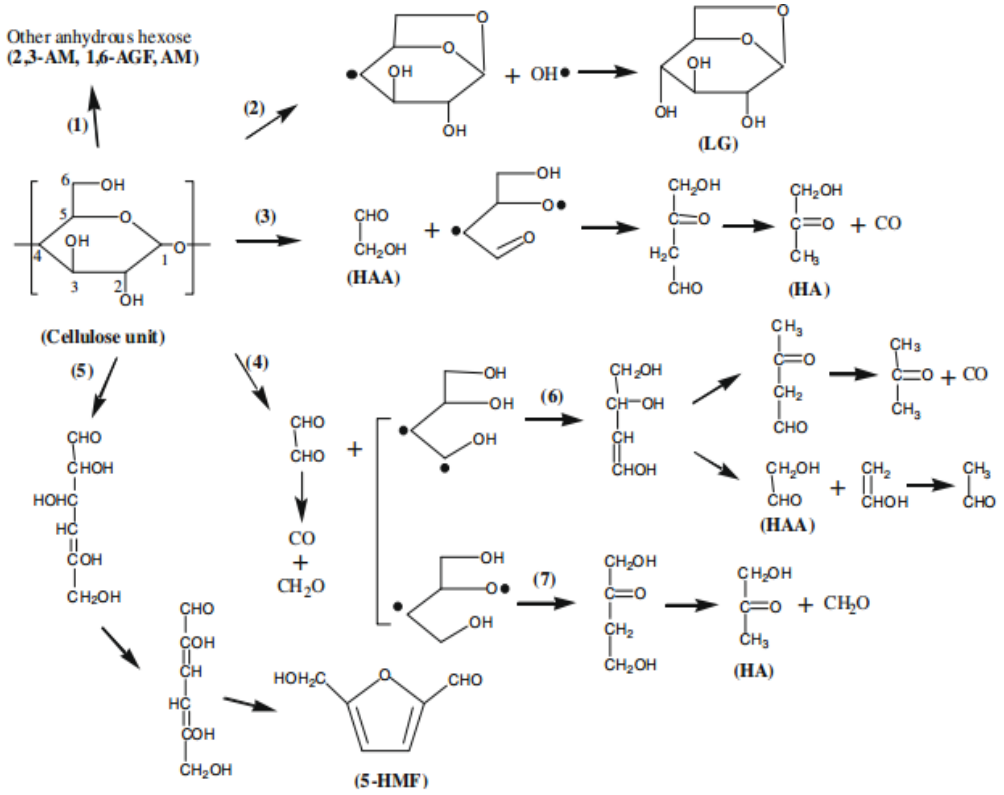

Figure 16: Pathways for direct conversion of cellulose unit to chemicals [171].

In contrast to cellulose, the other two components- hemicellulose and lignin involve much more sophisticated decomposition mechanisms due to their complex structures. Zhang *et al.* [172] proposed several potential opportunities to develop commercially feasible routes to extract and covert biomass lignin and hemicelluloses

for high-value applications along with biofuel production from cellulose. Since thermal depolymerization of lignin will inevitably produce complex mixture of chemicals due to a series of complicated and random reaction sequences, delignification before lignocellulosic biomass pyrolsis is very promising. Six main reactions involving lignin and peroxyacids interactions have been well demonstrated in pulp bleaching process, and the reaction mechanism could be a useful reference for lignin pyrolysis [173]. As for hemicellulose, a pre-extraction of hemicellulose from woody biomass is promising.

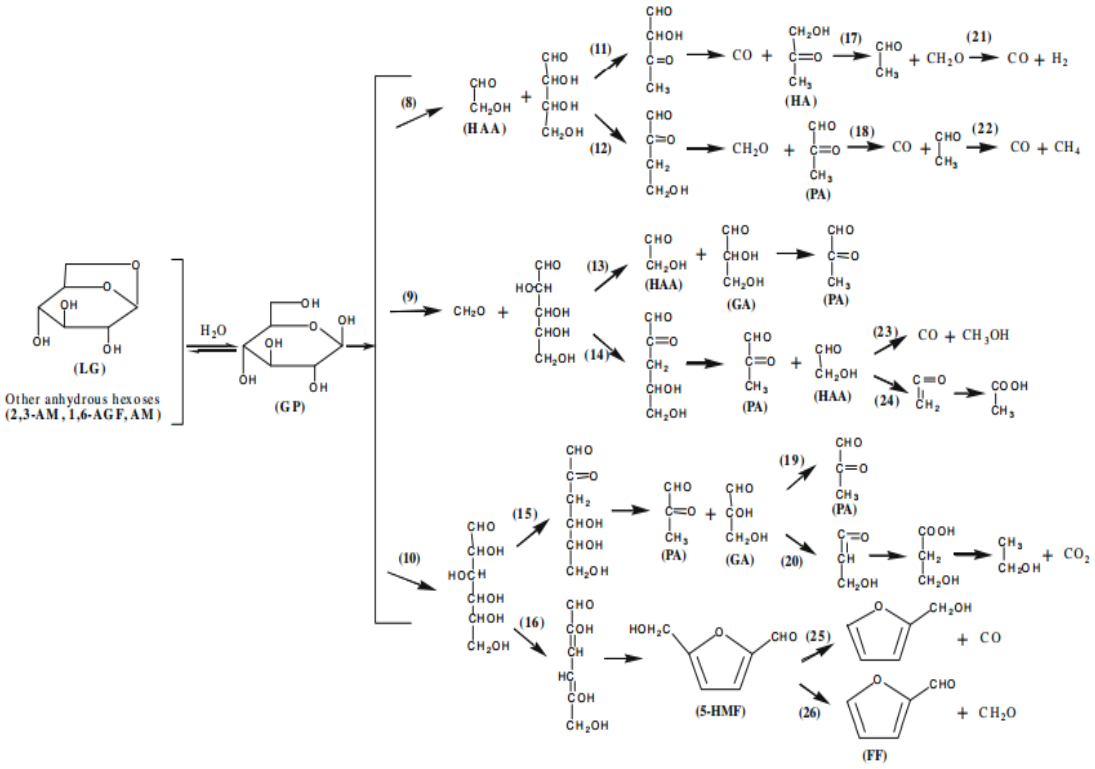

Figure 17: Pathways for direct conversion of LG to chemicals [171].

In summary, unlike cellulose conversions in aqueous solution which undergo reactions such as cellulose to glucose, isomerization of glucose to fructose and then decomposition of fructose to small molecules, pyrolysis of cellulose may directly convert cellulose unit to small molecules, such as HMF-5, furfural, and acetic acid. Currently, no mechanism of pyrolysis of lignocellulosic biomass has been proposed.

Chapter 3. Methodology

This chapter provides an overview of the experimental methodology. The specific goals of the experiment, materials used, molten salt selection, experimental setup and procedures, data acquisition, GC/MS and TGA experiment, and safety procedures are presented below.

3.1 Objectives

For experimental studies, the broad goals were to:

(1) Determine the optimal carrier gas flow rate for bio-oil production from real biomass, not surrogate molecules.

(2) Determine the best pyrolysis temperature for bio-oil production.

(3) Determine the optimal particle size of biomass for the pyrolysis process.

(4) Determine the best molten salts combination in order to obtain the highest yield of bio-oil. Salts under consideration are listed below:

Zinc chloride ($ZnCl_2$); Potassium chloride (KCl); Lithium chloride (LiCl); Sodium chloride (NaCl); Cuprous chloride (CuCl); Stannous chloride ($SnCl_2$); Magnesium chloride (MgCl); Aluminium chloride ($AlCl_3$)

(5) Determine the effects of various catalysts on yields of bio-oil. Catalysts under consideration are listed below:

Phosphomolybdic acid; ZSM-5; $Ni(OH)_2$;

(6) Determine the composition of bio-oil for various temperatures, molten salts, and catalysts

(7) Determine the yields and compositions of bio-oil produced from newspaper and recycled print paper.

(8) Kinetics study on thermal decomposition of biomass with molten salts and catalysts.

3.2 Materials

Three kinds of biomass were used in this project. They are: pinewood sawdust (Figure 18), newspaper (Figure 19), and recycled print paper (Figure 19). Pinewood sawdust was purchased from *American Wood Fibers*; newspaper feed use was the

WPI student newspaper, *The Towers*; recycled print paper was purchased from *W.B. Mason*. Raw sawdust was ground in electric mixer and sieved by different meshes. Both newspaper and print paper were manually cut by scissors into very tiny pieces with average surface area of 0.04 cm^2/ piece. No further drying pretreatment was applied to these biomasses.

Figure 18: Raw sawdust (left) and sawdust powder (<116 μm).

Figure 19: Newspaper sample (left) and print paper sample (right).

Chemicals used include: CuCl (ACS, purity> 96.8%, *Fisher Scientific*); $AlCl_3$ (anhydrous, GR, purity> 98.0%, *EMD*); NaCl (food grade salt, *MORTON SALT, INC*); ZSM-5 (GR, *ACROS*); $MgCl_2$ (anhydrous, purity> 96.8%, *EMD*); LiCl (GR, purity> 99%, *EMD*); KCl (GR, purity> 99%, *EMD*); $ZnCl_2$ (ACS, *EMD*); $Ni(OH)_2$

(*SIGMA-ALDRICH*); $SnCl_2$ (purity> 98%, *SIGMA-ALDRICH*); phosphomolybdic acid (ACS, *MP Biomedicals*)

Table 15. Chloride salts used in pytolysis of biomass.

Molten Salts	Molar Ratio	Melting Point (℃)
$ZnCl_2$-KCl-LiCl	40:20:40 [a]	240 [b]
$AlCl_3$-KCl	67:33	128 [c]
$AlCl_3$-NaCl	55:45	133 [d]
CuCl-KCl	65:35	150 [c]
$ZnCl_2$-KCl-NaCl	52.9:33.7:13.4	204 [e]
$ZnCl_2$-KCl-NaCl	60:20:20	203 [c]
KCl-LiCl-NaCl	36:55:9	346 [c]
KCl-LiCl-NaCl	24:43:33	357 [c]
KCl-$MgCl_2$-NaCl	28.75:43.75:27.5	383 [d]
$ZnCl_2$	-	283 [c]
$ZnCl_2$-KCl	70:30	262 [c]
$ZnCl_2$-NaCl	70:30	255 [d]
$ZnCl_2$- $SnCl_2$	70:30	/

a. These mole percentages are based on the molecular weight of the metal cation.
b. Measured by Drew Martino, a PhD candidate at WPI.
c. Data retrieved from https://books.google.com.ezproxy.wpi.edu/books?isbn=0323144837.
d. Data retrieved from http://factsage.com/
e. Data retrieved from http://proceedings.asmedigitalcollection.asme.org.ezproxy.wpi.edu/proceeding.aspx?articleid=1920627.

3.3 Molten Salt Selection

As chlorides molten salts gave the highest yield of bio-oil according to the previous studies conducted by MQP groups at WPI [7-9], in this project, only chlorides molten salts were used. The selection criterion of molten salts was based on their melting point, pyrolysis performance, and cost. Low melting point, high performance in bio-oil production and lower costs are preferable. Single chloride salts usually have very high melting points, such as potassium chloride melts at 770 ℃, sodium chloride

at 801 ℃, and lithium chloride at 605 ℃ [8]. Compared with single salt, the melting point of mixed salts is usually much lower, especially at some compositions corresponding to eutectic points. Through the use of a phase diagram such as, Figure 20, it is possible to find a suitable composition of a eutectic that will melt at a given temperature. Table 3 listed types of molten salts used in this project.

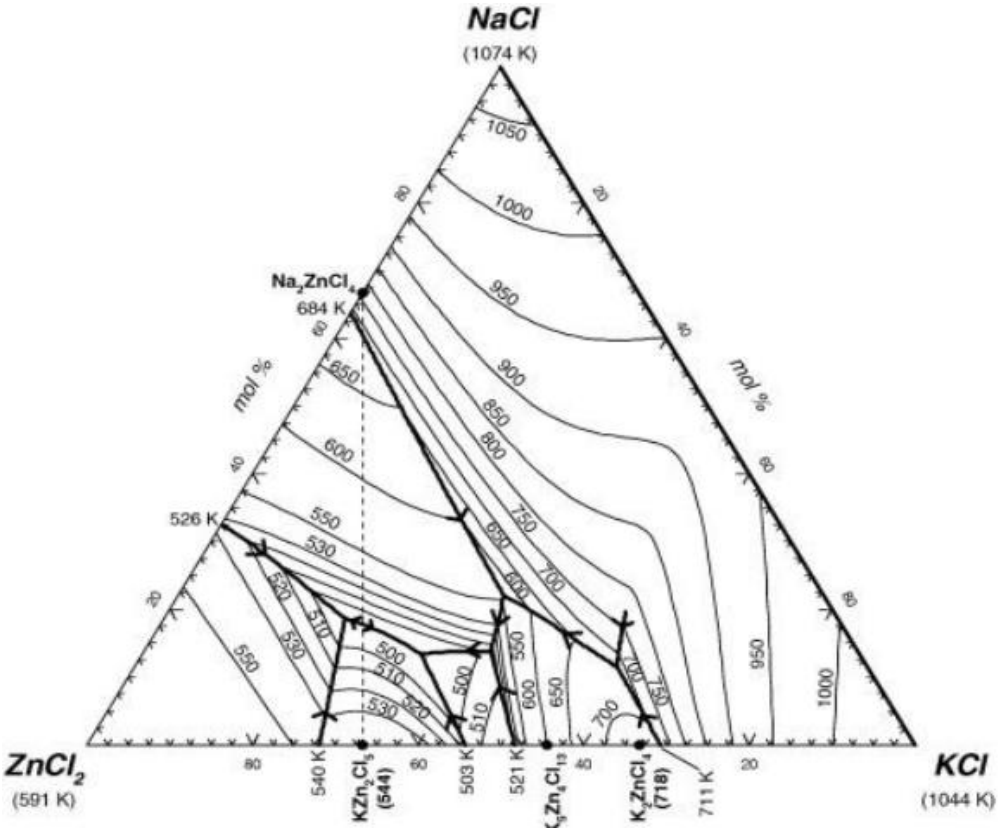

Figure 20: Ternary eutectic phase diagram [174].

All kinds of salts listed in Table 3 were tested in the pyrolysis reaction system. It was found that salt groups containing $AlCl_3$ and $MgCl_2$ were not suitable for pyrolysis in the proposed experimental setup. When $AlCl_3$ was used as molten salt component, the outlet of reactor released white smog over 100 ℃; carrier gas flow rate kept unstable irrationally; white powders were collected in the condensation flasks; strong smell of acid gas would be detected. This is due to the decomposition of $AlCl_3$ during the pyrolysis. Molten salts with $MgCl_2$ produced char/salt-contained bio-oil which resulted in yield of bio-oil higher than 100%.

For thermogravimetric analysis of sawdust MSCP, four groups of molten salts were

selected initially: CuCl-KCl, $ZnCl_2$-KCl-LiCl, $ZnCl_2$-KCl-NaCl, and KCl-LiCl-NaCl. Since the crucible used in TGA instrument is made of alumina, it was felt that some of these molten salts may react with alumina at high temperature, thus causing damage to the TGA instrument. So testing the reactivity of the four kinds of molten salts with alumina was first necessary. The results showed that CuCl-KCl molten salt did in fact corrode alumina tube in the test. As a result, CuCl-KCl was not used in thermogravimetric investigation of sawdust molten salt pyrolysis.

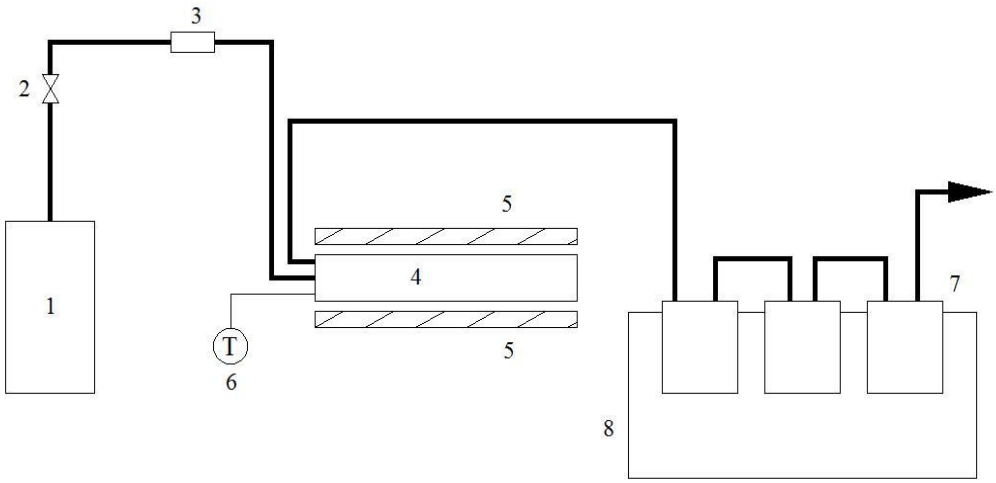

Figure 21: Pyrolysis process flow chart.
1-Helium gas tank; 2-Pressure control valve; 3-Gas flow meter; 4-Tubular reactor; 5-Furnace; 6-Thermocouple; 7-Bio-oil collection flasks; 8- Ice bath.

3.4 Experimental Setup and Procedures

In order to understand and improve the application of MSCP process with real natural biomass, many factors which affect the performance of MSCP process were tested, including carrier gas flow rate, pyrolysis temperature, types of biomass, reactor configuration, varying combinations and compositions of molten salts, reaction time, mass radio of biomass-to-molten salts and the performance of different catalysts. Although heating rate is a vital factor that affects the pyrolysis process, the influence of heating rate was not studies in this work, as it could not be precisely controlled in the current setup. The average heating rate used in experiment was 95 ±15 ℃/min.

As shown in Figure 21, a self-designed pyrolysis setup mainly consisted of a tubular reactor, an electric furnace, a condenser, a thermocouple, a gas flow meter, as

well as pressure indicator and control valve. The stainless steel tubular reactor (Figure 22) of 9/10 inch in inner diameter, 16.5 inches in length was set horizontally in consideration of the dimension of the furnace (TF55035A-1, *Thermo Scientific*). Glass wool was used to block the space between furnace and reactor at each end. Liquid yields tended to decrease sharply when the reactor was placed vertically, as heat loss occurred at the bottom. Three bio-oil collection flasks connected in series ensured that all volatile substances could be condensed at experiment conditions. An Ice bath was used for condensation. Two temperature indicators were used in experiment: the first one provided inner temperature of pyrolysis temperature via a thermocouple (JQIN-116U-18, *OMEGA Engineering*) which was inserted into the mixture of reactants; the second one displayed the temperature of outer wall of the reactor. Temperature in reactor was always 50 ℃ higher than that of exterior. Helium gas was chosen as the carrier gas for its inert characteristics.

Figure 22: Reactor tube.

The experiments consisted of a series of crucial steps as highlighted below. For each run, 5.0 g sawdust powder in a certain diameter range was placed into a mortar and pestle followed by addition of desired salts in sequence. The weight of sawdust and salts were massed on a scale (XL-5K, *Denver Instrument*) before mixing. The mixture was then ground thoroughly to guarantee a homogenous state. The mixing time should be appropriate for this: too short time would cause uneven composition; too long time would lead to absorption of water in the air by zinc chloride. Next, the whole mixture was transferred into the reactor. After putting the reactor back into the furnace, the helium gas tank was turned on and the whole reaction system was fully

saturated in helium to ensure an inert atmosphere. Before heating up to the pyrolysis temperature, the furnace was first set to 130 ℃ for 30 mins, in order to dry off water existing within the biomass and salts. Once the preheating was completed, the reactor was heated to the desired temperature at a desired rate. Once the final temperature was reached, the reaction was then allowed to proceed for about one hour. The volatiles were purged out by helium, whose flow rate could be controlled by gas flow meter. Then the carrier gas together with volatiles entered into condensation system cooled by ice bath, where volatiles condensed in three consecutive flasks. Once the reaction ended, the condensed oil was collected into a vial, weighted and kept in refrigerator. The reactor was also weighted after being cooled to room temperature in order to determine the mass of char. All the experiments were conducted at atmospheric pressure. Since huge amount of experiments were conducted in this work, not all runs were duplicated. Only parts of the experiments were repeated three times or more, and the data variability thus calculated is within 10%.

3.5 Data Acquisition

For each set of experiment, two different kinds of yields were calculated and recorded, i.e., total percent bio-oil yield and total char yield. In order to calculate liquid yield, the three flasks used were weighted before and after each run. Therefore, the liquid yield was equal to the difference between the masses of the three flasks divided by the mass of sawdust used (Eq. 1).

$$\frac{\text{Mass of flasks after} - \text{Mass of flasks before}}{\text{Mass of sawdust charged}} \times 100\% = \text{Percent liquid yield} \quad (1)$$

Similarly, the char yield (Eq. 2) was determined by the difference between the mass of original feed and mass of violates (both condensable and non-condensable). The mass of violates was calculated by the difference between mass of reactor plus load before and after. Load here contains both salts and feedstocks.

$$\left(1 - \frac{\text{Mass of reactor plus load before} - \text{Mass of reactor plus load after}}{\text{Mass of sawdust charged}}\right) \times 100\%$$

$$= \text{Percent char yield} \quad (2)$$

Finally, the non-condensable gas yield was obtained by simple subtraction (Eq. 3).

$$1 - \text{Percent liquid yield} - \text{Percent char yield} = \text{Percent gas yield} \quad (3)$$

3.6 GC-MS Analysis Methods

The liquid product contained organic oil and water. A Gas Chromatograph- Mass Spectrometer (GC-MS) was used to determine the individual chemical substances in the bio-oil obtained from pyrolysis of biomass. Agilent 7890 GC was used along with Agilent HP-5MS 30 m × 0.25 mm × 0.25 μm column and Agilent 5183-4637 (870 μL) split inlet liner. Other parts used were Agilent 5975C VL MSD with Triple Axis Detector and Inert EI source, as well as Agilent G453A auto-sampler tower with Agilent G4514A 150 sample tray.

Each liquid sample was firstly transferred to Thompson 35540 filter vials in order to be filtered of any solid carbon residue present in the sample. Then prepared samples were placed into the sample tray and the operation parameters for the auto analysis process were set. The split ratio was set to 100:1; helium carrier gas flow rate was 54 mL/ min. The temperature programming for GC was set as follows: the column oven first rose to 50 ℃ and kept for 10 mins. Then the temperature was increased to 180 ℃ at a heating rate of 5 ℃/ min. Once up to 180 ℃, the temperature went up to a final temperature of 300 ℃ at a heating rate of 15 ℃/ min. After passing through GC, each separate substance entered the MS, where each substance was fragmented into various ions of different mass-to-charge ratios. Then each ion was recorded in a plot of mass spectra. Finally, the original chemical could be identified by comparing the mass spectra with standard mass spectra in MS database. The operation parameters for MS were set as follows: the MS source was kept at 230 ℃ and the MS quad held at 150 ℃; the scan mode for the MS was m/z 5-500. The total run time for one sample was about 45 mins.

The chemicals in bio-oil could hence be identified by MS and quantified by GC. However, the percentage report of GC only gave the percent area of each substance in bio-oil. Percent mass could be more accurate the percent area. In order to obtain percent mass of each substance, calibration was prepared. In this study, only three main components in bio-oil were calibrated, they were water, furfural, and acetic acid,

as these were the main products in many experiments.

3.7 TGA Experiment

TGA experiments were conducted by using the Netzsch 209 F1 Libra with Al_2O_3 85 μL crucible. Before each run, the crucible must be burned out for several seconds until it glowed. This step was necessary to ensure that no organic chemicals residue remained in crucible. After the crucible cooled down, the crucible was weighed and recorded. Then the sample was loaded into the crucible and weighed again. Next the experiment was commenced. The temperature program for this experiment was to start temperature at 30.0 ℃ and end temperature at 700 ℃ with a heating rate of 10 K/min. Finally, data was analyzed by software Proteus Analysis.

3.8 Safety Procedures

As high temperature operation environment, high pressure gases, some delicate instruments and many corrosive chemicals were involved in this project, extreme caution should be exercised during the whole experimental process. Inattentive operation could lead to great danger to both people and instrument. So laboratory safety training was of crucial importance before conducting research in the lab.

When dealing with high temperature procedures, heat resistant gloves must be worn and hawkbill might be used in some cases. Another notice was to keep hot substance away from people, flammable and heat-sensitive matters. With respect to chemicals, lots of attention should be given: stored various chemicals properly in case of light, temperature, humidity, etc.; wear latex gloves and lab clothing all the time when exposed to dangerous chemicals; chemical wastes should be handled properly.

All experiment operations should be abided by the regulations. In pyrolysis experiment, every tiny error might contribute to wrong results; In TGA experiment, special attention should be given to the procedures. Wrong steps could cause severe damage to the instruments.

Chapter 4. Results and Discussion

In this chapter, the results are mainly divided into four parts: yield of bio-oils, composition/selectivity of bio-oils, kinetics studies on thermal degradation of biomass and preliminary study on pyrolysis of newspaper and print paper. The feedstocks used in the first three parts were limited to sawdust only. In the first part, the sequence of results is organized by first illustrating the effects of gas flow rate, temperature and particle size. Then the effects of varied combinations of different chloride molten-salts and varied compositions of certain molten-salt eutectic are demonstrated. Finally, the influence of catalysts is investigated.

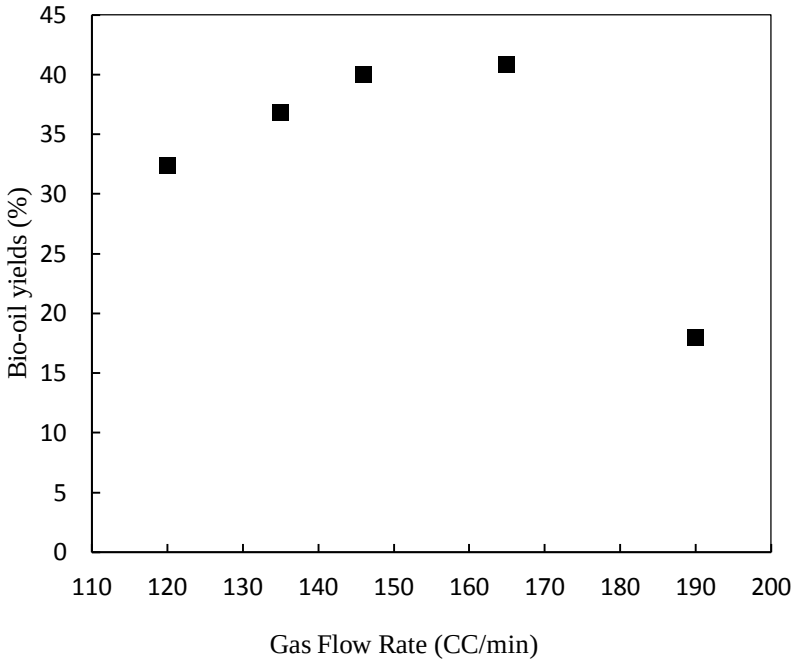

Figure 23: Bio-oil yield at various carrier gas flow rates.

(Condition: Feed: 5 g sawdust; Molten salt: $ZnCl_2$ (40% mol), KCl (20% mol), LiCl (20% mol); Temperature: 350 ℃; Mass ratio of feed to molten salt: 1:10; Particle size: 106-212 μm)

4.1 Optimizing Bio-oil Yield

4.1.1 Carrier Gas Flow Rate

Few publications discuss the effect of gas flow rate on the yield of bio-oil. N_2, H_2, helium and even steam could be utilized as the carrier gas. In this work, helium gas was selected for its inert properties. The carrier gas has three main functions in pyrolysis process: first, take the volatiles formed away from the reactor; second,

exclude oxygen to provide an inert environment for the pyrolysis; third, the gas could bubble in the reaction mixture to make heat and mass transfer more efficient.

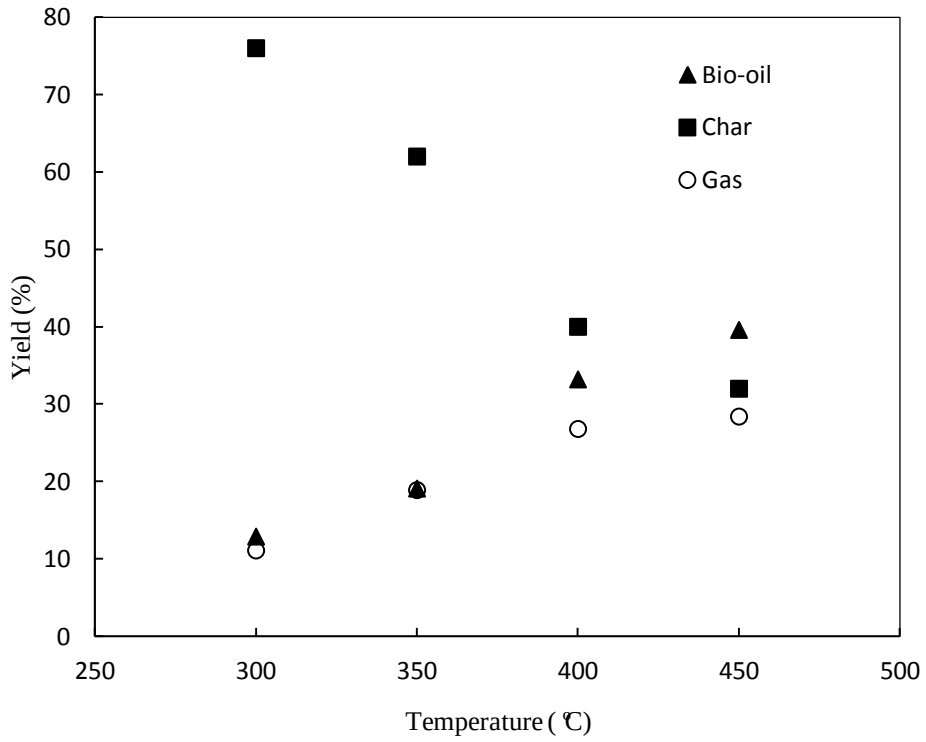

Figure 24: Temperature effect on yield of products without molten salts.

(Condition: Feed: 5 g sawdust; Flow rate: 165 CC/ min; Particle size: 106-212 μm.)

Figure 23 shows the yield of bio-oil at different carrier gas flow ratse. Changing gas flow rate directly affects the volatiles residence time in the reactor. The higher flow rate simply residence times for the primary products in the reactor, so that the higher bio-oil yield might be expected, as the second cracking reaction and repolymerization would be inhibited. However, as shown in Figure 23, there existed an optimal value rather than a monotonic increase. Two possible reasons might explain this phenomenon at high flow rate: one is the flow rate was too high for a reasonable residence time for the decomposition reactions; the other is due to the limited condensation efficiency, bio-oils might not be condensed totally at higher flow rates. Experimental results showed that at the highest flow rate under investigation (190 CC/min), all the three flasks collected oils which means some volatiles might be blown away. Thus, the second reason above appears likely. So the flow rate of 165

CC/min was chosen as the best for this system and was hence set as a fixed flow rate for subsequent experiments.

4.1.2 Pyrolysis Temperature

Figure 24 shows that temperature had a great impact on the products yields in absence of molten salts. The yield of char was reduced sharply from 76 to 32% as the temperature was increased from 300 to 450 ℃. This indicated that char formation was favored at lower temperatures. The gas content increased from 11.1 to 28.4 % with this increase in temperature. Similarly, the yield of bio-oil also increased from 12.9 to 39.6 % in the same temperature range. Clearly, the increase rated of bio-oil yield with temperature was faster than that of gas, which indicated that the loss mass of char mainly contributed to the formation of bio-oil compared with gas, as the temperature rose.

Typically, a maximum liquid yield could exist with monotonic increasing of gas yield and monotonic decreasing yield of char, since higher temperature improved volatiles' decomposition to gas. However, the maximum liquid yield didn't appear in this experiment for the reason that the maximum liquid yield from biomass usually occurs over 500 ℃ which was beyond the range of temperatures investigated in this work. An assumption might be made that if temperature was elevated to above 500 ℃, an optimal value might appear. Although the highest yield was obtained at 450 ℃, the main temperatures under investigation in this work were 350 ℃ and 400 ℃, as a goal of the MSCP is to reduce the operating temperature of pyrolysis process.

4.1.3 Particle Size

Another important factor in determination of bio-oil yield is the particle size of biomass material and discussion about this is rarely presented in previous literatures. Four groups of sawdust with different particle size range were tested. The mass of sawdust in each run was 5 g and the reaction was conducted at carrier gas flow rate of 165 CC/min and at a temperature of 350 ℃. Table 4 shows the effect of particle size of biomass on bio-oil yield without molten salts. Theoretically, the finer the particle

size that biomass has, the higher the bio-oil yield should be. Since sawdust itself is not a good thermal conductivity material, fine particle size biomass has the ability of transferring heat to its inner core faster than the bigger particle size biomass, which favors the formation of bio-oil. Moreover, smaller particles show better mass transfer characteristics than bigger particle size biomass, which means the products produced could leave the particle faster. However, results of this study showed that particle size between 106-212 μm gave slightly higher yield than the finest particle size, lower than 106 μm in the experiment. Of course it may be that a plateau is reached at 106-212 μm particle size, and smaller particle size does not increase the bio-oil yield.

Table 16. Effect of particle size on yield of bio-oil without molten salt.

Particle size (μm)	Yield (%)
<106	18.6
106-212	19.1
300-450	14
600-850	13.8

In order to get more information about the effect of particle size in the presence of molten salts, two types of molten salts were added into the reaction system. Figure 25 shows the improvement of addition of molten salts on the bio-oil yield. Compared with Table 2, 32.6% yield was obtained with CuCl-KCl molten salts for the particle size between 106-212 μm, while only 19.1% was attained without molten salts at the same temperature. This improvement was even more significant for the particle size lower than 106 μm, i.e., 41% with molten salts and 18.6% without salts. In the persence of CuCl-KCl molten salts, biomass of particle size between 106-212 μm exhibited lower yield of bio-oil than that of particle size < 106 μm. This finding not only proved that fine particle should produce high yield of bio-oil, but also illustrated that the advantage of molten salts. Thus, biomass particles would be evenly distributed within a molten salt solvent which could suppress the possible agglomeration of fine particles in the absence of molten salts. The ternary molten salts,

$ZnCl_2$-KCL-LiCl also had the same function and gave higher yield below 450 ℃.

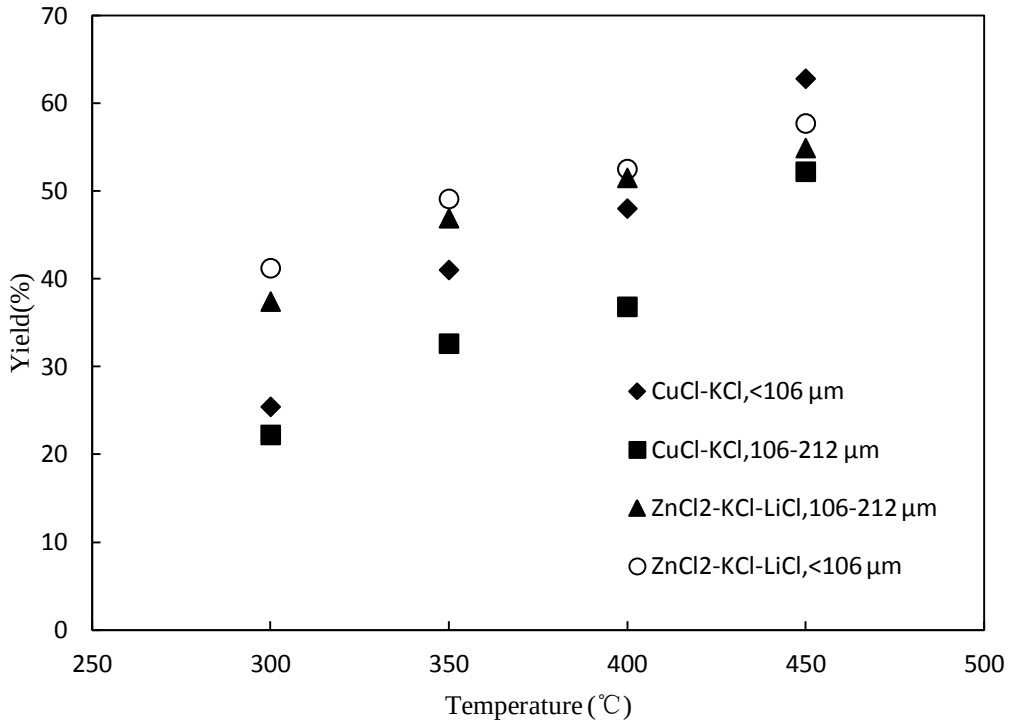

Figure 25: Effect of particle size on the liquid yield based on different salts combinations.

(Condition: Feed: 5 g sawdust; Flow rate: 165 CC/min; Mass ratio of feed to molten salt: 1:10; Diamond: CuCl (65% mol), KCl (35% mol), particle size: <106 μm; Square: CuCl (65% mol), KCl (35% mol), particle size: 106-212 μm; Triangle: $ZnCl_2$ (40% mol), KCl (20% mol), LiCl (20% mol), particle size: <106 μm. Circle: $ZnCl_2$ (40% mol), KCl (20% mol), LiCl (20% mol), particle size: 106-212 μm.) Mole percentages in $ZnCl_2$- KCl- LiCl were based on the molecular weight of the metal cation.

In Figure 25, it's shown that biomass of smaller particle size gave higher bio-oil yield no matter what type of molten salt was used and what temperature it is. $ZnCl_2$-KCl-LiCl molten salts performed better than CuCl-KCl molten salts when temperature was at 300 ℃, 350 ℃ and 400 ℃, while at 450 ℃, the situation was reversed. At 300 ℃, the difference between the highest and lowest yield was 19%, while at 450 ℃ this difference changed to 10.6%, which indicates that different types of molten salts play a more important role at lower temperatures than that at higher temperatures. Besides, the difference of bio-oil yields from different particle size in CuCl-KCl molten salts was larger than that in $ZnCl_2$-KCl-LiCl molten salts.

4.1.4 Varying Composition of $ZnCl_2$-KCL-LiCl Molten Salt

The molten salt group of $ZnCl_2$-KCl-LiCl had been proved to be effective in pyrolysis of cellulose in previous MQP study [8]. In this project, a systematic study on the effect of varying compositions of this type of molten salt on bio-oil yield from sawdust was carried out. The results of the effect of varying compositions of $ZnCl_2$-KCl-LiCl on bio-oil yield are presented in Table 5. For each run, 5 g sawdust with particle size of 106-212 μm was used. The reaction was carried out at 400 ℃ with carrier gas flow rate of 165 CC/min. The molar ratio used in Table 5 was in the format of $ZnCl_2$: KCl: LiCl and based on the molecular weight of the metal cation. The mass ratio of feed to molten salts was set to 1: 10.

Table 17. Effect of composition of molten salt on bio-oil yield.

Molar ratio $ZnCl_2$:KCl:LiCl	Liquid yield (%)	Molar ratio $ZnCl_2$:KCl:LiCl	Liquid yield (%)	Molar ratio $ZnCl_2$:KCl:LiCl	Liquid yield (%)
4:2:1	54.9	4:0.2:4	20.7	3:2:4	53.4
4:2:2	57.5	4:0.5:4	56.1	5:2:4	66.5
4:2:3	56.6	4:1:4	51.5	6:2:4	58.2
4:2:4	51.5	4:3:4	50.1	7:2:4	58.3

In this section, the different compositions were selected arbitrarily, as no phase diagram for $ZnCl_2$-KCl-LiCl was available. The only data could be found out was the minimum melting point at a specific combination of each salt component, a tiny change in composition might alter the melting point greatly, which could result in solid phase in the reactor. This could explain why there was an extremely low yield of 20.7 %, when the molar ratio was 4:0.2:4 in Table 5. In contrast, the highest yield was 66.5% with the group of $ZnCl_2$ (5)-KCl (2)-LiCl (4). As shown in column 1 in Table 5, if the molar ratio of $ZnCl_2$ to KCl was kept unchanged, the yield of bio-oil had an optimal value with an increase of LiCl content. The same trends occurred if the molar ratio of $ZnCl_2$ to LiCl or KCL to LiCl remained unchanged, with a gradual increase in KCl or $ZnCl_2$, respectively. Furthermore, the highest three yields obtained with molar ratio of 5:2:4 (yield of 66.5%), 7:2:4 (yield of 58.3%), and 6:2:4 (yield of 58.3%)

indicated that relative high concentration of $ZnCl_2$ (a Lewis acid) could improved the yield of bio-oil. Undoubtedly, changes of composition lead to variation of salts properties such as melting point and thermal conductivity, along with Lewis acidity. The contributions of these changes on yield are still unclear.

4.1.5 Dosage of Catalyst

In this work, whether the amount of a catalyst could affect the yield of bio-oil during pyrolysis of sawdust was investigated and the results were presented in Figure 26. The three different dosages of catalyst gave the same yield of bio-oil when phosphomolybdic acid was used as the catalyst. The result showed that the yield of bio-oil was independent of the mass of the catalyst used in this case.

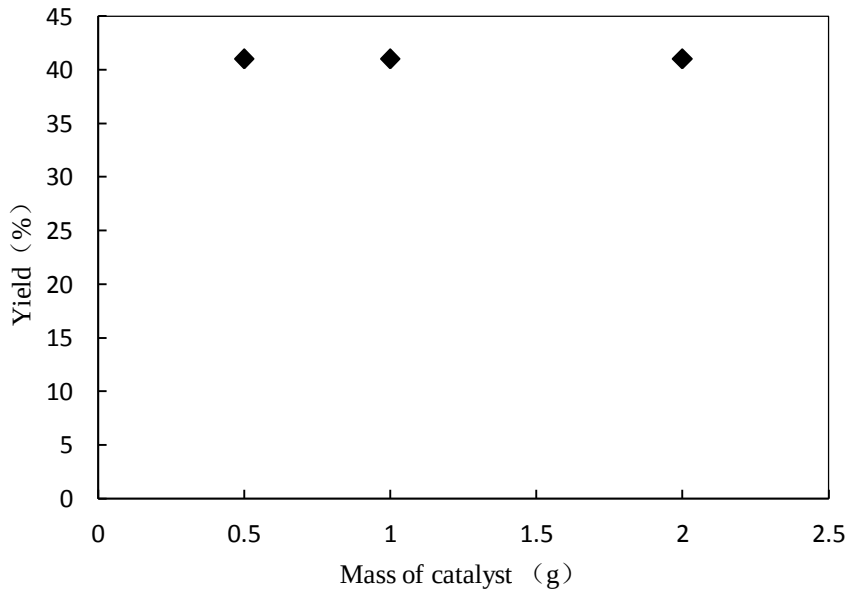

Figure 26: Effect of mass of catalyst on bio-oil yield.

(Condition: Feed: 5 g sawdust; Molten salt: CuCl (65% mol), KCl (35%); Flow rate: 165 CC/min; Temperature: 350 ℃; Mass ratio of feed to molten salt: 1:10; Particle size: 106-212 μm.)

4.1.6 Effect of Catalyst on Yield in different Molten Salts System

Figure 27 gives a good demonstration of the enhancement of bio-oil yield with addition of molten salts and catalysts at four selected temperature. The results show that molten salts could improve the bio-oil yield significantly no matter whether a

catalyst is added or not. The group of $ZnCl_2$-KCl-LiCl together with phosphomolybdic acid provided the highest yield at all temperature range. Especially at 300 ℃, the yield was increased by a factor of 4 over the case of pyrolysis without molten salt. It could hence be concluded that molten salts not only act as effective solvents, but also provide catalysis function in the pyrolysis of biomass as $ZnCl_2$ is a Lewis acid. Brønsted acid such as phosphomolybdic acid can also catalyze pyrolysis of biomass. Thus, the introduction of phosphomolybdic acid to the molten salts reaction system further improved the liquid yield (Figure 27).

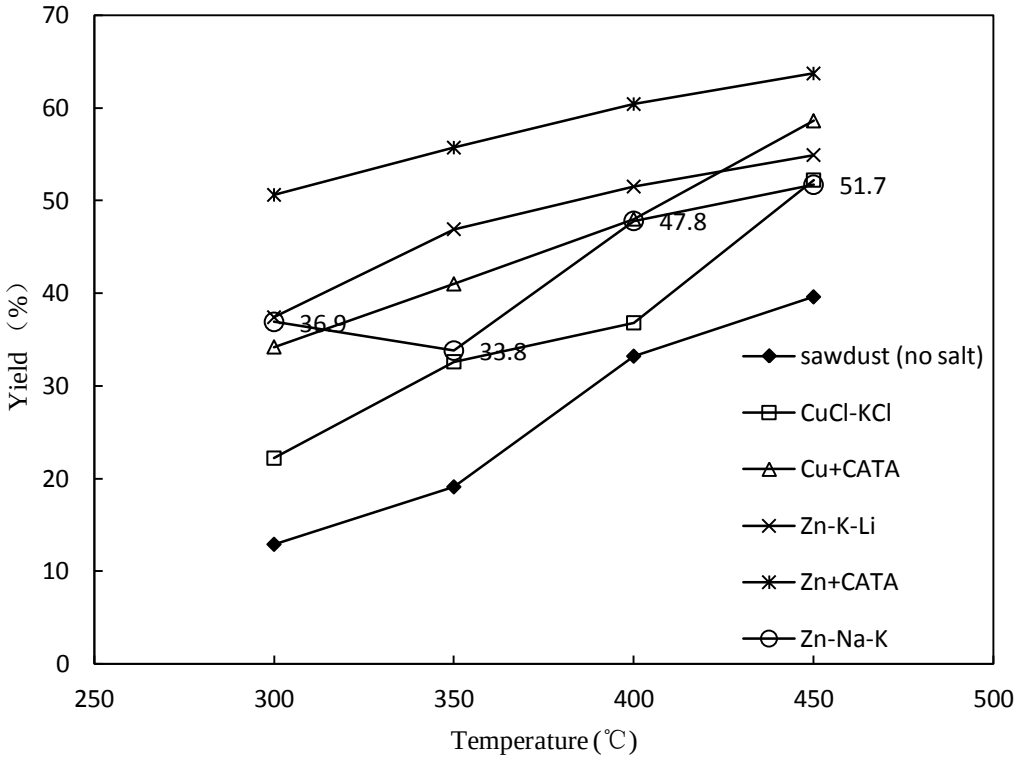

Figure 27: Yield dependency on temperature with varied salts combination and catalyst.

(Condition: Feed: 5 g sawdust; Flow rate: 165 CC/min; Mass ratio of feed to molten salt: 1:10; Particle size: 106-212 μm. Diamond: no molten salt; Square: CuCl (65% mol), KCl (35%mol); Triangle: CuCl (65% mol), KCl (35%) + 2 g phosphomolybdic acid; Crossing: $ZnCl_2$ (40% mol), KCl (20% mol), LiCl (20% mol), molar ratio based on the molecular weight of the metal cation; Asterisk: $ZnCl_2$ (40% mol), KCl (20% mol), LiCl (20% mol) + 1 g g phosphomolybdic acid, molar ratio based on the molecular weight of the metal cation; Circle: $ZnCl_2$ (52.9% mol), KCl (33.7% mol), NaCl (13.4% mol).)

Generally, the performance of $ZnCl_2$-KCl-LiCl was better than CuCl-KCl, with the exception for temperature at 450 ℃. The result confirmed that CuCl-KCl favored

high temperatures. Another ternary molten salt $ZnCl_2$-KCl-NaCl was tested in which LiCl was substituted by NaCl, a cheaper kind of salt. The overall performance of $ZnCl_2$-KCL-NaCl fell in between $ZnCl_2$-KCl-LiCl and CuCl-KCl, and its behavior was close to $ZnCl_2$-KCl-LiCl. The irregular point at 350 ℃ for $ZnCl_2$-KCl-NaCl might be due to the experimental error. Still when temperature was at 450 ℃, the differences among all groups of molten salts became smaller. This observation was quite similar to the results derived from Figure 25. Nonetheless, the highest yield at 450 ℃ with $ZnCl_2$-KCl-LiCl molten salt plus phosphomolybdic acid was 63.7% which was much higher than 39.6% without molten salt at 450 ℃.

Table 18. Effect of combination of different molten salts (yield 1) and addition of catalyst (yield 2) on bio-oil yield.

Molten salt	Yield 1	Yield 2
Cu-K	36.80%	48%
Zn-K-Li	51.50%	60.40%
Zn-Na-K	47.80%	51.60%
Zn-Na-K[1]	46.70%	54.60%
K-Li-Na	36.20%	43.00%
K-Li-Na[1]	39.50%	46.00%

(Condition: Feed: 5 g sawdust; Flow rate: 165 CC/min; Mass ratio of feed to molten salt: 1:10; Particle size: 106-212 μm; Temperature: 400 ℃. Cu-K: CuCl (65% mol), KCl (35% mol); 2 g phosphomolybdic acid was used as catalyst; Zn-K-Li: $ZnCl_2$ (40% mol), KCl (20% mol), LiCl (20% mol), molar ratio based on the molecular weight of the metal cation; 1 g phosphomolybdic acid; Zn-Na-K: $ZnCl_2$ (52.9% mol), NaCl (13.4% mol), KCl (33.7% mol); 1 g phosphomolybdic acid; Zn-Na-K[1]: $ZnCl_2$ (60% mol), NaCl (20% mol), KCl (20% mol); 1 g phosphomolybdic acid; K-Li-Na: KCl (36% mol), LiCl (55% mol), NaCl (9% mol); 1 g phosphomolybdic acid; K-Li-Na[1]: KCl (24% mol), LiCl (43% mol), NaCl (33% mol); 1 g phosphomolybdic acid.)

$ZnCl_2$, KCl, LiCl and NaCl are the most used molten salt components, and selected ternary combination from the four components was investigated for pyrolysis process. As seen in Table 6, yield 1 represented bio-oil yields obtained without catalyst, while yield 2 represented bio-oil yields obtained with phosphomolybdic acid catalyst. In most cases shown in Table 6, ternary molten salt provided higher bio-oil yield than binary molten salt. The groups containing $ZnCl_2$ gave higher yield than those without

$ZnCl_2$. In $ZnCl_2$ containing salts, the one with LiCl showed higher yield than the ones with Na. In $ZnCl_2$-NaCl-KCl ternary system, two different compositions groups didn't show much difference in yields. However, in KCl-LiCl-NaCl ternary system, increasing NaCl content tended to give higher yield. When catalyst was introduced into molten salts system, the yield for each group increased. In $ZnCl_2$-NaCl-KCl groups, the one with higher $ZnCl_2$ content gave higher yield than the one with lower $ZnCl_2$ content.

There was an interesting observation that when phosphomolybdic acid was added into reation system, the yields increased were always kept at around 10% in absolute value no matter what the reaction system is.

Table 19. Effects on different kinds of catalyst on bio-oil yield in a KCl-LiCl-NaCl molten salt.

Catalyst No.	Yield (%)
None	39.5
1	46
2	48.3
3	48
4	37.4
5	42.1
6	47.8
7	43.5

4.1.7 Effect of Different Catalysts

The final aspect studied in this work about bio-oil yield was to investigate the effect of different types of catalyst on the yield of bio-oil, and the results were shown in Table 7. For each run, 5 g sawdust with particle size of 106-212 μm was used. The reaction was carried out at 400 ℃ with carrier gas flow rate of 165 CC/min. The molten salts used was KCl (24% mol): LiCl (43% mol): NaCl (33% mol), i.e., without $ZnCl_2$. The mass ratio of feed to molten salts was set to 1: 10. Catalyst 1 was 1 g of phosphomolybdic acid; catalyst 2 was 1g $ZnCl_2$; catalyst 3 was 0.5 g

phosphomolybdic acid + 0.5 g $ZnCl_2$; catalyst 4 was 1 g $SnCl_2$; catalyst 5 was 0.5 g phosphomolybdic acid + 0.5 g $SnCl_2$; catalyst 6 was 1 g $Ni(OH)_2$; catalyst 7 was 1 g ZSM-5.

Thus, Brønsted acid catalyst (phosphomolybdic acid), Lewis acid catalyst ($ZnCl_2$, $SnCl_2$, and ZSM-5), and base catalyst ($Ni(OH)_2$) were tested. Almost all types of catalysts had a positive effect on improving liquid yield except for $SnCl_2$. Catalyst 2, 3, and 6 gave higher liquid yield than others, indicating that $ZnCl_2$ and $Ni(OH)_2$ were preferable in pyrolysis of sawdust. For catalyst 1,2, and 3, it could be concluded that $ZnCl_2$ played more important role in catalytic pyrolysis of sawdust than phosphomolybdic acid. For catalyst 3 and 4, both acted as Lewis acid catalysts, however, the performances were quite different. $ZnCl_2$ was better than $SnCl_2$ in the pyrolysis process, even below the performance without catalyst. The probable explanation could be that the $SnCl_2$ was kept in pieces rather than powders stored in the bottle. These pieces configurations made $SnCl_2$ very difficult to be ground into tiny particles.

Apparently, $ZnCl_2$ and $Ni(OH)_2$ catalyzed bio-oil formation reaction performed the best, however, water content was not excluded from bio-oil. Considering $ZnCl_2$ would produce more water, so the best catalyst for the highest yield of organic bio-oil needs to be determined by considering the compositions of the samples.

4.1.8 Other Miscellaneous Factors

Reaction time- The reaction time for all the samples was set 2 hours. Major volatiles come out in the first 30 mins, and remaining oil could be condensed within the subsequent 75 mins. No oil comes out after that for at least 15 mins, so that the total reaction time was set 2 hours.

Mass ratio of sawdust to molten salts- The mass ratio of sawdust to molten salts was set as 1 to 10 in all the experiment. This value was determined by pervious work done by WPI research group [7-9]. The ideal condition was that biomass would be fully immersed into the molten salt medium with the least amount of molten salt and a relatively high bio-oil yield.

Mass of sawdust- Due to the limitation of the reactor size and the mass ratio mentioned above, both 4g and 6 g of biomass were also tested with mass ratio of sawdust to molten salts set as 1: 10. Neither one provided a higher yield than that when 5 g was used under the same condition. When 4 g was used, the residence time of volatiles was too long, when secondary cracking reactions happen. When 6 g was used, the mixture of biomass and salts filled nearly all the space in the reactor, so that volatiles had difficulty coming out from reactor, which suppressed the formation of bio-oil.

Reactor orientation- The furnace used in this project could only heat the reactor in horizontal orientation effectively. When turned the reactor and furnace vertically, the bottom part could not be heated efficiently which could leave unreacted residue in the reactor.

Table 20. Selected samples for GC-MS composition analysis.

No.	Temperature/ ° C	Molten salt	Molar ratio of salt	Yield/ %
1	350	-	-	18.4
2	400	-	-	31.7
3	450	-	-	41.1
4	400	Cu,K	65:35	37.2
5	400	Zn,Na	70:30	53.3
6	400	Zn,k	70:30	52.2
7	400	Zn,Na,K	52.9:13.4:33.7	49.0
8	400	K,Li,Na	24:43:33	38.7
9	400	Zn,K,Li	4:2:4	51.5
10	400	Zn,K,Li	5:2:4	66.5
11	400	Zn,K,Li	6:2:4	58.2
12	400	Zn,K,Li	4:0.5:4	56.1
13	400	Zn,K,Li	4:2:1	54.9

4.2 Compositions of Bio-oils

The second major part of this project is to have a basic understanding of the effect of molten salts on the bio-oil composition both qualitatively and quantitatively (Appendix A). Figure 28 shows some bio-oil samples obtained from pyrolysis of sawdust. Gas chromatography–mass spectrometry (GC-MS) is an ideal analytical method to determine the composition of the samples that were produced. Identification of products distribution was characterized by retention time in GC graph, as well as mass fragmentation patterns in comparison with those of in database library. Product percentages were determined directly by percent area of each component peak in GC graph, where area percentage was generated by computer software controlling the GC-MS.

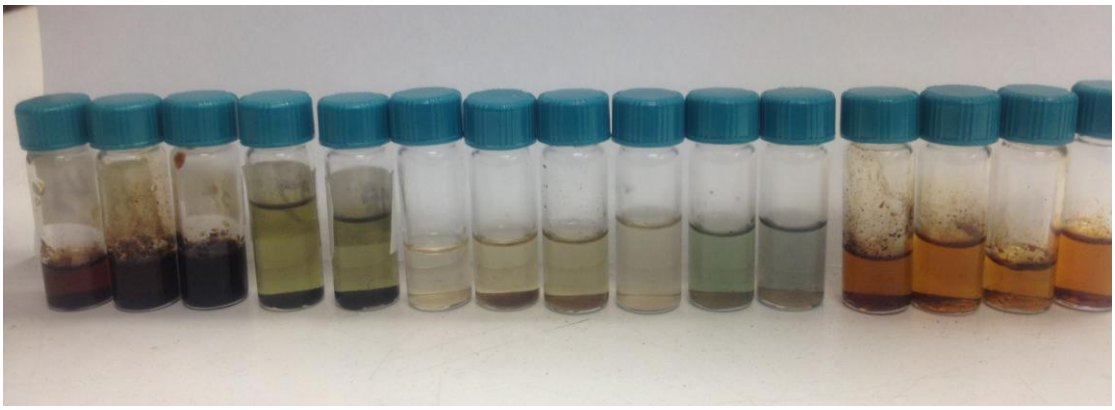

Figure 28: Bio-oil samples obtained from pyrolysis of sawdust.

Due to the large amount of samples obtained from the pyrolysis experiments, not all samples were analyzed by GC-MS. A certain group of samples was selected to illustrate the influence of molten salts on the composition of bio-oil. All the conditions of selected samples were listed and labeled in Table 8. All samples listed were obtained under the condition of carrier gas flow rate of 165 CC/min, mass ratio of feed to molten salt of 1:10 and particle size within 106- 212 μm.

In view of the results listed in Table 9, from No. 1 to No. 3, it was evident that as the pyrolysis temperature increased, the water content of the sample decreased significantly from 28.63% to 14.28%. Acetic acid, furfural and (2-propanone,1-hydroxy-) were the main products in runs without molten salts. The product distribution of No. 2 was closer to those of in No. 1, while No. 3 was quite

distrinct from No. 1 and gave a wider distribution. In this case, high temperature group tended to produce less water and a broader distribution of products. Compared with No. 2, the product distribution of No.9 narrowed down to only three species. Both water content and furfural increased when ternary molten salts were introduced at the same temperature.

Table 21. GC/MS results (area %) with (No.9) and without (No.1-3) molten salts

Content	No. 1	No. 2	No. 3	No. 9
Water	28.63	24.51	14.28	49.89
Acetic acid	25.06	25.81	19.82	25.86
Furfural	11.63	14.11	6.90	21.62
2-propanone,1-hydroxy-	11.20	11.50	10.36	-
Acetic acid, methyl ester	2.98	2.73	1.96	-
Propanic acid	2.02	2.28	1.15	-
1-hydroxy-2-butanone	0.97	1.81	1.87	-
2-cyclopenten-1-one,2-hydroxy-	-	1.46	2.6	-
Phenol,2-methoxy-4-methyl	2.50	1.23	3.66	-
Ethanone,1-(2-furanyl)-	1.47	1.18	2.34	-
Undefined organic products	10.88	9.78	66.68	-

Table 22. GC/MS results (area %) for different kinds of molten salts.

Content	No. 4	No. 5	No. 6	No. 7	No. 8	No. 9
Water	34.94	53.58	46.46	43.60	25.53	49.89
Acetic acid	23.12	26.33	29.77	27.49	26.38	25.86
Furfural	19.37	13.71	16.57	23.61	16.31	21.62
Formic acid	7.82	3.10	1.45	1.01	1.46	-

Table 10 demonstrates the effect of varying combinations of molten salt on the product distribution of the bio-oil. First, No. 8 had the least amount of water- almost the same level as it was without molten salt (No. 1 – No. 3), which was caused by the

absence of zinc chloride. It could be concluded that zinc chloride had the tendency to produce more water. No .4 had relative high water content than No. 8 mainly because the effect of cuprous chloride. Second, no matter what kind of salts mixture was used, the amount of acetic acid kept as a constant especially in the groups from No.5 to No. 9. Third, in terms of furfural, No. 4, 7, and 9 provided high furfural content. It indicates that ternary molten salts system containing zinc and potassium chloride favored high furfural content. Forth, binary molten salts system tended to render high formic acid content, especially for cuprous and potassium chloride. Fifth, water, acetic acid and furfural were the main products in groups from No. 5 to No. 9, however, No. 4 had a wider product distribution which also included (acetaldehyde, chloro-), dichloroacetaldehyde, 2(5H)- furanone and 2-furancarboxaldehyde 5-methyl.

Table 23. GC/MS results (area %) for effect of ratio of $ZnCl_2$-KCl-LiCl on bio-oil composition.

Content	No. 9	No. 10	No. 11	No. 12	No. 13
Water	49.89	52.48	54.57	59.63	44.40
Acetic acid	25.86	26.62	26.46	32.63	30.70
Furfural	21.62	17.41	15.08	3.46	17.90

Table 11 indicates the effect of different molar ratio in zinc, potassium and lithium chloride system on the product distribution. As shown in Table 11, acetic acid and furfural were the only main products in exception of water in all cases. From No. 9 to No. 11, it could be concluded that as the zinc chloride portion increased monotonously, water content increased while furfural deceased with acetic acid remaining unchanged. Comparing No. 9 with No. 12, it was evident that the amount of water and acetic acid improved sharply while furfural dropped tremendously. The molten salt combination of No. 12 was mostly a zinc-lithium binary system which gave quite different result. Compared No. 9 with No. 13, the amount of water and furfural dropped while acetic acid increased. This was due to relatively high zinc chloride and less lithium chloride in No. 13.

Since bio-oil produced based on zinc, potassium and lithium chloride molten salts

only contained water, acetic acid, and furfural as the main products; these components were calibrated and presented in mass percentages when ternary molten salts group of zinc, potassium and lithium chloride was used in the following. The calibration curves for water, acetic acid, and furfural are shown in Appendix B.

Table 12. GC/MS results (wt %) for effect of ratio of $ZnCl_2$-KCl-LiCl on bio-oil composition.

Content	No.9	No.10	No.11	No.12	No.13
Water	90.30	91.26	91.91	92.99	88.43
Acetic acid	6.27	6.19	5.99	6.88	8.44
Furfural	3.43	2.55	2.11	0.12	3.12

Table 12 shows the composition of bio-oil (wt %) derived from pyrolysis of sawdust in $ZnCl_2$-KCl-LiCl molten salt. In all samples, water content was about 90 wt%, which means the summation of mass parentages of acetic acid and furfural stays at around 10%. No. 13 gave the highest yield of acetic acid in weight, while No. 12 provided the highest yield of acetic acid in area percent. So it is concluded that area percent- based composition might lead to errors in getting real composition of bio-oil samples. As seen in Table 12, No.13 offered the highest yield of organics compared with other samples, while No. 9 gave the highest yield of furfural.

In summary, the composition of bio-oil derived from pyrolysis of sawdust can be very complicated which could contain hundreds of substances. Moreover, as the pyrolysis temperature increasing, the composition of bio-oil became more complicated. Introduction of molten salt to the pyrolysis system can narrow down the product distribution significantly. Among the salts under investigation, CuCl-KCl gave a relative high yield of formic acid than other salts. Ternary molten salts can narrow the bio-oil components to 3 or 4 substances, especially when $ZnCl_2$-KCl-LiCl was used, the only main organic products were acetic acid and furfural. Furthermore, changes of composition of certain molten salt, such as $ZnCl_2$-KCl-LiCl can slightly alter the composition of bio-oil.

4.3 Kinetics Studies on Biomass Pyrolysis

4.3.1 Thermogravimetric analysis

The thermal degradation of sawdust without molten salts was first investigated, as shown in Figure 29. Sample 1 was sawdust with particle size of below 106 μm and the sample was dried in oven at 150 ℃ for 24 hrs; sample 2 represented sawdust with particle size of 106-212 μm and the sample was dried in oven at 150 ℃ for 24 hrs; sample 3 was sawdust with particle size of 106-212 μm and no drying treatment applied. Approximate 2.5 mg sawdust was used in each sample.

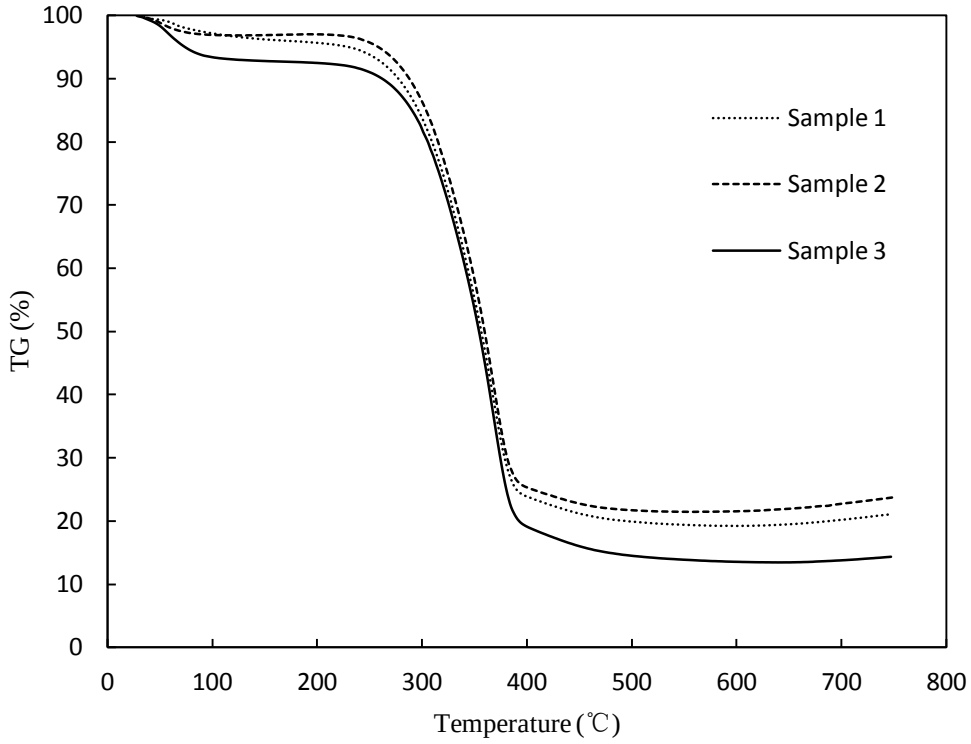

Figure 29: TG curves of sawdust without molten salts.

The three weight loss curves (TG) shown in Figure 29 had similar trends in the whole temperature range: water evaporation at 100 to 150 ℃; main pyrolysis process at 160 to 500 ℃; pyrolysis of residue from 500 ℃. The major pyrolysis process began with decomposition of hemicelluloses in sawdust at around 160 ℃ followed by primary decomposition of lignin. This observation was similar to the results from other research [166].The significant mass loss occurred between 260 and 400 ℃ was

attributed to the pyrolysis of cellulose. When pyrolysis temperature was higher than 500 ℃, slightly decreasing curves were observed due to the pyrolysis of remaining lignin portion, when changes of mass could be very small. As shown in Figure 29, compared with sample 2, the main decomposition reaction occurred at lower temperature for sample 1. This was because the smaller particle size of sample 1, with more effective mass and heat transfer, thus lead to more efficient decomposition reaction. Furthermore, the final residues increased with an increase of particle size, which indicating that larger particles could reduce the degree of pyrolysis and produce more chars. The main difference between sample 2 and 3 was the curves in water evaporation temperature zone. Sample 3 showed a relative strong decrease in this zone as this sample didn't undergo a pre-drying process.

Table 13. Characteristics of sample 3 to sample 7.

Sample No.	Mass of sawdust (mg)	Typle of molten salt	Molar ratio of molten salt (%)	Mass of molten salt (mg)
Sample 3	2.5	-	-	-
Sample 4	3.7	$ZnCl_2$-KCl-LiCl	40-20-40 [a]	23.8
Sample 5	2.5	$ZnCl_2$-NaCl-KCl	52.9-13.4-33.7	11.6
Sample 6	2.5	KCl-LiCl-NaCl	36-55-9	20.6
Sample 7	0	$ZnCl_2$-KCl-LiCl	40-20-40 [a]	25.5

a. Molar ratio based on the molecular weight of the metal cation.

Then second set of experiments was focused on the effects of molten salts on TGA results. Three types of molten salts with sawdust were under investigation. The description of each sample is listed in Table 13. Sample 3 was the same as the one used in Figure 29. The sawdust used in samples from 4 to 6 all have particle size of 106-212 μm and no drying treatment was applied to sawdust. All molten salts were prepared as follows: first, weighed each salt component individually after calculating the mass of salt in the mixed salts by molar ratio; second, added each weighted salt to a crucible and mixed them thoroughly to perform a homogenous mixed salts sample,

then put the sample into oven and hold at a temperature at least 50 ℃ higher than the melting point of this mixed salts for 24 hrs; at last, took the salts out after cooling down to room temperature then sealed the sample for future use. For the TGA experiment, sawdust was first added into the crucible followed by addition of molten salt. No pre-mix procedure applied to sawdust and molten. Sample 7 was only the molten salt without sawdust, aced as a control group. Figure 30 shows the difference of TG curves of sawdust with and without $ZnCl_2$-KCl-LiCl molten salts. The presence of molten salt shifts the main decomposition reaction of sawdust to lower temperature region (at around 220 ℃), while the main decomposition temperature of sawdust without molten salts was at 280 ℃. Sample 4 was continuous decreasing, whereas sample 3 showed a sharp decrease from 150 to 450 ℃.

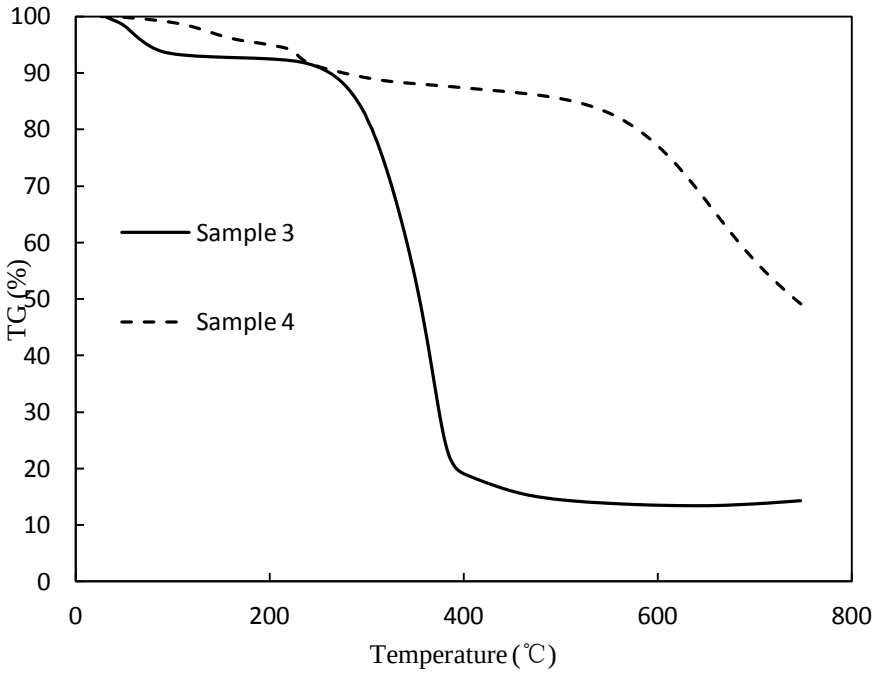

Figure 30: TG curves of sawdust with and without molten salts.

Figure 31 shows TG curves of sawdust with different molten salts. The main decomposition temperature of sample 4 was the lowest (at around 220 ℃) compared to other samples. In contrast, sample 5 and 6 presented almost the same main decomposition temperature at 280 ℃. It could be concluded that $ZnCl_2$-KCl-LiCl molten salt had a positive effect on decreasing the temperature of initial

decomposition reaction of sawdust. The second major mass loss of sample 4 and 5 after 550 ℃ was mainly attributed to the decomposition of $ZnCl_2$. This was proven by the experiment of decomposition of sample 7, which has no biomass. Furthermore, sample 6 didn't show the same trend after 550 ℃, in which the molten salt used was without $ZnCl_2$. In terms of samples with molten salt, the TG curves showed huge distinctions in the temperature range from 150 to 400 ℃. The reason why $ZnCl_2$-KCl-LiCl behaved differently is still unclear.

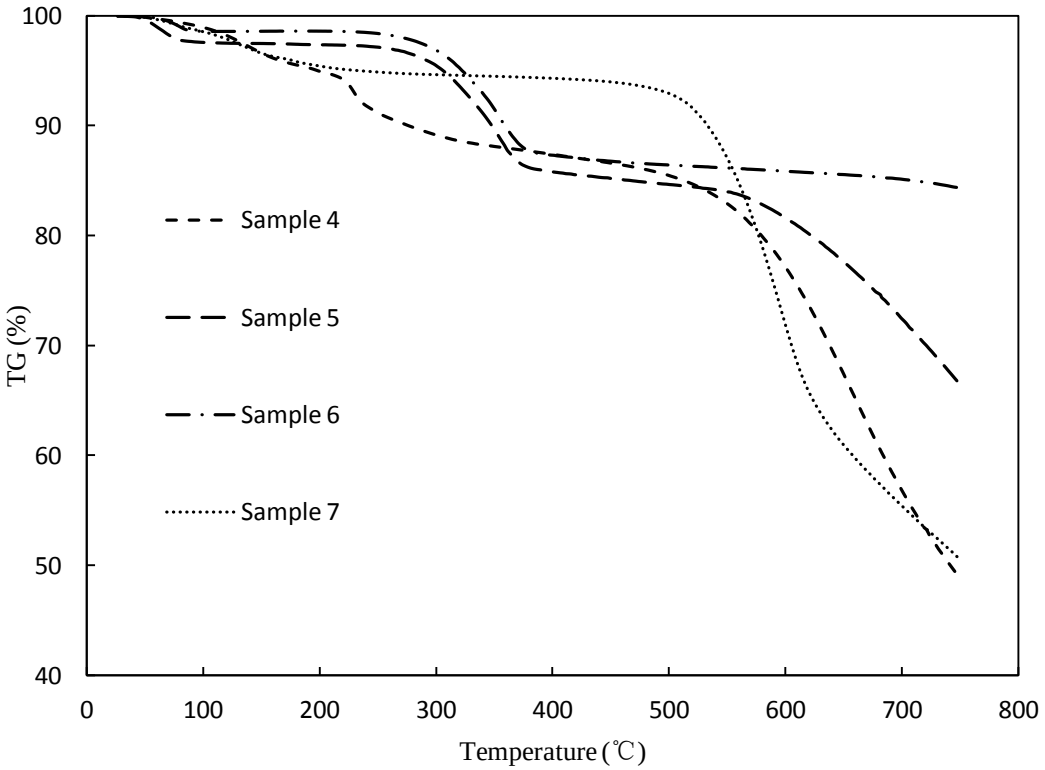

Figure 31: TG curves of sawdust with different molten salts.

The quantitative effects of molten salts on decomposition of sawdust in TGA could not be obtained directly by the TG curves. Rigorous assumptions and data analysis should be made. First, temperatures from 150 to 500 ℃ was selected as the temperature region that decomposition reaction of sawdust occurred completely; second, no decomposition reaction of molten salts occurred at this region. All data regarding TGA could be found in Appendix C. The calculating procedures were presented below:

(1) Sample 3

The conversions were 92.79% and 14.78 % at 150 ℃ and 500 ℃, respectively. So the overall conversion of sawdust was 78.01% (92.79%- 14.78 %=78.01%).

(2) Sample 4

The total mass of sawdust and molten salts was 27.5 mg (see Table 1). The conversions were 96.61% and 85.47 % at 150 ℃ and 500 ℃, respectively. So the overall conversion was 11.14% (96.61%- 85.47 %=11.14%). The mass loss of sawdust was 3.06 mg (11.14% × 27.5 mg = 3.06 mg). So the overall conversion of sawdust was 82.80% (3.06 mg/ 3.7 mg ×100%=82.80%).

So the conversion of sawdust in $ZnCl_2$-KCl-LiCl was somewhat higher than the one without salts.

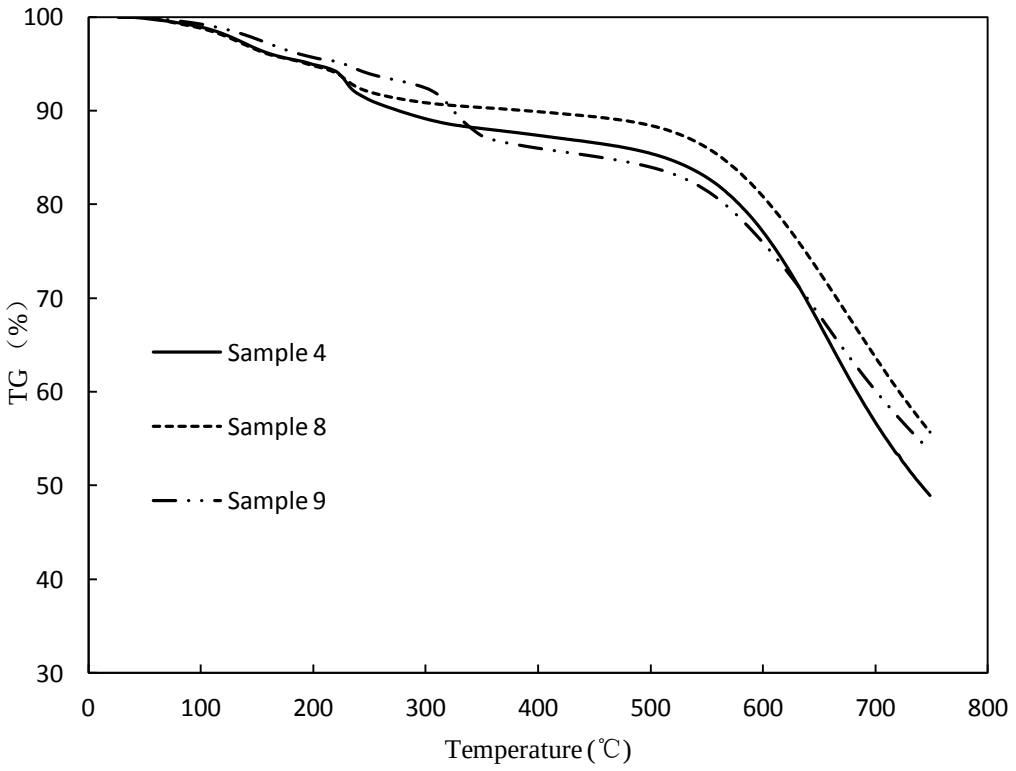

Figure 32: TG curves of sawdust with molten salt and catalysts.

To investigate the influence of catalysts on pyrolysis of sawdust, ZSM-5 and $Ni(OH)_2$ were used as catalysts in TGA. In Figure 32, sample 4 was the same one in Figure 31; sample 8 contained 2.1 mg sawdust, 2.6 mg ZSM-5, and 22.0 mg

$ZnCl_2$-KCl-LiCl molten salt; sample 9 contained 4.3 mg sawdust,11.3 mg $Ni(OH)_2$, and 34.8 mg $ZnCl_2$-KCl-LiCl molten salt. As shown in Figure 32, sample 4 and 8 had same initial decomposition temperature, while $Ni(OH)_2$ had a remarkable shift to the high temperature region.

4.3.2 Kinetic analysis

Kinetic study on pyrolysis of biomass is mainly to obtain the kinetic parameters of the pyrolysis process such as reaction order, pre-exponential factor, and activation energy. Several models have been proposed to fit the TGA data; in this project, only Coats- Redfern model [162] (see Eq. 4) was used in determining the activation energy of pyrolysis of sawdust and the reaction order was assumed to be 1 in all cases.

$$\ln\left[\frac{-\ln(1-C)}{T^2}\right] = \ln\left[\frac{AR}{\beta E}\left(1-\frac{2RT}{E}\right)\right] - \frac{E}{RT} \quad (4)$$

where C is conversion with respect to initial mass; T is reaction temperature; A is pre-exponential factor; E is activation energy; β is heating rate;

Eq. 4 is derived from isothermal rate of conversion model (see Eq. 5)

$$F(C) = \int_0^C \frac{dC}{f(c)} = \frac{A}{\beta}\int_{T_0}^{T} e^{(-E/RT)}\,dT = \frac{AE}{\beta R}\left\{-\frac{e^x}{x} + \int_{-\infty}^{X}\frac{e^x}{x}dx\right\} = \frac{AE}{\beta R}p(x) \quad (5)$$

where F(C) is the integrated function of conversion (F(C)= ln(1-C), when the reation order is fixed to 1); x=(-E/RT);

The slope of curve $\ln\left[\frac{-\ln(1-X)}{T^2}\right]$ versus 1/T produces activation energy. The intercept $\ln\left[\frac{AR}{\beta E}\left(1-\frac{2RT}{E}\right)\right]$ gives the value of the pre-exponential factor. Calculated activation energy values of selected samples were listed in Table 13. The data used to calculate activation energy for each sample were confined to a temperature range, in which main decomposition of sawdust occurred. In other words, these data were collected around the most dominant peak in Differential Thermogravimetry (DTG) curve.

As shown in Table 14, samples (1, 2, and 3) without molten salt provided higher activation energy, from 46.7 to 56.5 KJ/mol. Compared with sample 1, sample 2 offered high activation energy, indicating a smaller energy barrier for smaller particle

sample. Pre-drying treatment to the sample increased activation energy, as sample 3 showed lower activation energy than sample 2. Introduction of molten salts could lower the activation energy no matter what types of molten salts used. The degree of improvement could be ranked in sequence: $ZnCl_2$-KCl-LiCl > $ZnCl_2$-NaCl-KCl> KCl-LiCl-NaCl. Continuous addition of catalyst could further decrease the activation energy (sample 8 and 9) and the activation energy required for sample 8 was only 13% of that required for sample 2.

Table 14. The activation energy of pyrolysis of sawdust in selected samples

Sample No.	E (KJ/mol)	Temperature (K)	r
sample 1	48.0	488-674	0.980
sample 2	56.5	492-672	0.988
sample 3	46.7	504-672	0.972
sample 4	10.1	434-564	0.952
sample 5	31.4	523-653	0.982
sample 6	36.2	504-655	0.974
sample 8	7.5	434-532	0.958
sample 9	9.7	488-628	0.918

r: fitting degree.

However, the calculations in this part are quite rough approximations. Several factors could affect the performance of decomposition of sawdust in TGA, such as, he mass of each component in sample, the sequence of sample preparation, etc. More experiments need to be conducted to obtain a solid knowledge regarding TGA with molten salts. Also, Coats- Redfern model used was not very suitable to pytolyis of sawdust, more accurate model should be adopted, for example, independent parallel model.

4.4 Trials for Newspaper and Recycled Print Paper

4.4.1 Experiment on Newspaper

Preliminary experiment on newspaper was carried out in a smaller reactor, which was a 3/4 inch stainless steel tube with 14 inches in length. 2 g newspaper was used in each trial. $ZnCl_2$ (40% mol) - KCl (20% mol) – LiCl (20% mol) was selected as molten salt. In all runs, the carrier gas flow rate was fixed to 100 CC/min and pyrolysis temperature was set to 350 ℃. The first operation parameter investigated was mass ratio of feed to molten salt: when the mass ratio was set 1:5, the bio-oil sample was black in color and high-viscosity, which could not be analyzed GC/MS; mass ratio of 1:10 gave a satisfactory results with bio-oil yield of 30 %; further increased mass ratio led to lower yield, because of the limited space in the small reactor. Moreover, when switching the reactor orientation vertically, the liquid yield could increase to 34% in contrast to the reactor in horizontal orientation in the same condition. When adding catalyst into the vertical system, introduction of 1g ZSM-5 gave a liquid yield of 32%, while 1 g $Ni(OH)_2$ improved the liquid yield to 38%.

Table 15. Composition of bio-oil derived from newspaper.

Content	Area percentage (%)
Water	21.436
Formic acid	4.090
Acetic acid	21.003
2-Propanone, 1-hydroxy-	11.753
Propanoic acid	2.758
1-Hydroxy, 2-butanone	1.832
Furfural	10.112
2-Propanone, 1-(acetyloxy)-	1.730
2(5H)-Furanone	2.030
2-Cyclopenten-1-one,2-hydroxy-	1.458
2-Furancarboxaldehyde, 5-methyl-	2.391
2-Cyclopenten-1-one,2-hydroxy-3-methyl-	2.596
Phenol,2-methoxy-	4.263
Phenol,2-methoxy-4-methyl	3.355

In order to get more product in quantity, a bigger reactor was then used (the same one for sawdust experiment). 5 g newspaper was used in this beginning and all other conditions were kept the same as small reactor experiment. In this case, the reactor set vertically only produced a liquid yield of 16%, while reactor set in horizontal orientation provided 32% liquid yield. This finding confirmed that this reactor was not suitable to be set vertically in this project. Then the optimal mass of newspaper was investigated: 4g newspaper used gave a liquid yield of 25% and 6 g newspaper used only provided 10% liquid yield.

To explore the composition of bio-oil from newspaper, 5 g newspaper was used in the bigger reactor without molten salts and the pyrolysis temperature was set to 400 ℃. Table 15 lists the main products in bio-oil derived from newspaper. It had a similar product distribution as sawdust. Primary small reactor tests showed that introduction of molten salts could narrow down the product distribution, and enhance particular products formation like furfural.

Table 24. Composition of bio-oil derived from print paper.

Content	Area percentage (%)
Water	21.625
Formic acid	1.922
Acetic acid	9.180
2-Propanone, 1-hydroxy-	11.242
Propanoic acid	3.974
1-Hydroxy, 2-butanone	2.640
Furfural	12.312
2-Propanone, 1-(acetyloxy)-	1.547
2(5H)-Furanone	2.013
2-Cyclopenten-1-one,2-hydroxy-	2.095
2-Furancarboxaldehyde, 5-methyl-	4.415
2-Cyclopenten-1-one,2-hydroxy-3-methyl-	2.545
1,4:3,6-Dianhydro-α-d-glucopyranose	1.621

4.4.2 Experiments on Recycled Print Paper

Similar experiments were conducted on print paper. Molten salts could increase the liquid yield from 25% to 35% at pyrolysis temperature of 400 ℃. KCl (24% mol)-LiCl (43% mol)- NaCl (33% mol) was selected as the molten salts.

To explore the composition of bio-oil from print paper, 5 g paper was used in the big reactor without molten salts and the pyrolysis temperature was set to 400 ℃. Table 16 listed the main products in bio-oil derived from print paper. It had a similar product distribution as sawdust and newspaper. Compared with newspaper, print paper produced two times higher concentration of formic acid and acetic acid. Newspaper oil had a relative high concentration of phenols, while print paper oil had a relative high concentration of anhydrosugars. Figure 33 shows the bio-oils obtained from pyrolysis of newspaper and print paper.

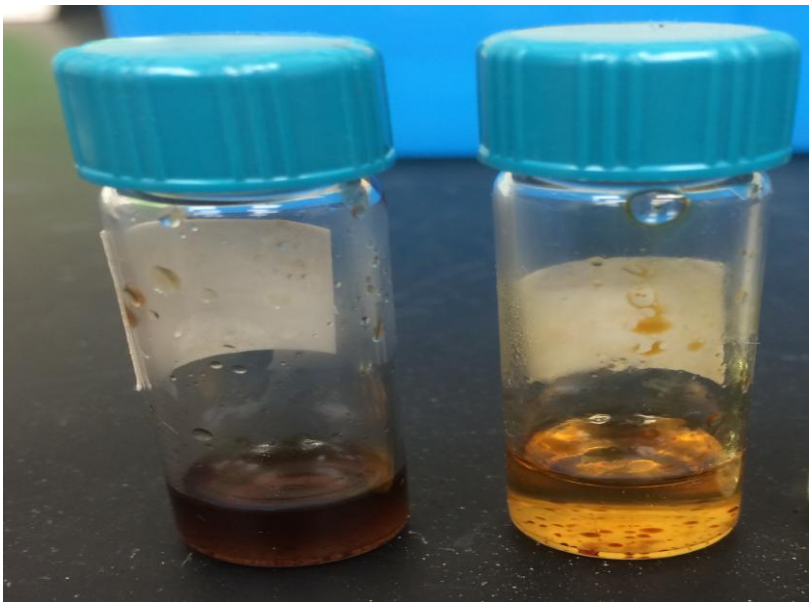

Figure 33: Bio-oil samples derived from pyrolysis of newspaper (left) and print paper (right) without molten salt.

Chapter 5. Conclusions and Future Work

5.1 Conclusions

The single-pot, molten-salt catalytic pyrolysis (MSCP) process described in this report is much more promising, as it produces relatively high bio-oil yield in an easily-built and moderate conditions system (atmospheric pressure and 400 ℃). Through analysis of all the experimental results above, several conclusions could be made. First, pyrolysis temperature is a curial factor in determining the yield of bio-oil. When in the absence of molten salt, bio-oil yield could be up to 39.6% at 450 ℃, while only 12.9% was obtained at 300 ℃. Second, an optimal carrier gas flow rate existed, i.e., 165 CC/min in this work. Third, it can be concluded that sawdust with particle size in 106-212 μm could achieve higher bio-oil yield. The introduction of molten salts could improve the liquid yield significantly. The highest liquid yield was 66.5% in presence with $ZnCl_2$-KCl-LiCl molten salt, compared with 33.2% at the same conditions without molten salts. Different combinations of molten salts and use of catalyst had certain differences in the quality and quantity of the bio-oil produced. Ternary salts had a better performance than binary salts, usually around 10% higher yield. The usage of catalyst could improve the yield by 10~40% depending upon the molten salts pyrolysis system.

The composition of bio-oil derived from pyrolysis of sawdust was studied. Introduction of molten salt to the pyrolysis system can narrow down the product distribution significantly. When $ZnCl_2$-KCl-LiCl was used, the only main organic products were acetic acid and furfural. The highest yield of acetic acid and furfural in bio-oil sample was 8.44 wt % and 3.43 wt %, respectively.

The kinetics study of pyrolysis of sawdust with molten salt was also investigated by using TGA. TGA results showed that $ZnCl_2$-KCl-LiCl molten salt had a positive effect on decreasing the temperature of initial decomposition reaction of sawdust, while $ZnCl_2$-NaCl-KCl and KCl-LiCl-NaCl presented similar trends as the one without molten salt. Moreover, the activation energy of pyrolysis of sawdust was calculated based on Coats- Redfern model. The activation energy was 10.1 KJ/mol for pyrolysis of sawdust in $ZnCl_2$-KCl-LiCl, while it was 46.7 KJ/mol for sawdust

without molten salt.

Finally, preliminary trials on pyrolysis of newspaper and print paper were carried out. The liquid yield for both cases was around 32% in $ZnCl_2$-KCl-LiCl molten salt at 350 ℃ and 35 % without molten salt at 400 ℃. In terms of composition of bio-oil, newspaper and print paper had a similar product distribution as sawdust, whereas, print paper oil had a relative high concentration of anhydrosugars.

5.2 Recommendations for Future Work

First, in this work, one major factor that can affect bio-oil yield was untested, i.e., heating rate. High heating rate could provide high liquid yields. A method to realize this goal is to use a fluidized bath reactor which can enhance the heating rate tremendously. Another method is to use a heater that can offer different level of heating rate.

Second, the gas products were not captured and analyzed. Knowing gas composition would be beneficial to have a better understanding of the mechanism of pyrolysis of biomass. Also, the pyrolysis-derived gas contains fuel gas such as, H_2, CO, and CH_4, which could be utilized in downstream process. Similarly, the char product could be analyzed in the future, as the solid char could be utilized in many ways.

Third, a more effective way to analyze composition of bio-oil should be adopted in future work. Organic substances can be analyzed by dissolving bio-oil sample in methanol or acetone and water content can be analyzed by Karl Fischer titration.

Fourth, a more accurate value of activation energy of pyrolysis of sawdust could be calculated by three-independent reaction model or iso-conversion model. Also, the in-depth molten salts-aid pyrolysis mechanism should be developed.

Finally, a systematic investigation on pyrolysis of newspapers and/or paper should be conducted in the future.

References

1 CV Stevens and R Verhe. Renewable bioresources scope and modification for nonfood application. *England: John Wiley and Sons Ltd* 2004.

2 C Hu, Y Yang, *et al.*. Recent advances in the catalytic pyrolysis of biomass. *Front. Chem. Sci. Eng.* **2011**, 5(2), 188-193.

3 RH Venderbosch and W Prins. Fast pyrolysis technology development. *Biofuels Bioproducts and biorefining* **2010**, 4, 178-208.

4 PR Patwardhan. "Understanding the product distribution from biomass fast pyrolysis"(2010). *Graduate Theses and Dissertations*. Paper 11767.

5 GW Huber and A Corma. Synergies between bio- and oil refineries for the production of fuels from biomass. *Angewandte Chemie International Edition* **2007**, 46(38), 7184-7201.

6 JR Regalbuto. Cellulosic biofuels— got gasoline? *Science* **2009**, 325(5942), 822-824.

7 K Bordage, T McGee, *et al.*. "A study of biofuel production using molten salt catalysts" (2010). Worcester MA: WPI.

8 R O'Hara, J Rynkar, *et al.*. "Production of furanic liquid compounds from cellulosic biomass based on molten salts and catalysis" (2012). Worcester MA: WPI.

9 CL Welsh. "Production of bioliquids from cellulosic biomass through molten salt pyrolysis using molten salt catalysts" (2013). Worcester MA: WPI.

10 RC Brown. Biorenewable resources: engineering new products from agriculture. *Iowa: Iowa State Press* 2003.

11 GW Huber, S Iborra and A Corma. Synthesis of transportation fuels from biomass: chemistry, catalysis, and engineering. *Chem. Rev.* **2006**, 106, 4044-4098.

12 CA Koufopanos, *et al.*. Kinetic modelling of the pyrolysis of biomass and biomass components. *Can. J. Chem. Eng.* **1989**, 67, 75-83.

13 P Mckendry. Energy production from biomass (part 1): overview of biomass. *Bioresource Technology* **2002**, 83, 37-46.

14 D Mohan, *et al.*. Pyrolysis of wood/biomass for bio-oil: a critical review. *Energy & Fuels* **2006**, 20, 848-889.

15 CE Wyman, *et al.*. In polysaccharides, 2nd ed. *New York: Marcel Dekker* 2005.

16 RM Rowell. Handbook of wood chemistry and wood composites, 2nd ed. *Boca Raton: CRC Press* 2012.

17 TA Hsu, *et al.*. Alcohol from cellulose. *Chemical Technology* **1980**, 10, 315–319.

18 MM Ahmed. Biomass as a renewable source of chemicals for industrial application. *International journal of engineering science and technology* **2012**, 4, 721-730.

19 TE Timell. Recent progress in the chemistry of wood hemicelluloses. *Wood Sci. Technol*. **1967**, 1, 45-70.

20 J McCarthy, *et al.*. Lignin chemistry, technology, and utilization: a brief history. In lignin: historical, biological, and materials perspectives. W Glasser, *et al.* ACS Symposium Series; American Chemical Society: Washington, DC, 1999.

21 RJ Evans, *et al.*. Direct mass-spectrometric studies of the pyrolysis of carbonaceous fuels: III. Primary pyrolysis of lignin. *Anal. Appl. Pyrolysis* **1986**, 9, 207-236.

22 N Mosier, C Wyman, *et al.*. Features of promising technologies for pretreatment of lignocellulosic biomass. *Bioresour. Technol.* **2005**, 96, 673.

23 A Brandt, *et al.*. Deconstruction of lignocellulosic biomass with ionic liquids. *Green Chem.*

2013, 15, 550-583.

24 M Himmel, *et al*.. Biomass recalcitrance: engineering plants and enzymes for biofuels production. *Science* **2007**, 315, 804-807.

25 L Sousa, *et al*.. 'Cradle-to-grave'assessment of existing lignocellulose pretreatment technologies. *Curr. Opin. Biotechnol*. 2009, 20, 339-347.

26 SPS Chundawat, *et al*.. Multi-scale visualization and characterization of lignocellulosic plant cell wall deconstruction during thermochemical pretreatment. *Energy Environ. Sci*. 2011, 4, 973-984.

27 SPS Chundawat, *et al*.. Deconstruction of lignocellulosic biomass to fuels and chemicals. *Annu. Rev. Chem. Biomol. Eng*. **2011**, 2, 6.1-6.25.

28 J Lehmann and S Joseph. Biochar for environmental management: science and technology. *London: Earthscan* 2009.

29 BT Nguyen, *et al*.. Temperature sensitivity of black carbon decomposition and oxidation. *Environ. Sci. Technol.* **2010**, 44, 3324–3331.

30 J Lehmann, *et al*.. Biochar effects on soil biota- A review. *Soil Biology & Biochemistry* **2011**, 43, 1812-1836.

31 M Essandoh, *et al*.. Sorptive removal of salicylic acid and ibuprofen from aqueous solutions using ping wood fast pyrolysis biochar. *Chemical Engineering Journal* **2015**, 265, 219-227.

32 KT Klasson, *et al*.. Influence of biochar pyrolysis temperature and post-treatment on the uptake of mercury from flue gas. *Fuel Processing Technology* **2014**, 123, 27-33.

33 S Ren, *et al*.. Hydrocarbon and hydrogen-rich syngas production by biomass catalytic pyrolysis and bio-oil upgrading over biochar catalysts. *RSC Adv.* **2014**, 4, 10731-10737.

34 AJ Ashworth, *et al*.. Influence of pyrolysis temperature and production conditions on switchgrass biochar for use as a soil amendment. *BioResources* **2014**, 9(4), 7622-7635.

35 LV Zwieten, *et al*.. Effects of biochar from slow pyrolysis of papermill waste on agronomic performance and soil fertility. *Plant Soil* **2010**, 327, 235-246.

36 D Mohan, *et al*.. Organic and inorganic contaminants removal from water with biochar, a renewable, low cost and sustainable adsorbent- A critical review. *Bioresource Technology* **2014**, 160, 191-202.

37 M Keiluweit, *et al*.. Dynamic molecular structure of plant biomass-derived black carbon (biochar). *Environ. Sci. Technol*. **2010**, 44, 1247-1253.

38 M Zhao, *et al*.. Short- and long- term flammability of biochars. *Biomass Bioenergy* **2014**, 69, 183-191.

39 X Domene, *et al*.. Ecotoxicological characterization of biochars: Role of feedstock and pyrolysis temperature. *Science of the Total Environment* **2015**, 512-515, 552-561.

40 G Lv, *et al*.. Characteristics of corn stalk hemicelluloses pyrolysis in a tubular reactor. *BioResources* **2010**, 5(4), 2051-2062.

41 A Demirbas. Effects of temperature and particle size on bio-char yield from pyrolysis of agricultural residues. *J. Anal. Appl. Pyrolysis* **2004**, 72, 243-248.

42 X Liu, *et al*.. Characterization of corncob-derived biochar and pyrolysis kinetics in comparison with corn stalk and sawdust. *Bioresource Technology* **2014**, 170, 76-82.

43 N Ai, *et al*.. Co-production of activated carbon and bio-oil from agricultural residues by molten salt pyrolysis. *BioResources* **2013**, 8(2), 1551-1562.

44 Monthly Energy Review May 2014, Report No. DOE/EIA-0035. U.S. Energy Information

Administration, Washington DC, 2014.

45 RD Perlack, LL Wright, *et al*.. Biomass as feedstock for a bioenergy and bioproducts industry: the technical feasibility of a billion-ton annual supply, Report No. DOE/GO-102995-2135. Oak Ridge National Laboratory, Oak Ridge TN, 2005.

46 DL Klass. Biomass for renewable energy, fuels and chemicals. *San Diego: Academic Press* 1998.

47 U.S. Energy Information Administration, Washington DC, 2014.

48 RE Sims, W Mabee, *et al*.. An overview of second generation biofuel technologies. *Bioresource Technology* **2010**, 101, 1570-1580.

49 SN Naik, VV Goud, *et al*.. Production of first and second generation biofuels: A comprehensive review. *Renewable and Sustainable Energy Reviews* **2010**, 14, 578-597.

50 J Fargione, *et al*.. Land clearing and the biofuel carbon det. *Science* **2008**, 319, 1235-1238.

51 T Searchinger, *et al*.. Use of US croplands for biofuels increases greenhouse gases through emissions from land use change. *Science* **2008**, 319, 1238-1240.

52 K Dutta, A Daverey, and J Lin. Evolution retrospective for alternative fuels: First to fourth generation. *Renewable Energy* **2014**, 69, 114-122.

53 E Suali and R Sarbatly. Conversion of microalgae to biofuel. *Renew. Sust. Energ. Rev.* **2012**, 16, 4316-4312.

54 J Maity, J Bundschuh, *et al*.. Microalgae for third generation biofuel production, mitigation of greenhouse gas emissions and wastewater treatment: Present and future perspectives e A mini review. *Energy* **2014**, 78, 104-113.

55 J Singh and S Gu. Commercialization potential of microalgae for biofuels production. *Renew. Sust. Energ. Rev.* **2010**, 14, 2596-2610.

56 C Branca, P Giudicianni, and C DiBlasi. GC/MS characterization of liquids generated from low-temperature pyrolysis of wood. *Ind. Eng. Chem. Res.* **2003**, 42, 3190-3202.

57 JP Diebold. A review of the chemical and physical mechanisms of the storage stability of fast pyrolysis bio-oils. Report No. NREL/SR-570-27613. National Renewable Energy Laboratory: Golden, CO, 2000. http://www.osti.gov/bridge.

58 LD Gomez, *et al*.. Sustainable liquid biofuels from biomass: the writing's on the walls. *New Phytol* **2008**, 178, 473-485.

59 JH Clark, *et al*.. Green chemistry and the biorefinery: a partnership for a sustainable future. *Green Chem* **2006**, 8, 853-860.

60 J Jensen, *et al*.. Kinetics characterization of biomass dilute sulfuric acid hydrolysis: mixtures of hardwoods, softwood, and switchgrass. *AICHE J* **2008**, 54, 1637-1645.

61 FEI Dewarte, *et al*.. Toward an integrated straw-based biorefinery. *Biofuel Biopord Biorefineries* **2007**, 1, 245-254.

62 M Sasaki, *et al*.. Cellulose hydrolysis in subcritical and supercritical water. *J Supercrit Fluid* **1998**, 13, 261-268.

63 WN Rowlands, *et al*.. The biorefinery-challenges, opportunities and an Australian perspective. *Bull Sci Technol Soc* **2008**, 28(2), 149-158.

64 A Demirbas. Current technologies for the thermo-conversion of biomass into fuels and chemicals. *Energy Sources* **2004**, 26, 715-730

65 F Goudnaan, *et al*.. Thermal efficiency of the HTU® process for biomass liquefaction, in Progress in thermochemical biomass conversion (ed A. V. Bridgwater). *Oxford: Blackwell*

Science Ltd 2010.

66 S Lee, *et al*.. Hand book of alternative fuel technologies. *USA: CRC Taylor and Francis Group* 2007.

67 M Balat. Sustainable transportation fuels from biomass materials. *Energy Educ Sci Technol* **2006**, 54, 559-568.

68 F Shafizafeh. Introduction to pyrolysis of biomass. *J Anal Appl Pyrolysis* **1982**, 3, 283-305.

69 Y Zheng, J Zhao, *et al*.. Pretreatment of lignocellulosic biomass for enhanced biogas production. *Prog. Energy Combust. Sci.* **2014**, 42, 35-53.

70 Y Yang, T Li, *et al*.. Catalytic pyrolysis of tobacco rob: Kinetic study and fuel gas produced. *Bioresource Technology* **2011**, 102, 11027-11033.

71 G Cheng, L Zhang, *et al*.. Pyrolysis of ramie residue: Kinetic study and fuel gas produced in a cyclone furnace. *Bioresource Technology* **2011**, 102, 3451-3456.

72 W Wijayantia and K Tanoueb. Char formation and gas products of woody biomass pyrolysis. *Energy Procedia* **2013**, 32, 145 – 152.

73 B Zhao, X Zhang, *et al*.. High quality fuel gas from biomass pyrolysis with calcium oxide. *Bioresource Technology* **2014**, 156, 78-83.

74 J RemÓn, F Broust, *et al*.. Production of a hydrogen-rich gas from fast pyrolysis bio-oils: Comparison between homogeneous and catalytic steam reforming routes. *Int. J. Hydrogen Energy* **2014**, 39, 171-182.

75 PL Spath and DC Dayton. Preliminary screening - technical and economic assessment of synthesis gas to fuels and chemicals with emphasis on the potential for biomass-derived syngas. Report No.NREL/TP-510-34929; National Renewable Energy Laboratory, Golden, CO, 2003; http://www.osti.gov/bridge.

76 P Kumar, DM Barrett, *et al*.. Methods for pretreatment of lignocellulosic biomass for efficient hydrolysis and biofuel production. *Ind. Eng. Chem. Res.* **2009**, 48, 3713–3729.

77 E Palmqvist and B Hahn-Hägerdal. Fermentation of lignocellulosic hydrolysates. I: Inhibition and detoxification. *Bioresource Technology* **2000**, 74, 17–24.

78 S Mood, AH Golfeshan, *et al*.. Lignocellulosic biomass to bioethanol, a comprehensive review with a focus on pretreatment. *Renewable and Sustainable Energy Reviews* **2013**, 27, 77–93.

79 MJ Taherzadeh and K Karimi. Pretreatment of lignocellulosic wastes to improve ethanol and biogas production: a review. *International Journal of Molecular Science* **2008**, 9, 1621–1651.

80 TC Hsu, GL Guo, *et al*.. Effect of dilute acid pretreatment of rice straw on structural properties and enzymatic hydrolysis. *Bioresource Technology* **2010**, 101, 4907–4913.

81 X Li, TH Kim and NP Nghiem. Bioethanol production from corn stover using aqueous ammonia pretreatment and two-phase simultaneous saccharification and fermentation (TPSSF). *Bioresource Technology* **2010**, 101, 5910-5916.

82 WE Karr and MT Holtzapple. The multiple benefits of adding non-ionic surfactant during the enzymatic hydrolysis of corn stover. *Biotechnol. Bioeng.* **1998**, 59, 419-427.

83 WE Mabee, DJ Gregg, *et al*.. Updates on softwood-to-ethanol process development. *Appl. Microbiol. Biotechnol.* **2006**, 129–132, 55–70.

84 MT Holtzapple, JH Jun, *et al*.. The ammonia freeze explosion (AFEX) process: A practical lignocelluloses pretreatment. *Appl. Biochem. Biotechnol.* **1991**, 28-29, 59-74.

85 SPS Chundawat, G Bellesia, *et al*.. Restructuring the crystalline cellulose hydrogen bond network enhances its depolymerization rate. *J. Am. Chem. Soc.* **2011**, 133, 11163–11174.

86 M Sasaki, Z Fang, *et al.*. Dissolution and hydrolysis of cellulose in subcritical and supercritical water. I*nd. Eng. Chem. Res.* **2000**, 39, 2883-2890.

87 KH Kim, Juan Hong, *et al.*. Supercritical CO_2 pretreatment of lignocellulose enhances enzymatic cellulose hydrolysis. *Bioresour. Technol.* **2001**, 77, 139-144.

88 AV Bridgwater. Principles and practice of biomass fast pyrolysis processes for liquids. *J. Anal. Appl. Pyrolysis* **1999**, 51, 3-22.

89 AV Bridgwater, *et al.*. Fast pyrolysis process for biomass. *Renewable and Sustainable Energy Reviews* **2000**, 4, 1-73.

90 WNRW Isahak, MWM Hisham, *et al.*. A review on bio-oil production from biomass by using pyrolysis method. *Renewable and Sustainable Energy Reviews* **2012**, 16, 5910–5923.

91 J Akhtar and NS Amin. A review on operating parameters for optimum liquid oil yield in biomass pyrolysis. *Renewable and Sustainable Energy Reviews* **2012**, 16, 5101–5109.

92 Q Zhang, *et al.*. Review of biomass pyrolysis oil properties and upgrading research. *Energy Conversion and Management* **2007**, 48, 87-92.

93 AV Bridgwater. Review of fast pyrolysis of biomass and product upgrading. *Biomass and Bioenergy* **2012**, 38, 68-94.

94 Z Luo, *et al.*. Research on biomass fast pyrolysis for liquid fuel. *Biomass and Bioenergy* **2004**, 26, 455-462.

95 J Zheng, *et al.*. Bio-oil from fast pyrolysis of rice husk: yields and related properties and improvement of the pyrolysis system. *J. Anal. Appl. Pyrolysis* **2007**, 80, 30-35.

96 H Chen, *et al.*. Pyrolysis characteristics of sucrose biomass in a tubular reactor and a thermogravimetric analysis. *Fuel* **2012**, 95, 425-430.

97 S Kim, *et al.*. Pyrolysis characteristics and kinetics of the alga Saccharina japonica. *Bioresource Technology* **2012**, 123, 445-451.

98 PR Patwardhan, *et al.*. Product distribution from fast pyrolysis of glucose-based carbohydrates. *J. Anal. Appl. Pyrolysis* **2009**, 86, 323-330.

99 PR Patwardhan, *et al.*. Distinguishing primary and secondary reactions of cellulose pyrolysis. *Bioresource Technology* **2011**, 102, 5265-5269.

100 S Li, J Lyons-Hart, *et al.*. Real-time evolved gas analysis by FTIR method: an experimental study of cellulose pyrolysis. *Fuel* **2001**, 80, 1809-1817.

101 HS Choi, *et al.*. Fast pyrolysis of Kraft lignin-vapor cracking over various fixed-bed catalysts. *J. Anal. Appl. Pyrolysis* **2013**, 100, 207-212.

102 X Wang, W Morrison, *et al.*. Biomass temperature profile development and its implications under the microwave-assisted pyrolysis condition. *Applied Energy* **2012**, 99, 386–392

103 AA Salema and FN Ani. Microwave induced pyrolysis of oil palm biomass. *Bioresour. Technol.* **2011**, 102, 3388–3395.

104 X Zhao, Z Song, *et al.*. Microwave pyrolysis of corn stalk bale: a promising method for direct utilization of large-sized biomass and syngas production. *J. Anal. Appl. Pyrolysis* **2010**, 89, 87–94.

105 K Raveendran, *et al.*. Influence of mineral matter on biomass pyrolysis characteristics. *Fuel* **1995**, 74, 1812-1822.

106 FA Shafizadez. Pyrolysis and combustion of cellulosic materials. A*dv. Carbohydrate Chem.* **1968**, 23, 419-474.

107 N Shimada, *et al.*. Different action of alkali/alkine earth metal chloride on cellulose pyrolysis. *J.*

Anal. Appl. Pyrolysis **2008**, 81, 80-87.

108 PR Patwardhan, *et al*.. Influence of inorganic salts on the primary pyrolysis products of cellulose. *Bioresource Technology* **2010**, 101, 4646-4655.

109 M Nik-Azar, MR Hajaligol, *et al*.. Mineral matter effects in rapid pyrolysis of beech wood. *Fuel Process. Technol.* **1997**, 51, 7-17.

110 Q Lu, *et al*.. Selective fast pyrolysis of biomass impregnated with $ZnCl_2$ to produce furfural: analytical Py-GC/MS study. *J. Anal. Appl. Pyrolysis* **2011**, 90, 204-212.

111 Q Lu, *et al*.. Selective fast pyrolysis of biomass impregnated with $ZnCl_2$: furfural production together with acetic acid and activated carbon as by-products. *J. Anal. Appl. Pyrolysis* **2011**, 91, 273-279.

112 AS Amarasekara and CC Ebede. Zinc chloride mediated degradation of cellulose at 200 ℃ and identification of the products. *Bioresour. Technol.* **2009**, 100, 5301–5304.

113 L Yang, G Li, *et al*.. Direct conversion of cellulose to 1-(furan-2-yl)-2-hydroxyethanone in zinc chloride solution under microwave irradiation. *Carbohydr. Res.* **2011**, 346, 2304-2307.

114 DM Alonso, JQ Bond and JA Dumesic. Catalytic conversion of biomass to biofuels. *Green Chem.* **2010**, 12, 1493-1513.

115 M Samolada. A Papafotica and I Vasalos, Catalyst evaluation for catalytic pyrolysis. *Energy Fuels* **2000**, 14, 1161-1167.

116 Changwei Hu, *et al*.. Recent advances in the catalytic pyrolysis of biomass. *Front. Chem. Sci. Eng.* **2011**, 5(2), 188-193.

117 S Thangalazhy-Gopakumar, S Adhikari, *et al*.. Production of hydrocarbon fuels from biomass using catalytic pyrolysis under helium and hydrogen environments. *Bioresour. Technol.* **2011**, 102, 6742–6749.

118 D Fabbri, *et al*.. Effect of zeolites and nanopowder metal oxides on the distribution of chiral anhydrosugars evolved from pyrolysis of cellulose: an analytical study. *J. Anal. Appl. Pyrolysis* **2007**, 80, 24-29.

119 C Torri, IG Lesci and D Fabbri. Analytical study on the pyrolytic behaviour of cellulose in the presence of MCM-41 mesoporous materials. *J. Anal. Appl. Pyrolysis* **2009**, 85, 192–196.

120 M Zabeti, *et al*.. *In situ* catalytic pyrolysis of lignocellulose using alkali-modified amorphous silica alumina. *Bioresource Technology* **2012**, 118, 374-381.

121 Y Wan, P Chen, *et al*.. Microwave-assisted pyrolysis of biomass: Catalysts to improve product selectivity. *J. Anal. Appl. Pyrolysis* **2009**, 86, 161–167.

122 G Yang, EA Pidko and EJM Hensen. Mechanism of Brønsted acid-catalyzed conversion of carbohydrates. *J. Catal.* **2012**, 295, 122-132.

123 Y Román-Leshkov and ME Davis. Activation of carbonyl-containing molecules with solid Lewis acids in aqueous media. *ACS Catal.* **2011**, 1, 1566-1580.

124 N Shi, Q Liu, *et al*.. Direct degradation of cellulose to 5-hydroxymethylfurfural in hot compressed steam with inorganic acidic salts. *RSC Adv.* **2014**, 4, 4978–4984.

125 V Choudhary, *et al*.. Insights into the interplay of lewis and brønsted acid catalysts in glucose and fructose conversion to 5-(Hydroxymethyl)furfural and levulinic acid in aqueous media. *J. Am. Chem. Soc.* **2013**, 135, 3997-4006.

126 E Nikolla, *et al*.. "One-Pot" synthesis of 5-(Hydroxymethyl)furfural from carbonhydrates using Tin-Bata zeolite. *ACS Catal.* **2011**, 1, 408-410.

127 T Wang, *et al*.. Production of 5-hydroxymethyfurfural from glucose using a combination of

lewis and brønsted acid catalysts in water in a biphasic reactor with an alkylphenol solvent. *ACS Catal.* **2012**, 2, 930-934.

128 F Yang, J Fu, *et al.*. Synergy of Lewis and Brønsted acids on catalytic hydrothermal decomposition of hexose to levulinic acid. *Energy Fuels* **2013**, 27, 6973-6978.

129 MG Mazzotta, D Gupta, *et al.*. Efficient solid acid catalyst containing Lewis and Brønsted acid sites for the production of furfurals. *ChemSusChem* **2014**, 7, 2342 – 2350.

130 NV Plechkova and KR Seddon. Applications of ionic liquids in the chemical industry. *Chem. Soc. Rev.* **2008**, 37, 123–150.

131 H Tadesse and R Luque. Advances on biomass pretreatment using ionic liquids: An overview. *Energy Environ. Sci.* **2011**, 4, 3913-3929.

132 A Brandt, *et al*.. Deconstruction of lignocellulosic biomass with ionic liquids. *Green Chem.* **2013**, 15, 550-583.

133 S Bose, *et al.*. Enzyme-catalyzed hydrolysis of cellulose in ionic liquids: A green approach toward the production of biofuels. *J. Phys. Chem. B* **2010**, 114, 8221–8227.

134 JL Wen, *et al.*. Understanding the chemical transformation of lignin during ionic liquid pretreatment. *Green Chem.* **2014**, 16, 181-190.

135 GN Sheldrake and D Schleck. Dicationic molten salts (ionic liquids) as re-usable media for the controlled pyrolysis of cellulose to anhydrosugars. *Green Chem.* **2007**, 9, 1044-1046.

136 J Du, *et al*.. Fast Pyrolysis of biomass for bio-oil with ionic liquid and microwave irradiation. *J. Fuel. Chem. Technol.* **2010**, 38(5), 554-559.

137 JB Binder and RT. Raines. Fermentable sugars by chemical hydrolysis of biomass. *Proc. Natl. Acad. Sci.* U. S. A. **2010**, 107(10), 4516-4521.

138 E Olsen, *et al*.. Review of thermal processing of biomass and waste in molten salts for production of renewable fuels and chemicals. *International Journal of Low-Carbon Technologies* **2012**, 7, 318-324.

139 ES Hidehiro, *et al*.. Pyrolysis of lignins in molten salt media. *Ind. Eng. Chem. Res*. **1992**, 31, 612-616.

140 M Kudsy, H Kumazawa and E Sada. Pyrolysis of kraft lignin in molten salt $ZnCl_2$-KCl media with tetralin vapor addition. *Can. J. Chem. Eng.* **1995**, 73, 411-415.

141 M Kudsy, *et al*.. Pyrolysis of kraft lignin in the presence of molten $ZnCl_2$-KCl mixture. *Can. J. Chem. Eng.* **1999**, 77, 1176-1184.

142 M Wang, *et al.*. Study on pyrolytic liquefaction of biomass in molten salt. *Chemistry and Industry of Forest Products* **2009**, 29, 41-46. (in Chinses with English abstract)

143 H Jiang, N Ai, *et al*.. Experimental study on thermal pyrolysis of biomass in molten salt media. *Electrochemistry* **2009**, 77, 730-735.

144 T Cai, *et al*.. Characteristics of biomass pyrolysis in molten salt. Transactions of the CASE 2010, 26, 243-247. (in Chinses with English abstract)

145 D Ji, *et al*.. Conversion of sawdust to bio-fuels by pyrolysis within molten sodium hydroxide. 2012 International Conference on Biobase Material Science and Engineering (BMSE)

146 H Jiang, *et al.*. Hydrogen production from biomass pyrolysis in molten alkali. *AASRI Procedia* **2012**, 3, 217-223.

147 F Danielsen, *et al.*. Thermal history of wood particles in molten salt pyrolysis. *Energy Fuel* **2012**, 26, 6419-6425.

148 J Piskorz, *et al*.. Pretreatment of wood and cellulose for production of sugars by fast pyrolysis. *J.*

Anal. Appl. Pyrolysis **1989**, 16, 127-142.

149 PJ Dauenhauer, *et al.*. Reactive boiling of cellulose for integrated catalysis through an intermediate liquid. *Green Chem.* **2009**, 11, 1555-1561.

150 JH Flynn and LA Wall. General treatment of the thermogravimetry of polymers. *J. Res. Nat. Bur. Standards, Part A* **1966**, 70, 487-523.

151 MJJ Antal, *et al.*. Cellulose pyrolysis kinetics: the current state of knowledge. *Ind. Eng. Chem. Res.* **1995**, 34, 703-717.

152 A Broido, *et al.*. Char yield on pyrolysis of cellulose. *Combust. Flame* **1975**, 24, 263-268.

153 AGW Bradbury, *et al.*. A kinetic model for pyrolysis of cellulose. *J. Appl. Polym. Sci.* **1979**, 23, 3271-3280.

154 S Cooley, *et al.*. Kinetics of cellulose pyrolysis in the presence of nitric oxide. *J. Anal. Appl. Pyrolysis* **1988**, 14, 149-161.

155 JL Banyasz, *et al.*. Gas evolution and the mechanism of cellulose pyrolysis. *Fuel* **2001**, 80, 1757-1763.

156 MJ Antal, G Várhegyi and E Jakab. Cellulose pyrolysis kinetics: revisited. *Ind. Eng. Chem. Res.* **1998**, 37, 1267-1275.

157 JJM Órfão, FJA Antunes and JL Figueiredo. Pyrolysis kinetics of lignocellulosic materials - three independent reactions model. *Fuel* **1999**, 78, 349-358.

158 JJ Manyà, E Velo and L Puigjaner. Kinetics of biomass pyrolysis: a reformulated three-parallel-reactions model. *Ind. Eng. Chem. Res.* **2003**, 42, 434-441.

159 M Müller-Hagedorn, H Bockhorn, *et al.*. A comparative kinetic study on the pyrolysis of three different wood species. *J. Anal. Appl. Pyrolysis* **2003**, 68-69, 231-249.

160 S Hu, A Jess and M Xu. Kinetic study of Chinese biomass slow pyrolysis: Comparison of different kinetic models. *Fuel* **2007**, 86, 2778–2788.

161 T Sonobe and Na Worasuwannarak. Kinetic analyses of biomass pyrolysis using the distributed activation energy model. *Fuel* **2008**, 87, 414-421.

162 T Damartzis, D Vamvuka, *et al.*. Thermal degradation studies and kinetic modeling of cardoon (*Cynara cardunculus*) pyrolysis using thermogravimetric analysis (TGA). *Bioresour. Technol.* **2011**, 102, 6230–6238.

163 K Slopiecka, P Bartocci and F Fantozzi. Thermogravimetric analysis and kinetic study of poplar wood pyrolysis. *Applied Energy* **2012**, 97, 491-497.

164 M Gao, D Ji, *et al.*. Influence of molten salts on pyrolysis characteristics of rice straw. 2012 International Conference on Biobase Material Science and Engineering (BMSE).

165 O Ioannidou, CG Jung and A Zabaniotou. A thermogravimetric model to predict yield product distribution in pyrolysis of agricultural biomass. *Catal. Today* **2011**, 167, 129-134.

166 H Yang, *et al.*. Characteristics of hemicellulose, cellulose and lignin pyrolysis. *Fuel* **2007**, 86, 1781–1788.

167 H Yang, *et al.*. In-depth investigation of biomass pyrolysis based on three major components: hemicelluloses, cellulose and lignin. *Energy & Fuels* **2006**, 20, 388-393.

168 T. Hosoya, *et al.*. Cellulose–hemicellulose and cellulose–lignin interactions in wood pyrolysis at gasification temperature. *J. Anal. Appl. Pyrolysis* **2007**, 80, 118-125.

169 S Caratzoulas and DG Vlachos. Converting fructose to 5-hydroxymethylfurfural: a quantum mechanics/molecular mechanics study of the mechanism and energetics. *Carbohyd. Res.* **2011**,346, 664-672.

170 MS Mettler, *et al*.. Revealing pyrolysis chemistry for biofuels production: Conversion of cellulose to furans and small oxygenates. ***Energy Environ. Sci.*** **2012**, **5**, 5414-5424.

171 DK Shen and S Gu. The mechanism for thermal decomposition of cellulose and its main products. *Bioresour. Technol.* **2009**, 100, 6496–6504.

172 X Zhang, *et al*.. Routes to potential bioproducts from lignocellulosic biomass lighnin and hemicelluloses. *Bioenerg. Res.* **2011**, 4, 246-257.

173 J Sundquist, *et al*.. Environmentally friendly technologies for the pulp and paper industry (ed RA Young). *New York: Wiley* 1997.

174 K Nitta, *et al*.. Physicochemical properties of $ZnCl_2$-NaCl-KCl eutectic melt. *Electrochimica Acta* **2009**, 54, 4898-4902.

Appendix A

Table 17. Area percentage report for sample 1.

peak #	R.T. min	first scan	max scan	last scan	PK TY	peak height	corr. area	corr. % max.	% of total
1	1.264	176	190	203	BV	4294918	222520301	100.00%	27.178%
2	1.369	203	207	213	VV	1060110	20657424	9.28%	2.523%
3	1.457	213	221	224	VV 2	977908	23181493	10.42%	2.831%
4	1.493	224	227	235	VV	396601	9646217	4.33%	1.178%
5	1.606	235	245	247	VV 2	1073133	25757767	11.58%	3.146%
6	1.783	247	273	287	VV	2607214	195038294	87.65%	23.822%
7	2.028	297	313	328	VV	3586670	87351581	39.26%	10.669%
8	2.189	328	339	341	VV 2	146703	3889080	1.75%	0.475%
9	2.298	341	356	383	VB 3	310721	16166786	7.27%	1.975%
10	3.116	465	488	493	BV 2	328727	12462612	5.60%	1.522%
11	3.155	493	495	510	VB	162728	3161499	1.42%	0.386%
12	3.492	543	549	560	VV	135110	3979503	1.79%	0.486%
13	4.501	692	712	746	BB	2584361	90299450	40.58%	11.029%
14	5.235	801	830	839	BV	184701	6549902	2.94%	0.800%
15	5.749	892	913	938	BB 2	166101	9177406	4.12%	1.121%
16	7.786	1232	1241	1263	VV	282791	11446722	5.14%	1.398%
17	8.359	1314	1334	1358	BB 3	153725	7883678	3.54%	0.963%
18	10.992	1747	1758	1791	BB	289433	14204710	6.38%	1.735%
19	14.633	2330	2345	2355	BV	150739	4732077	2.13%	0.578%
20	17.450	2789	2799	2811	BV	628089	18310491	8.23%	2.236%
21	17.578	2811	2820	2839	VB	268720	9324800	4.19%	1.139%
22	21.298	3392	3420	3441	BB 2	692939	19653640	8.83%	2.400%
23	24.037	3847	3862	3875	BB	130753	3347033	1.50%	0.409%

Sum of corrected areas: 818742466

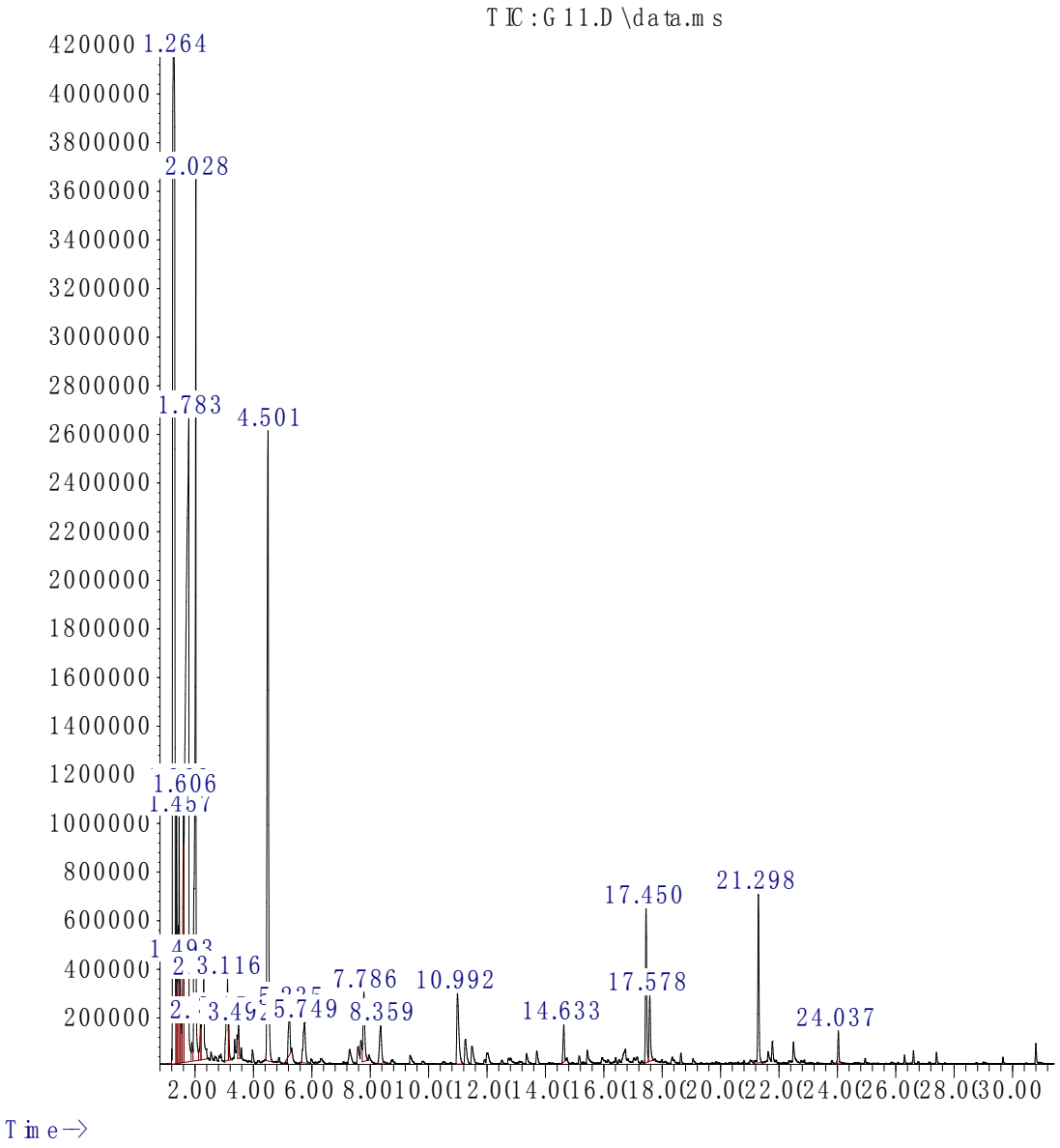

Figure 34: GC-MS graph for sample 1.

Table 18. Area percentage report for sample 2.

peak #	R.T. min	first scan	max scan	last scan	PK TY	peak height	corr. area	corr. % max.	% of total
1	1.265	175	190	203	BV	4319852	219388628	94.95%	23.909%
2	1.370	203	207	213	VV	1707209	32196101	13.93%	3.509%
3	1.437	213	218	225	VV 2	1971327	36814998	15.93%	4.012%
4	1.593	235	243	247	VV 2	1058990	26199262	11.34%	2.855%
5	1.802	247	276	287	VV	2996361	231044881	100.00%	25.179%
6	2.031	298	313	332	VV	4108185	102988788	44.58%	11.224%
7	2.190	332	339	344	VV	245576	6218769	2.69%	0.678%
8	2.344	344	364	381	VV 3	309343	20413151	8.84%	2.225%
9	3.119	465	489	513	BV 3	420042	16095841	6.97%	1.754%
10	3.360	513	528	537	PB	98792	1792459	0.78%	0.195%
11	4.526	685	716	752	BB	3305691	127462019	55.17%	13.891%
12	5.756	889	914	943	BB	178505	8671269	3.75%	0.945%
13	7.586	1196	1209	1224	BV	116502	5376051	2.33%	0.586%
14	7.788	1234	1242	1268	VV	260340	10674456	4.62%	1.163%
15	8.401	1315	1340	1368	BB 3	223256	13398649	5.80%	1.460%
16	11.007	1750	1761	1796	BV	563093	27387652	11.85%	2.985%
17	14.646	2331	2347	2357	BV 2	146740	4676948	2.02%	0.510%
18	17.457	2789	2801	2813	BV	555159	15491286	6.70%	1.688%
19	21.303	3402	3421	3447	BB	400305	11307093	4.89%	1.232%

Sum of corrected areas: 917598299

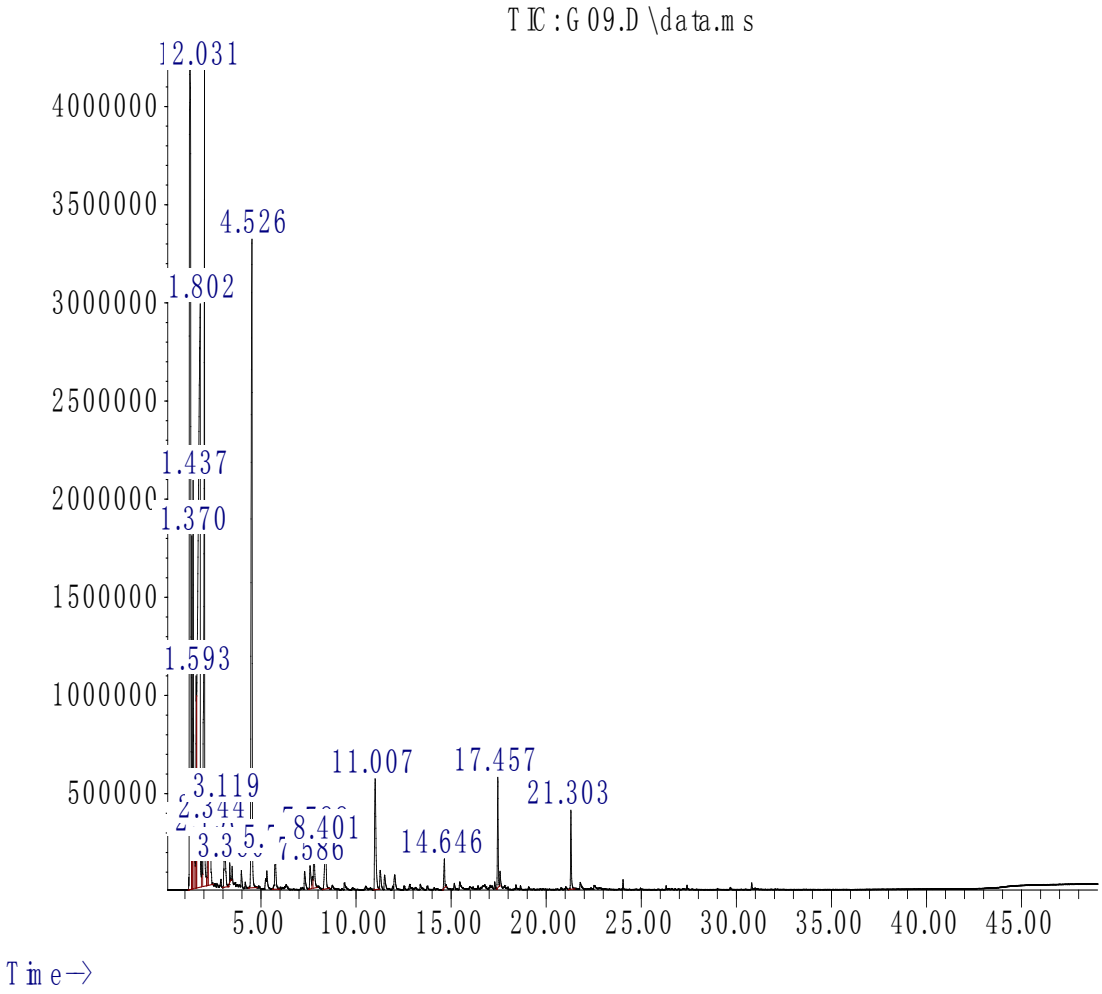

Figure 35: GC-MS graph for sample 2.

Table 19. Area percentage report for sample 3.

peak #	R.T. min	first scan	max scan	last scan	PK TY	peak height	corr. area	corr. % max.	% of total
1	1.262	177	189	203	BV	4350301	193180470	71.91%	12.870%
2	1.368	203	206	213	VV	1788076	37119486	13.82%	2.473%
3	1.436	213	217	224	VV 2	1078503	26527285	9.87%	1.767%
4	1.491	224	226	235	VV	391101	10071825	3.75%	0.671%
5	1.592	235	243	247	VV	2068746	41590079	15.48%	2.771%
6	1.815	247	279	286	VV	3245334	268657378	100.00%	17.898%
7	1.886	286	290	296	VV	250091	5413080	2.01%	0.361%
8	2.024	296	312	326	VV	4998958	140752063	52.39%	9.377%
9	2.188	332	339	344	VV	280218	6856716	2.55%	0.457%
10	2.291	344	355	360	VV 3	431399	16031908	5.97%	1.068%
11	2.375	360	369	389	VB 6	402771	18274208	6.80%	1.217%
12	3.107	465	487	490	BV	931644	25146029	9.36%	1.675%
13	3.142	490	492	512	VV	639376	12090695	4.50%	0.806%
14	3.337	519	524	537	PV	450742	9480117	3.53%	0.632%
15	3.486	537	548	562	VV 3	186607	6224159	2.32%	0.415%
16	4.495	677	711	734	BV 2	2141282	90662577	33.75%	6.040%
17	5.247	816	832	837	VV 3	452217	17885685	6.66%	1.192%
18	5.288	837	839	862	VB	290435	7729909	2.88%	0.515%
19	5.748	875	913	941	BV	469418	21653426	8.06%	1.443%
20	5.960	941	947	965	PB	110629	3883984	1.45%	0.259%
21	7.282	1141	1160	1187	BB 5	138769	6797045	2.53%	0.453%
22	7.579	1196	1208	1217	BV 2	107286	5201849	1.94%	0.347%
23	7.685	1217	1225	1232	VV 3	188496	8127424	3.03%	0.541%
24	7.859	1232	1253	1267	VV	499978	31588518	11.76%	2.104%
25	8.481	1312	1353	1378	BV	389853	35316863	13.15%	2.353%
26	10.999	1735	1759	1793	BV 4	413573	23337296	8.69%	1.555%
27	11.271	1793	1803	1826	PV 2	170249	7783906	2.90%	0.519%
28	11.494	1826	1839	1862	PB 2	142077	6388034	2.38%	0.426%
29	12.026	1892	1925	1952	BB 5	160529	11701347	4.36%	0.780%
30	14.761	2321	2366	2390	BB 2	531407	38900586	14.48%	2.592%
31	15.412	2464	2471	2483	BV	105548	3199308	1.19%	0.213%
32	17.005	2662	2728	2743	BV 7	240066	32486693	12.09%	2.164%
33	17.469	2787	2803	2816	VV	1230929	39767805	14.80%	2.649%
34	17.736	2816	2846	2878	VV	788560	55590550	20.69%	3.704%

35	18.428	2945	2957	2986	BV 2	200460	10203436	3.80%	0.680%
36	18.711	2986	3003	3022	VB	167627	5935798	2.21%	0.395%
37	21.056	3371	3381	3404	PV 6	118071	5103799	1.90%	0.340%
38	21.313	3404	3422	3452	PB 2	1495926	49728203	18.51%	3.313%
39	21.679	3452	3481	3499	BV	725644	30467230	11.34%	2.030%
40	21.869	3499	3512	3539	VB	355447	15787226	5.88%	1.052%
41	22.392	3581	3596	3611	BV 3	113469	4447450	1.66%	0.296%
42	22.580	3611	3627	3654	VV	219940	10155183	3.78%	0.677%
43	24.040	3846	3862	3870	PV	526957	13280080	4.94%	0.885%
44	24.443	3915	3927	3952	BV	197860	7242927	2.70%	0.483%
45	26.305	4203	4227	4238	VV	156074	4604497	1.71%	0.307%
46	27.413	4388	4406	4423	PV	211508	6155179	2.29%	0.410%
47	28.755	4593	4622	4656	BV 3	282168	10342107	3.85%	0.689%
48	29.690	4749	4773	4785	BV	244531	6183335	2.30%	0.412%
49	30.202	4785	4856	4888	VV 7	147638	28453496	10.59%	1.896%
50	30.819	4915	4955	4971	BB	474737	11178230	4.16%	0.745%
51	31.050	4974	4992	5017	BB 2	149265	7914040	2.95%	0.527%
52	33.560	5378	5397	5433	BB	201592	8416820	3.13%	0.561%

Sum of corrected areas: 1501017337

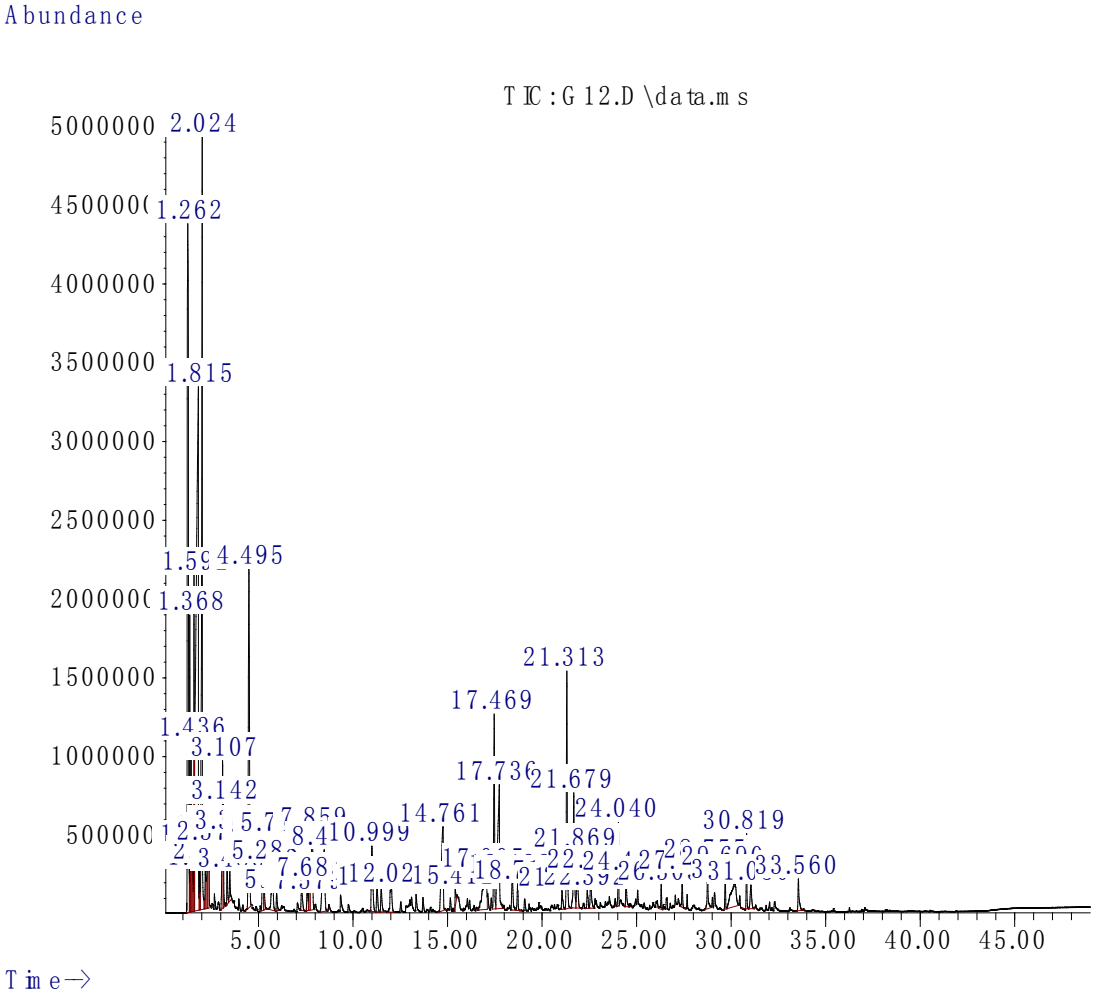

Figure 36: GC-MS graph for sample 3.

Table 20. Area percentage report for sample 4.

peak #	R.T. min	first scan	max scan	last scan	PK TY	peak height	corr. area	corr. % max.	% of total
1	1.243	176	186	187	BV 2	4202577	62101104	36.08%	8.024%
2	1.262	187	189	195	VV 2	4271001	121744391	70.74%	15.731%
3	1.308	195	197	203	VV	4289411	72306983	42.01%	9.343%
4	1.367	203	206	210	VV 2	1163971	20000192	11.62%	2.584%
5	1.439	210	218	230	VV 2	1835131	58180175	33.80%	7.518%
6	1.536	230	234	238	VV	727630	13878654	8.06%	1.793%
7	1.752	238	268	272	VV	2301889	172107163	100.00%	22.239%
8	1.800	272	276	298	VV	514027	22915356	13.31%	2.961%
9	2.009	298	310	311	VV	396783	9100534	5.29%	1.176%
10	2.031	311	313	320	VV	502848	6750570	3.92%	0.872%
11	2.242	327	347	359	VV 3	170065	10200643	5.93%	1.318%
12	2.395	359	372	393	VB 4	175538	8541950	4.96%	1.104%
13	4.520	684	715	745	BB	3751199	142278065	82.67%	18.385%
14	6.281	991	999	1029	VB	146574	6936723	4.03%	0.896%
15	7.779	1231	1240	1268	VB	237891	10716489	6.23%	1.385%
16	10.984	1744	1757	1791	BB	564517	26520592	15.41%	3.427%
17	14.617	2329	2343	2355	BV	131384	4366085	2.54%	0.564%
18	17.443	2789	2798	2813	BV	188761	5252900	3.05%	0.679%

Sum of corrected areas: 773898569

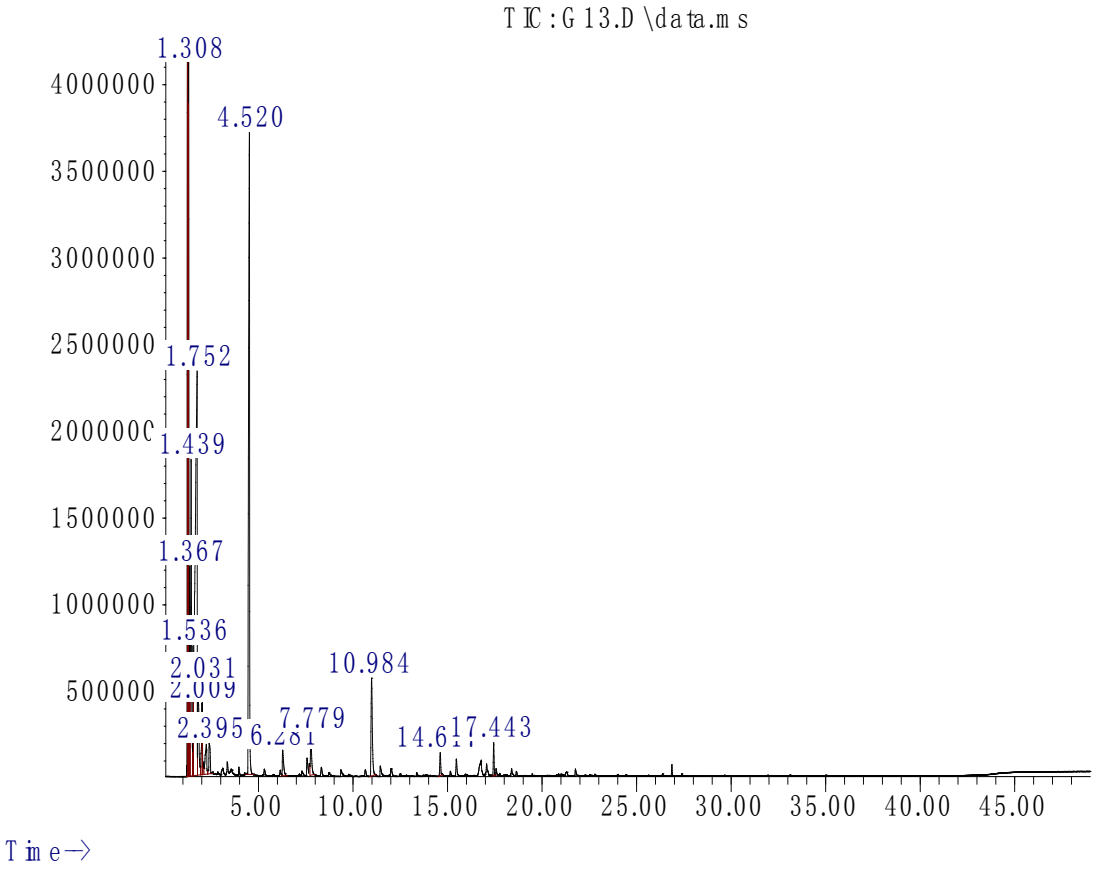

Figure 37: GC-MS graph for sample 4.

Table 21. Area percentage report for sample 5.

peak #	R.T. min	first scan	max scan	last scan	PK TY	peak height	corr. area	corr. % max.	% of total
1	1.259	177	189	195	BV	4048986	170564080	100.00%	37.546%
2	1.311	195	197	203	VV 2	4097340	71567883	41.96%	15.754%
3	1.366	203	206	213	VV	905933	14939974	8.76%	3.289%
4	1.462	213	222	234	VV 2	579546	14311691	8.39%	3.150%
5	1.734	234	266	298	VV	1831684	120521983	70.66%	26.530%
6	4.480	700	708	742	BB	2158488	62379401	36.57%	13.731%

Sum of corrected areas: 454285011

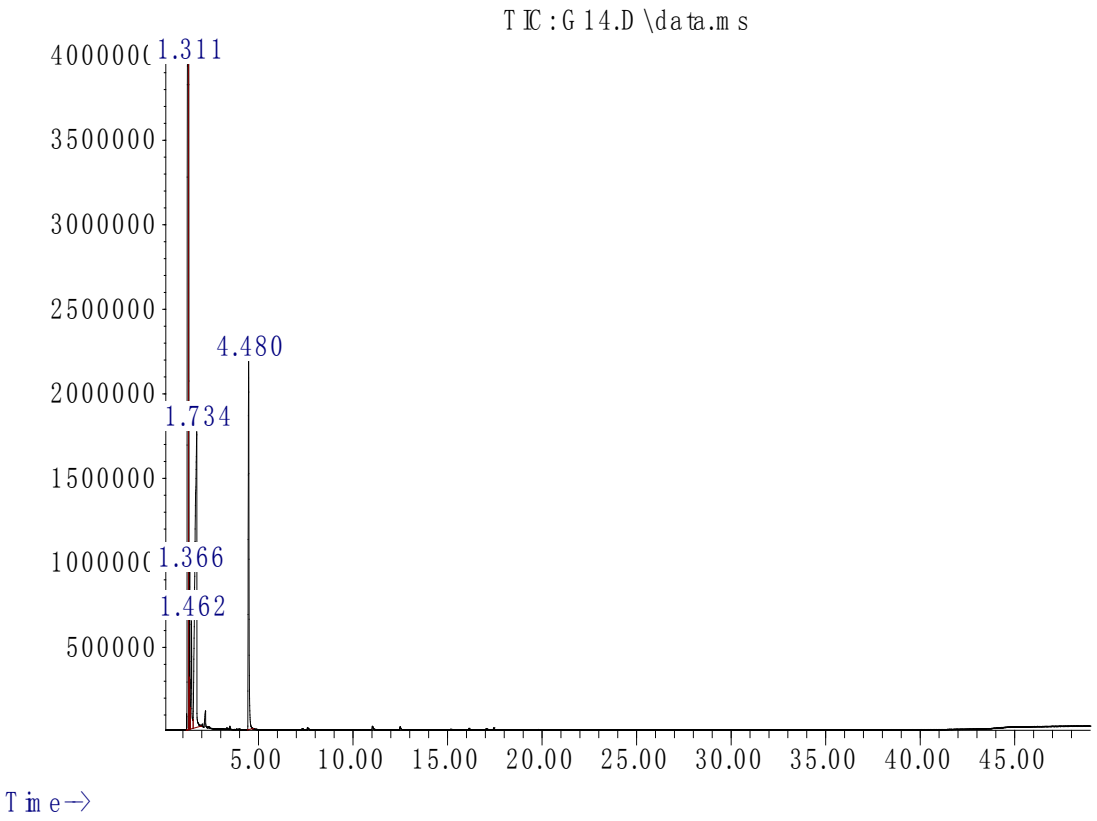

Figure 38: GC-MS graph for sample 5.

Table 22. Area percentage report for sample 6.

peak #	R.T. min	first scan	max scan	last scan	PK TY	peak height	corr. area	corr. % max.	% of total
1	1.261	181	189	195	VV 2	3994101	165247107	100.00%	30.745%
2	1.311	195	197	203	VV	4245645	77267610	46.76%	14.376%
3	1.365	203	206	212	VV	1655675	24472457	14.81%	4.553%
4	1.433	212	217	219	VV	468010	7299353	4.42%	1.358%
5	1.455	219	221	234	VV	547048	10353588	6.27%	1.926%
6	1.753	234	268	298	VB	2268696	161207447	97.56%	29.994%
7	2.226	322	345	358	BV	147013	5219193	3.16%	0.971%
8	4.491	697	710	747	BB	2831283	86407790	52.29%	16.077%

Sum of corrected areas: 537474544

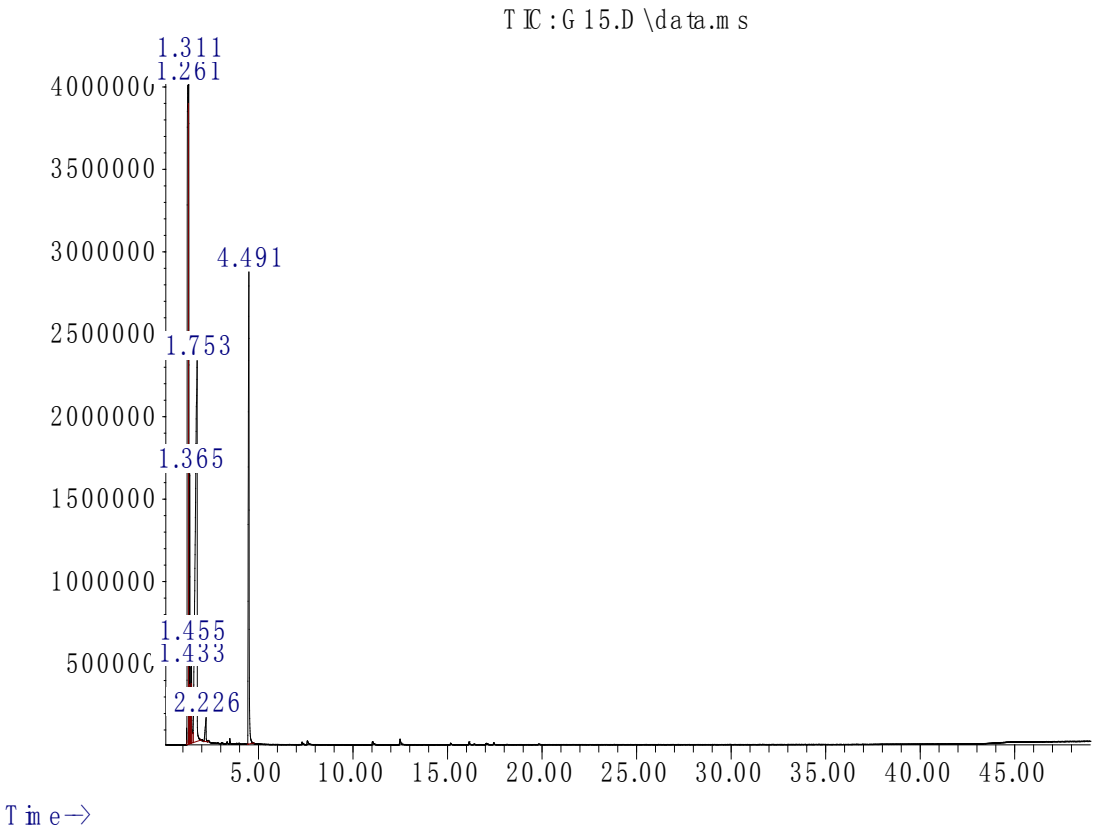

Figure 39: GC-MS graph for sample 6.

Table 23. Area percentage report for sample 7.

peak #	R.T. min	first scan	max scan	last scan	PK TY	peak height	corr. area	corr. % max.	% of total
1	1.262	181	189	203	VV 2	3989051	230901482	100.00%	43.208%
2	1.365	203	206	213	VV	1366127	19325783	8.37%	3.616%
3	1.432	213	217	219	VV	482610	6212080	2.69%	1.162%
4	1.462	219	222	231	VV	331913	5316599	2.30%	0.995%
5	1.746	231	267	287	VV	2101876	145630248	63.07%	27.251%
6	2.221	322	344	358	BV 4	132676	4629001	2.00%	0.866%
7	4.506	697	712	744	BB	3519715	122382839	53.00%	22.901%

Sum of corrected areas: 534398032

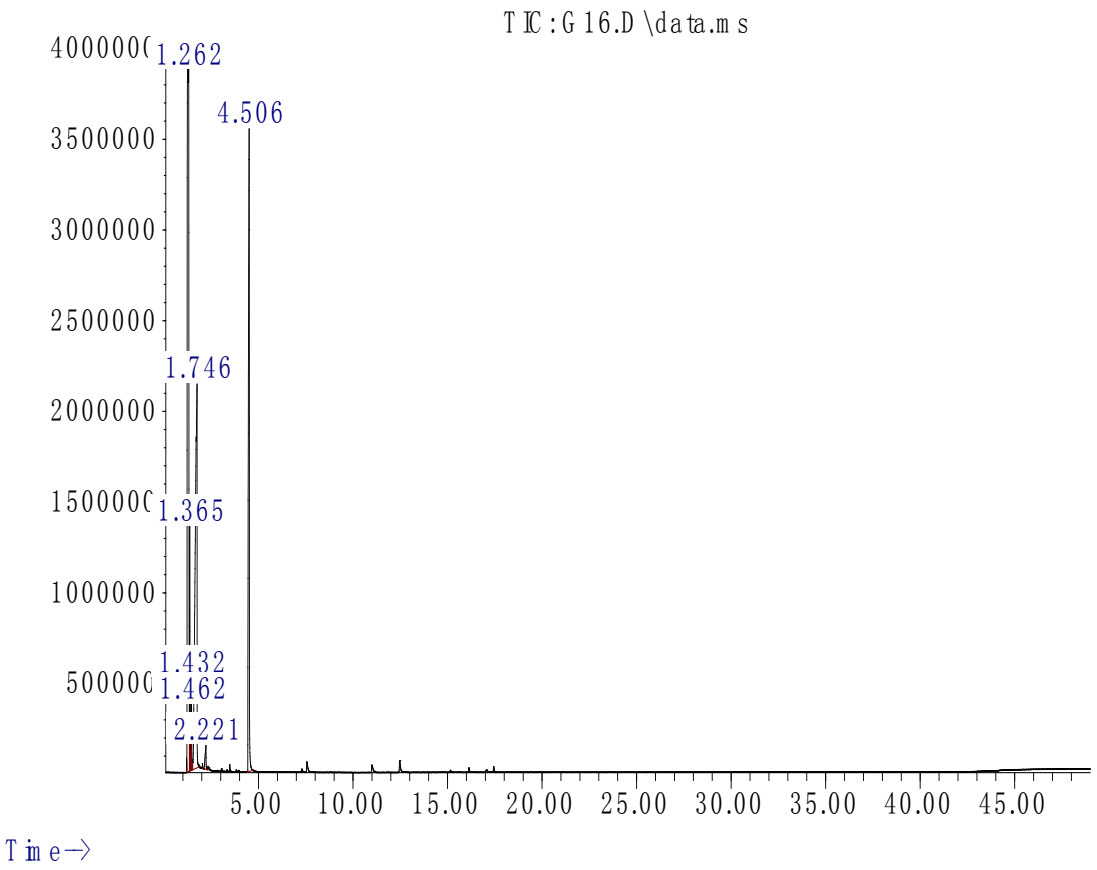

Figure 40: GC-MS graph for sample 7.

Table 24. Area percentage report for sample 8.

peak #	R.T. min	first scan	max scan	last scan	PK TY	peak height	corr. area	corr. % max.	% of total
1	1.262	181	189	203	VV 2	4032190	212234778	96.76%	24.980%
2	1.366	203	206	211	VV	1335187	22043882	10.05%	2.595%
3	1.433	211	217	219	VV	1147252	19094645	8.71%	2.247%
4	1.451	219	220	230	VV	946726	14487439	6.60%	1.705%
5	1.536	230	233	236	VV	291830	4662444	2.13%	0.549%
6	1.588	236	242	243	VV	1073743	16392394	7.47%	1.929%
7	1.783	243	273	286	VV 2	2767699	219349526	100.00%	25.818%
8	2.018	297	311	319	PV	3072071	64872108	29.57%	7.635%
9	2.087	319	322	331	VV	155508	2372746	1.08%	0.279%
10	2.181	331	338	342	PV	193061	3066019	1.40%	0.361%
11	2.315	342	359	366	VV 2	205487	9472477	4.32%	1.115%
12	3.110	468	487	513	BB 2	217832	8661321	3.95%	1.019%
13	4.510	692	713	752	BB	3551141	136339296	62.16%	16.047%
14	7.260	1150	1157	1183	BB 2	120276	5008485	2.28%	0.590%
15	7.544	1193	1202	1219	BV	220031	9833830	4.48%	1.157%
16	7.752	1229	1236	1267	VB	208312	8701619	3.97%	1.024%
17	8.327	1311	1329	1352	BB 2	110503	5483146	2.50%	0.645%
18	10.976	1742	1756	1793	BV	717872	37064848	16.90%	4.363%
19	14.624	2330	2344	2353	BV	178053	5966291	2.72%	0.702%
20	17.272	2763	2771	2786	VV	123910	3670305	1.67%	0.432%
21	17.439	2786	2798	2818	PV	1070130	30806910	14.04%	3.626%
22	21.282	3405	3417	3438	BV	382895	10028613	4.57%	1.180%

Sum of corrected areas: 849613123

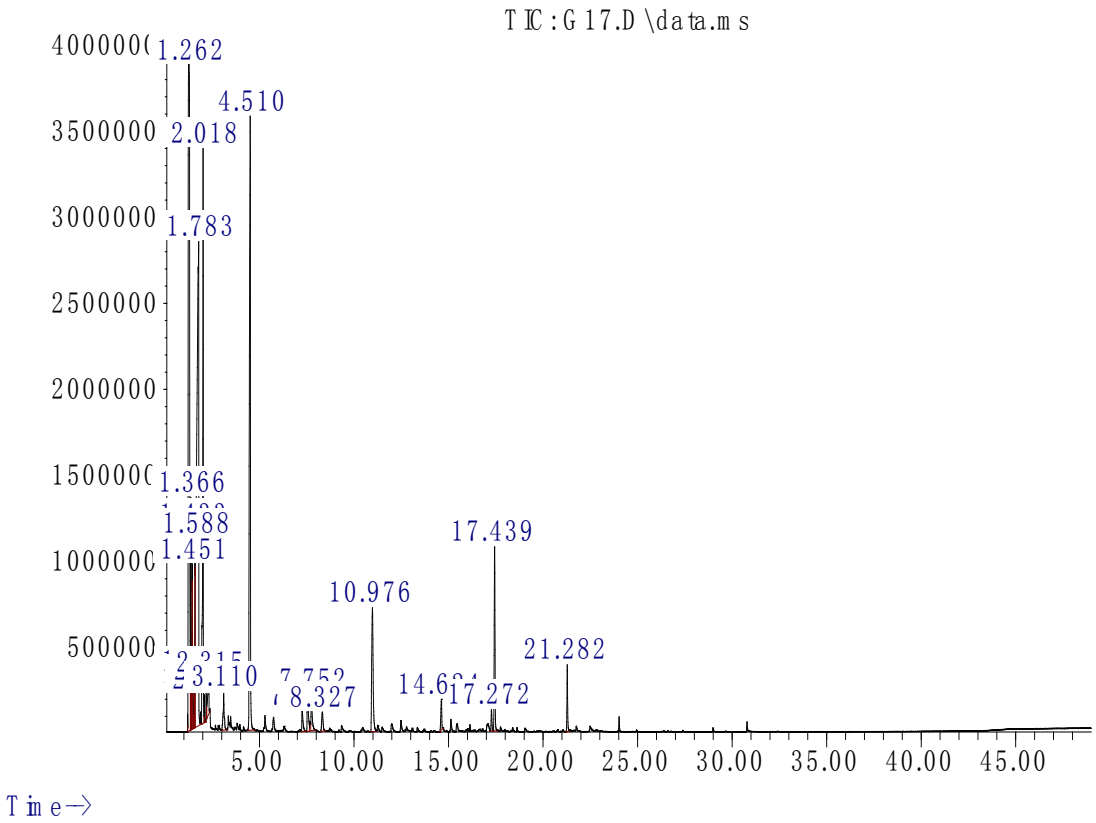

Figure 41: GC-MS graph for sample 8.

Table 25. Area percentage report for sample 9.

peak #	R.T. min	first scan	max scan	last scan	PK TY	peak height	corr. area	corr. % max.	% of total
1	1.258	176	189	203	BV 2	3697560	218482073	100.00%	48.928%
2	1.362	203	206	212	VV	933716	14015174	6.41%	3.139%
3	1.459	218	221	230	VV	252514	4575372	2.09%	1.025%
4	1.729	230	265	294	VB	1868184	115861910	53.03%	25.947%
5	4.484	697	709	742	BB	2979022	93604826	42.84%	20.962%

Sum of corrected areas: 446539354

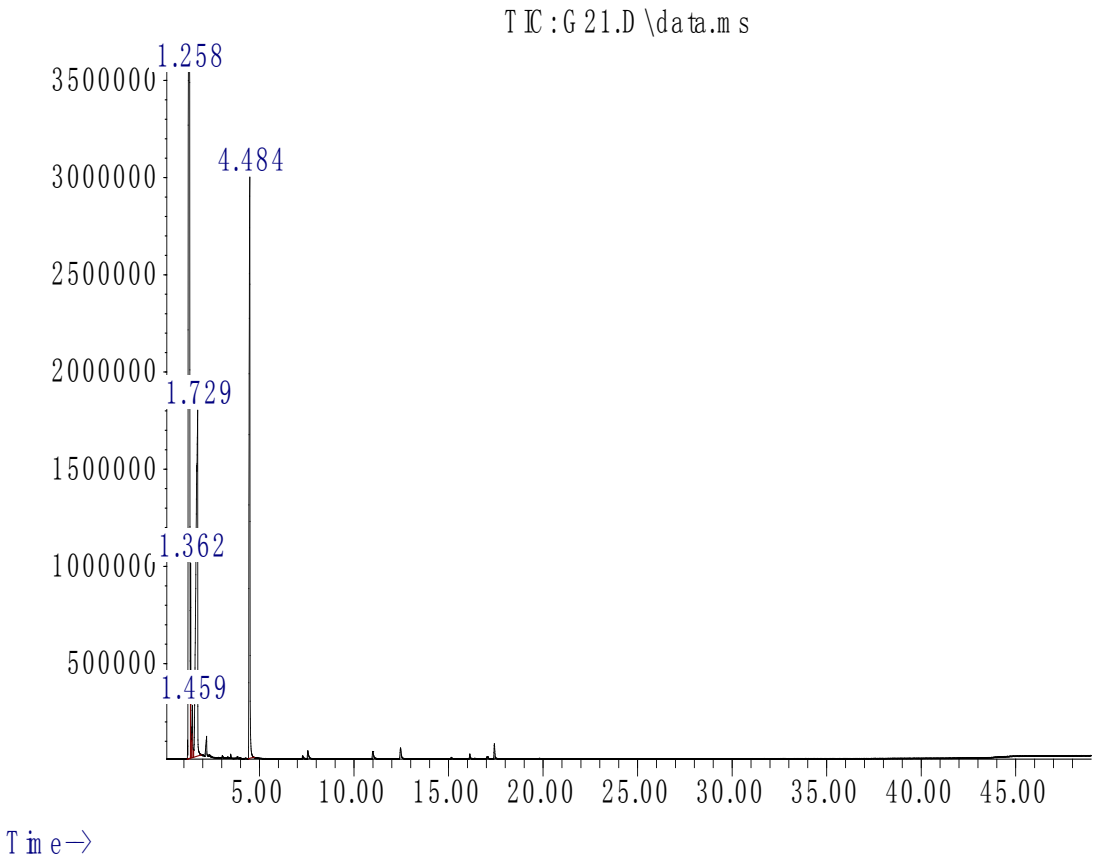

Figure 42: GC-MS graph for sample 9.

Table 26. Area percentage report for sample 10.

peak #	R.T. min	first scan	max scan	last scan	PK TY	peak height	corr. area	corr. % max.	% of total
1	1.260	173	189	203	BV	3682999	216455927	100.00%	51.423%
2	1.362	203	205	212	VV	1166289	16693155	7.71%	3.966%
3	1.460	218	221	231	VV	257535	4605665	2.13%	1.094%
4	1.729	231	265	293	VB	1807693	112017121	51.75%	26.612%
5	4.473	696	707	741	BB	2526975	71162808	32.88%	16.906%

Sum of corrected areas: 420934676

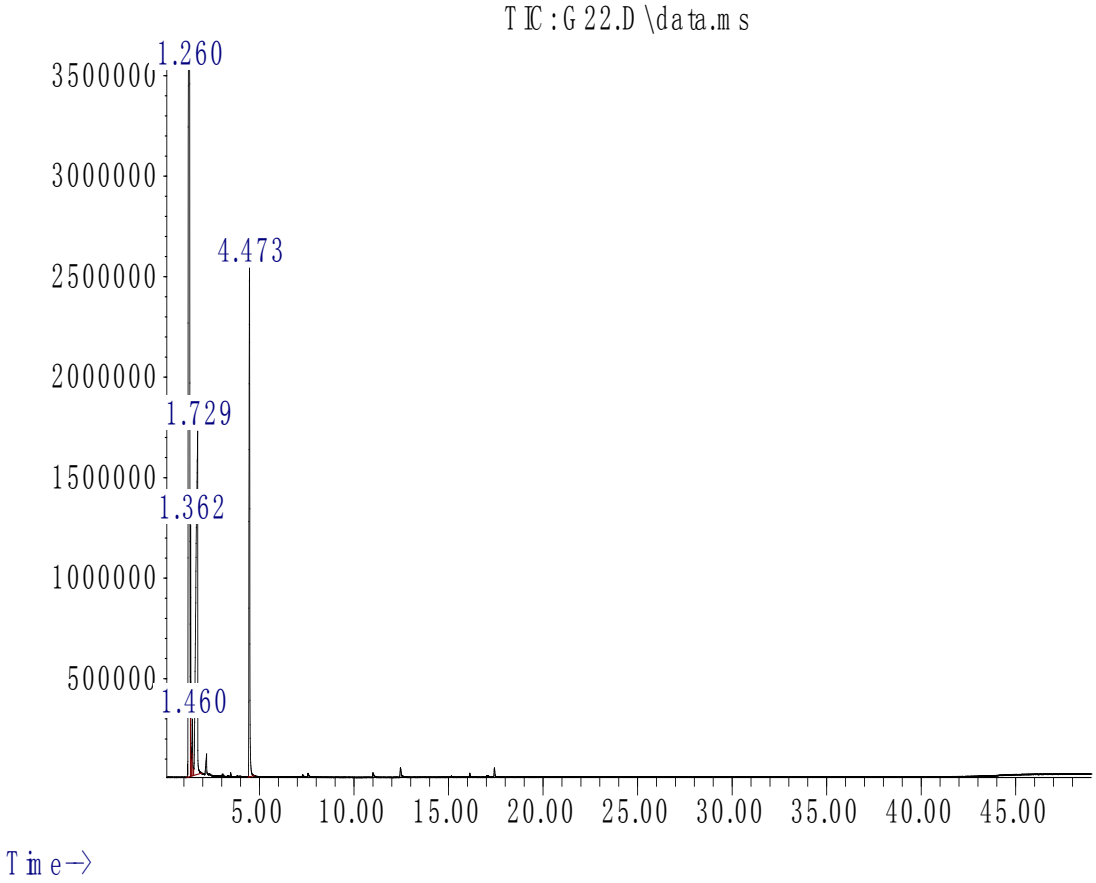

Figure 43: GC-MS graph for sample 10.

Table 27. Area percentage report for sample 11.

peak #	R.T. min	first scan	max scan	last scan	PK TY	peak height	corr. area	corr. % max.	% of total
1	1.259	181	189	195	PV 2	3815360	165650859	100.00%	37.616%
2	1.309	195	197	203	VV	3907686	68886799	41.59%	15.643%
3	1.362	203	205	213	VV	1315429	19218860	11.60%	4.364%
4	1.430	213	216	233	VB 2	251667	5505562	3.32%	1.250%
5	1.729	233	265	296	BB	1941691	112716928	68.04%	25.596%
6	2.206	323	342	356	BB 2	109892	3697967	2.23%	0.840%
7	4.471	697	707	743	BB	2272902	64694373	39.05%	14.691%

Sum of corrected areas: 440371349

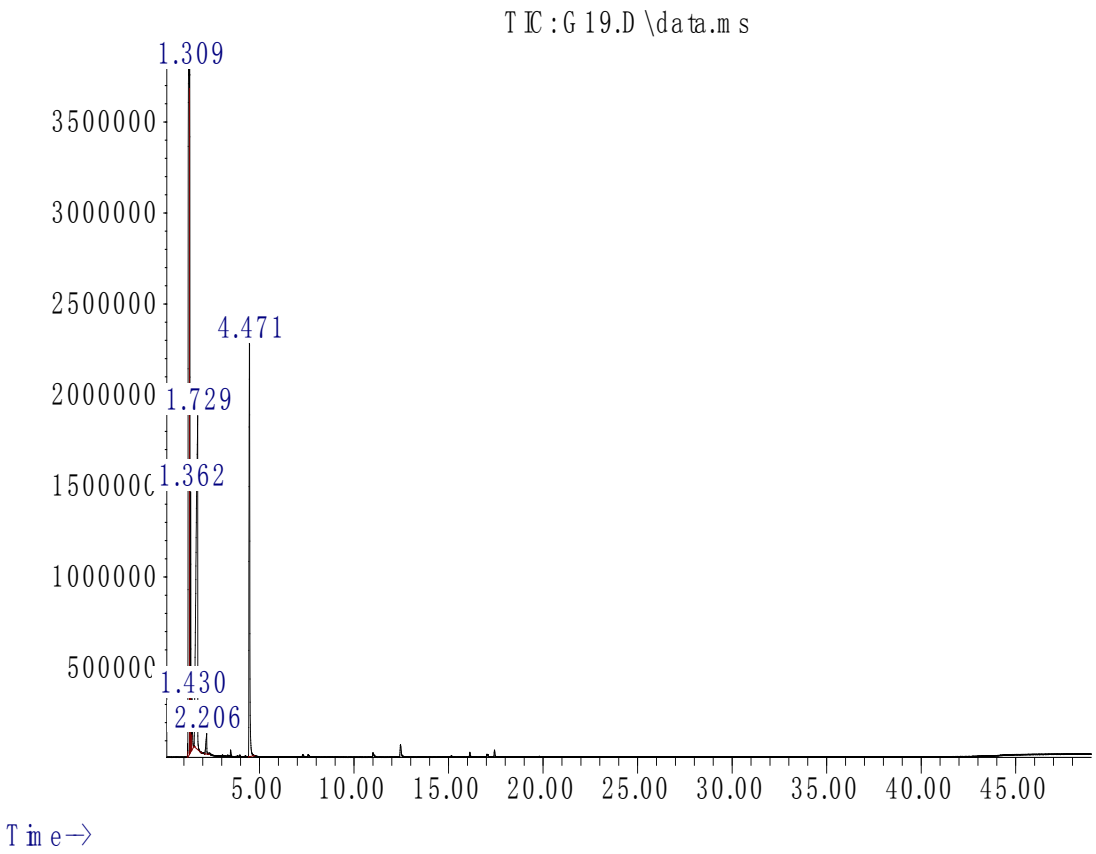

Figure 44: GC-MS graph for sample 11.

Table 28. Area percentage report for sample 12.

peak #	R.T. min	first scan	max scan	last scan	PK TY	peak height	corr. area	corr. % max.	% of total
1	1.259	181	189	203	PV 3	3727504	222619778	100.00%	58.931%
2	1.362	203	205	213	VV	1062924	15315057	6.88%	4.054%
3	1.460	218	221	230	VB	230450	3461800	1.56%	0.916%
4	1.735	232	266	296	BB	1901424	118639573	53.29%	31.406%
5	2.220	321	344	358	BB 3	138789	4610347	2.07%	1.220%
6	4.460	700	705	732	BB	468328	13114817	5.89%	3.472%

Sum of corrected areas: 377761371

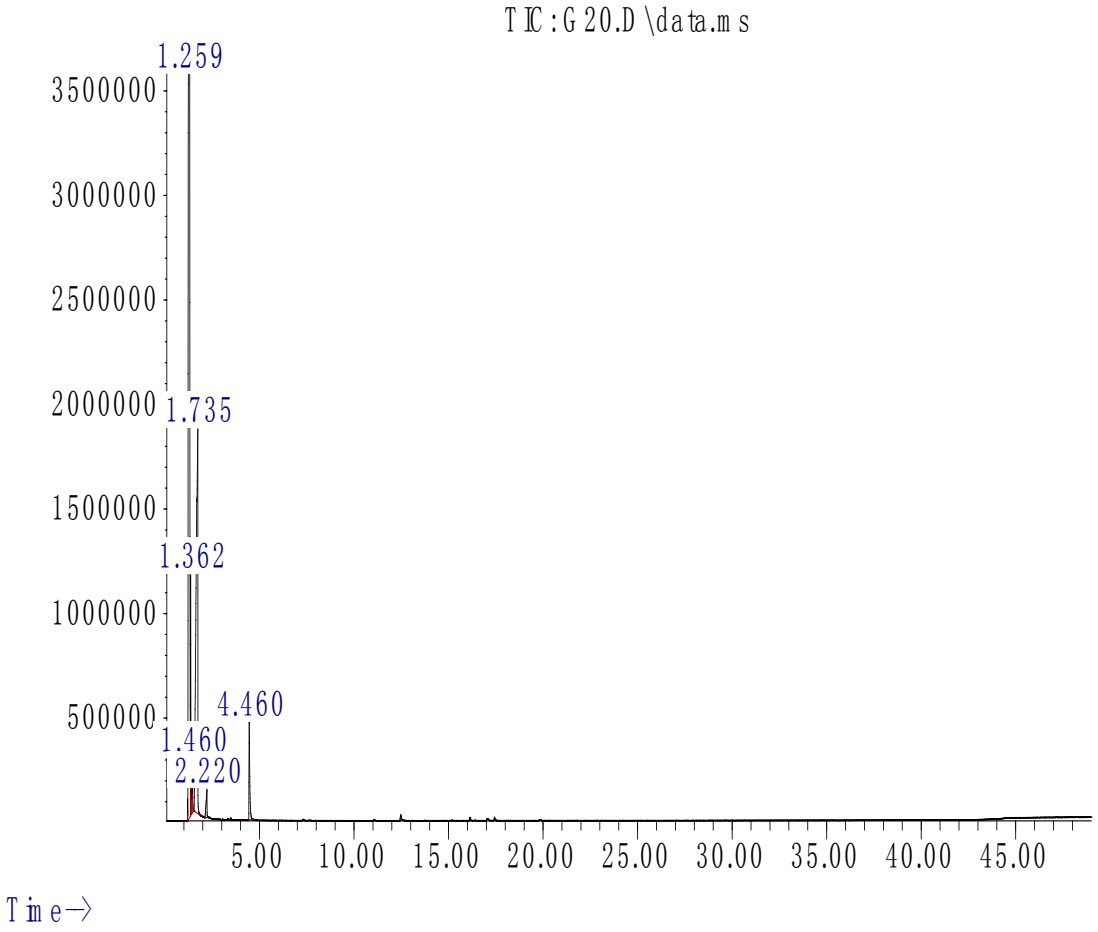

Figure 45: GC-MS graph for sample 12.

Table 29. Area percentage report for sample 13.

peak #	R.T. min	first scan	max scan	last scan	PK TY	peak height	corr. area	corr. % max.	% of total
1	1.259	181	189	203	PV 2	3880004	227281057	100.00%	42.715%
2	1.363	203	206	213	VV	1033812	15996497	7.04%	3.006%
3	1.432	213	217	219	VV	317318	4802858	2.11%	0.903%
4	1.461	219	221	231	VV	367604	6492370	2.86%	1.220%
5	1.753	231	269	298	VV	2199860	159517569	70.19%	29.980%
6	2.025	298	312	326	VV	141652	3637292	1.60%	0.684%
7	2.236	326	346	356	VV 3	158287	6550134	2.88%	1.231%
8	4.486	693	709	745	BB	2896540	91928090	40.45%	17.277%
9	12.464	1985	1996	2017	BB 2	107287	4351429	1.91%	0.818%
10	17.427	2787	2796	2814	BB	313492	8827505	3.88%	1.659%
11	21.281	3408	3417	3430	BB	114222	2702049	1.19%	0.508%

Sum of corrected areas: 532086851

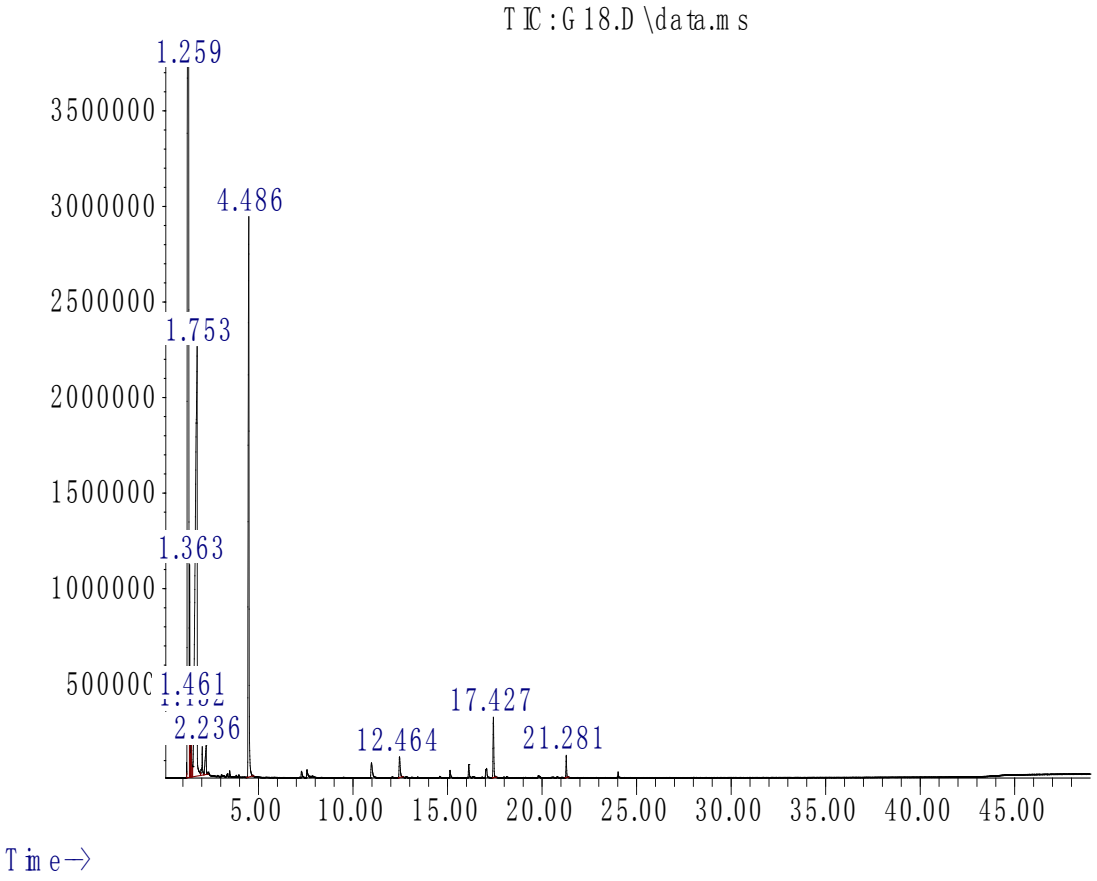

Figure 46: GC-MS graph for sample 13.

Table 30. Area percentage report for newspaper.

peak #	R.T. min	first scan	max scan	last scan	PK TY	peak height	corr. area	corr. % max.	% of total
1	1.261	176	189	203	BV	4224075	206062308	100.00%	19.727%
2	1.366	203	206	210	VV	1099826	19129250	9.28%	1.831%
3	1.444	210	219	224	VV 2	1326759	39309076	19.08%	3.763%
4	1.490	224	226	234	VV	342706	8935199	4.34%	0.855%
5	1.596	234	243	247	VV 2	1400216	31788917	15.43%	3.043%
6	1.791	247	275	286	VV	2832945	201849959	97.96%	19.324%
7	1.884	286	290	295	VV 2	165812	3528942	1.71%	0.338%
8	2.022	295	312	326	VV	4044208	112874687	54.78%	10.806%
9	2.186	326	338	343	VV	187261	5730954	2.78%	0.549%
10	2.297	343	356	360	VV 3	418658	16335368	7.93%	1.564%
11	2.331	360	362	379	VB 4	349352	10078771	4.89%	0.965%
12	3.107	466	487	490	BV	567689	17527800	8.51%	1.678%
13	3.143	490	493	512	VV	465033	10687931	5.19%	1.023%
14	3.340	512	524	534	VV	274363	6188003	3.00%	0.592%
15	3.482	534	547	559	VV 3	302026	12391749	6.01%	1.186%
16	4.495	692	711	742	BV	2307134	97202493	47.17%	9.306%
17	5.233	817	830	835	BV 2	123524	4565174	2.22%	0.437%
18	5.287	835	838	862	VB	132547	4288334	2.08%	0.411%
19	5.739	875	911	939	BV 2	282674	16829185	8.17%	1.611%
20	5.945	939	945	964	PB	105046	3503436	1.70%	0.335%
21	7.269	1142	1158	1186	BV 2	158800	7061217	3.43%	0.676%
22	7.561	1186	1205	1216	PV	156211	7424259	3.60%	0.711%
23	7.678	1216	1224	1232	VV 2	180433	8544476	4.15%	0.818%
24	7.819	1232	1247	1264	VV	391734	19521411	9.47%	1.869%
25	8.388	1311	1338	1366	BB 2	217158	14320436	6.95%	1.371%
26	10.984	1737	1757	1792	BB 4	420561	23630427	11.47%	2.262%
27	12.016	1891	1923	1948	BB 4	122711	8775397	4.26%	0.840%
28	14.710	2332	2358	2378	BV	443168	24953792	12.11%	2.389%
29	17.458	2785	2801	2813	PV	1324909	40915030	19.86%	3.917%
30	18.643	2982	2992	3007	BB	104667	2920477	1.42%	0.280%
31	21.302	3394	3421	3442	PB	1118605	32253533	15.65%	3.088%
32	21.629	3447	3473	3492	BV	153205	5980533	2.90%	0.573%
33	21.792	3492	3500	3512	VV	140168	4039274	1.96%	0.387%
34	24.032	3846	3861	3877	BB	301065	8210420	3.98%	0.786%

35	29.673	4754	4770	4796	BB	2	105004	3979383	1.93%	0.381%
36	30.799	4940	4952	4966	BV		132118	3210921	1.56%	0.307%

Sum of corrected areas: 1044548522

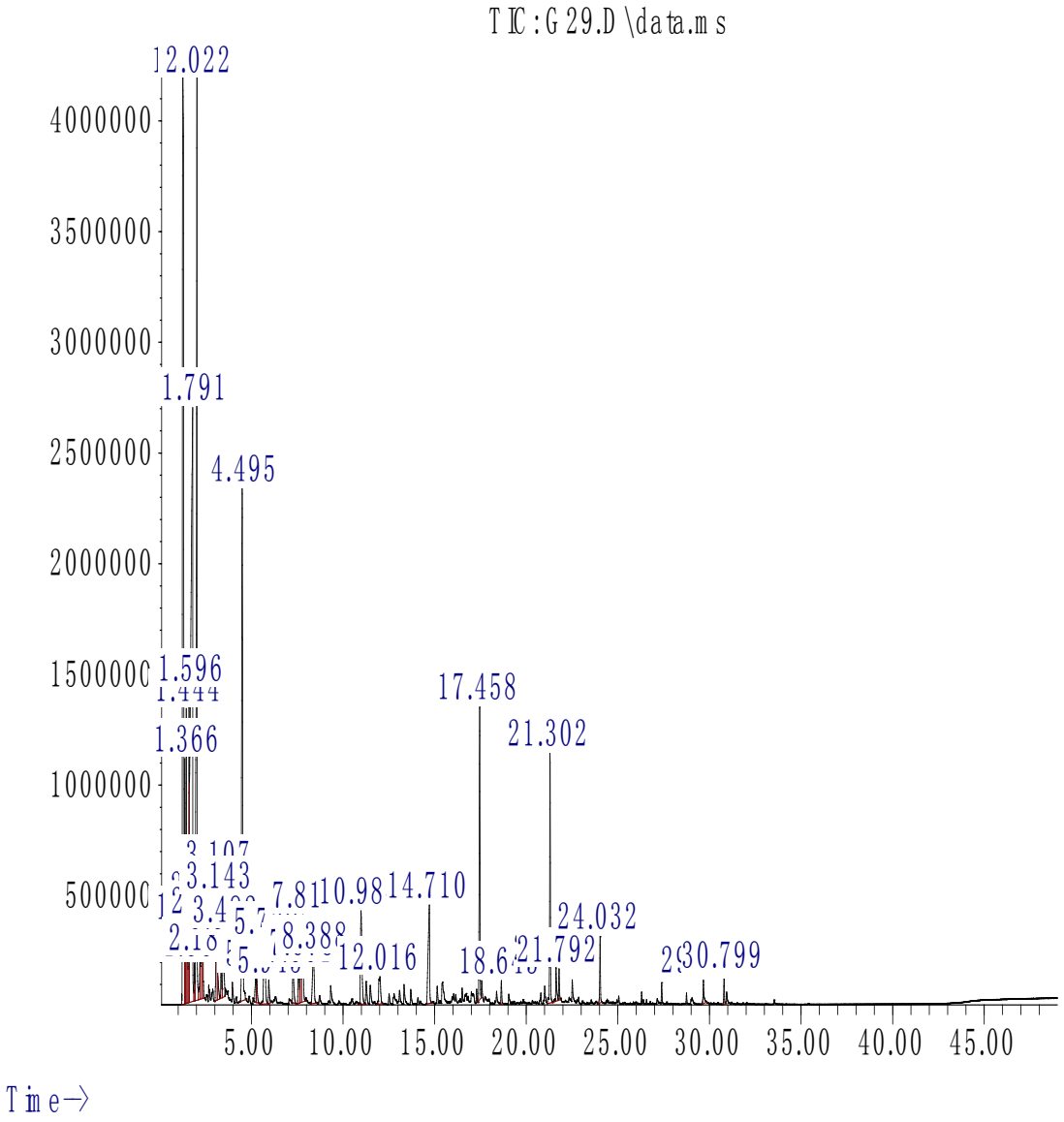

Figure 47: GC-MS graph for newspaper.

Table 31. Area percentage report for paper.

peak #	R.T. min	first scan	max scan	last scan	PK TY	peak height	corr. area	corr. % max.	% of total
1	1.262	177	189	203	BV 2	3957736	204449038	100.00%	21.616%
2	1.367	203	206	214	VV	1087685	19944558	9.76%	2.109%
3	1.451	214	220	231	VV 3	770517	18234804	8.92%	1.928%
4	1.598	231	244	247	VV 2	1410051	30977742	15.15%	3.275%
5	1.734	247	266	286	VV	1517845	87341609	42.72%	9.235%
6	2.025	296	312	326	VV	3848138	106118985	51.90%	11.220%
7	2.186	326	338	344	VV	239742	7614311	3.72%	0.805%
8	2.302	344	357	364	VV 3	423655	22094693	10.81%	2.336%
9	2.390	364	371	393	VB 3	419286	15430510	7.55%	1.631%
10	3.111	466	488	492	BV	490924	15242051	7.46%	1.612%
11	3.149	492	494	497	VV	94551	1045560	0.51%	0.111%
12	3.347	519	526	534	BV	197776	4249333	2.08%	0.449%
13	3.485	534	548	564	VV 4	259853	13449179	6.58%	1.422%
14	3.960	619	625	644	VB	115875	3618722	1.77%	0.383%
15	4.513	674	714	742	BB	2925580	116314382	56.89%	12.298%
16	5.237	816	830	836	BV 3	201829	8842721	4.33%	0.935%
17	5.292	836	839	860	VB	136281	4208589	2.06%	0.445%
18	5.664	892	899	902	VV 2	231504	5304902	2.59%	0.561%
19	5.741	902	912	939	VV	268741	14584636	7.13%	1.542%
20	5.944	939	944	963	PV	142692	4453646	2.18%	0.471%
21	7.269	1146	1158	1184	BV 2	183474	7889745	3.86%	0.834%
22	7.559	1184	1205	1218	PV 2	236835	10761219	5.26%	1.138%
23	7.676	1218	1224	1232	VV 3	112725	4632867	2.27%	0.490%
24	7.813	1232	1246	1265	VV	380172	18846511	9.22%	1.993%
25	8.412	1306	1342	1374	BB 4	262050	19707155	9.64%	2.084%
26	11.006	1739	1761	1792	BV	778170	42310693	20.69%	4.474%
27	11.254	1792	1801	1825	VV	236113	10604425	5.19%	1.121%
28	11.476	1825	1836	1865	PB	178775	8252286	4.04%	0.873%
29	12.018	1891	1924	1945	BB 4	156043	9094451	4.45%	0.962%
30	14.710	2333	2358	2377	BV 3	430519	24038535	11.76%	2.542%
31	15.135	2406	2426	2444	BV 3	129105	4514491	2.21%	0.477%
32	15.430	2463	2474	2505	BB 4	121514	7733883	3.78%	0.818%
33	16.894	2666	2710	2719	BV 4	125601	13354034	6.53%	1.412%
34	17.618	2814	2827	2837	PV	315530	11821073	5.78%	1.250%

35	18.391	2940	2951	2980	VB 3	170606	7866440	3.85%	0.832%
36	18.683	2983	2998	3015	BB	152056	4711406	2.30%	0.498%
37	19.049	3050	3057	3075	BV	109786	3891883	1.90%	0.411%
38	21.012	3358	3374	3394	BV 3	235027	7800430	3.82%	0.825%
39	21.641	3468	3475	3492	PV	176997	5755170	2.81%	0.608%
40	21.813	3492	3503	3513	VV	423831	12923269	6.32%	1.366%
41	22.521	3602	3617	3648	BB 2	176750	5776205	2.83%	0.611%

Sum of corrected areas: 945806140

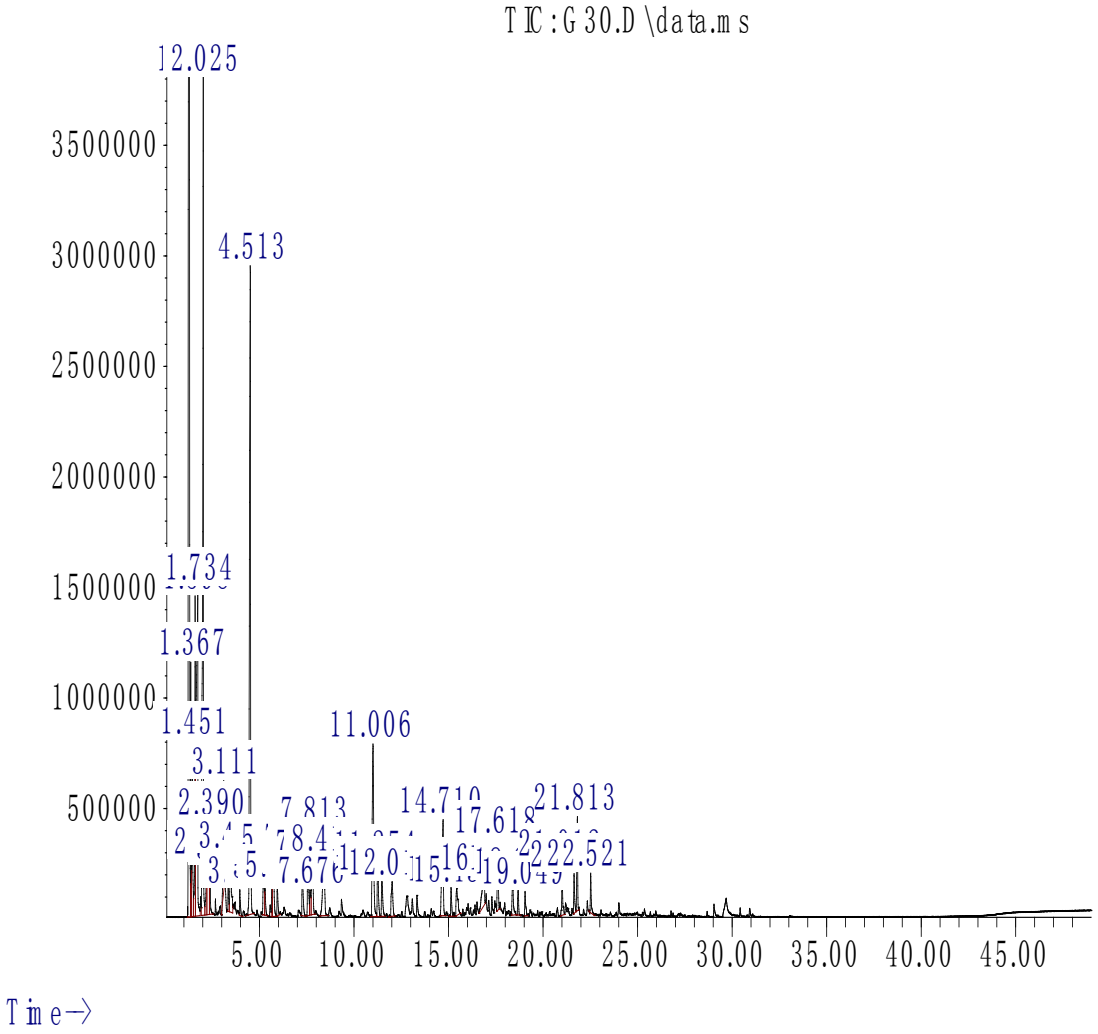

Figure 48: GC-MS graph for paper.

Appendix B

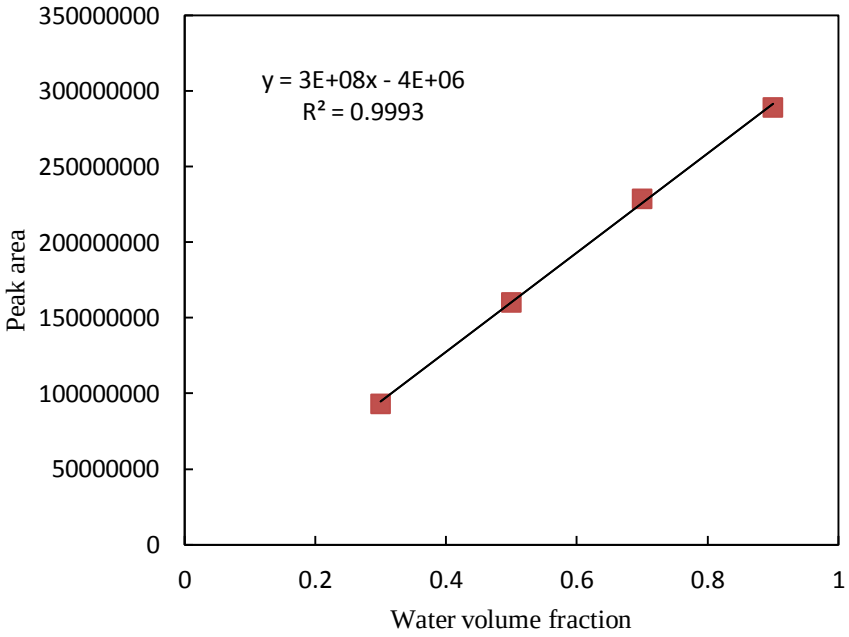

Figure 49: Calibration curve of water in acetic acid.

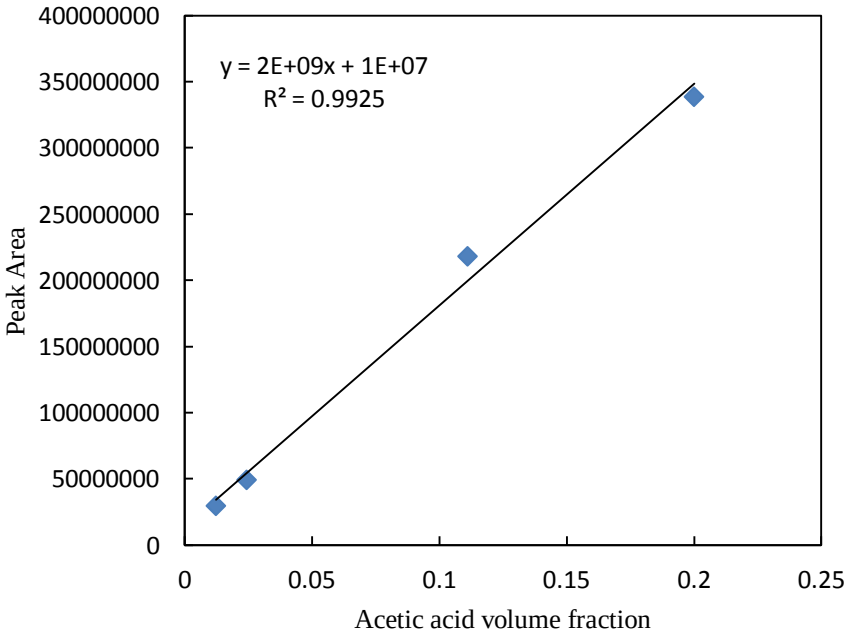

Figure 50: Calibration curve of acetic acid in methanol.

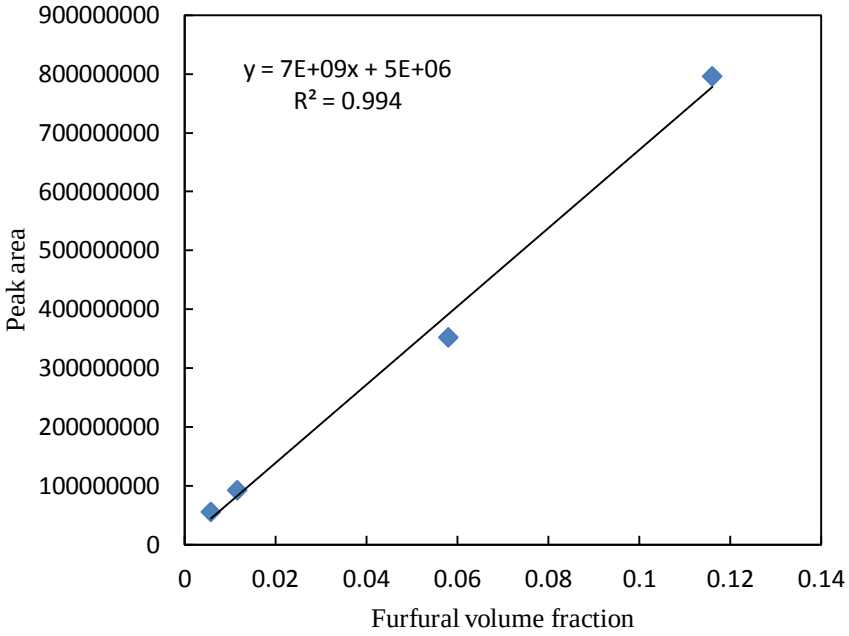

Figure 51: Calibration curve of furfural in methanol.

Appendix C

Table 32. TGA data for sample 1 to sample 3.

Sample 1		Sample 2		Sample 3	
Temperature (℃)	Residue percentage (%)	Temperature (℃)	Residue percentage (%)	Temperature (℃)	Residue percentage (%)
34.995	99.94568	27.937	99.97948	30.823	99.97288
34.882	99.87839	28.966	99.90117	31.561	99.87318
34.777	99.82259	31.224	99.81183	32.901	99.75298
34.675	99.76238	34.306	99.7157	34.88	99.59951
34.581	99.69766	37.802	99.63079	37.474	99.42378
34.486	99.64545	41.275	99.46686	40.439	99.21868
35.599	99.56429	44.447	99.2802	43.5	98.99405
39.209	99.48791	47.229	99.09267	46.446	98.72982
44.364	99.38029	49.668	98.89593	49.184	98.43386
49.748	99.30515	51.888	98.71068	51.71	98.11111
54.425	99.14807	54.023	98.51728	54.068	97.76027
58.027	98.98207	56.176	98.34115	56.341	97.40647
60.65	98.83346	58.404	98.16282	58.597	97.05182
62.623	98.6882	60.735	98.01665	60.888	96.69239
64.307	98.54615	63.143	97.86729	63.228	96.34963
66.003	98.43236	65.602	97.73085	65.626	96.01867
67.887	98.29923	68.076	97.60748	68.058	95.69197
70.037	98.17866	70.539	97.51532	70.504	95.38339
72.411	98.07247	72.981	97.42588	72.947	95.09972
74.941	97.97089	75.391	97.32821	75.375	94.8378
77.52	97.86423	77.786	97.25399	77.788	94.59443
80.087	97.77529	80.172	97.19157	80.189	94.38499
82.606	97.6744	82.561	97.14794	82.588	94.19142
85.059	97.59047	84.949	97.09877	84.979	94.02808
87.455	97.51026	87.337	97.05879	87.37	93.87899
89.824	97.43238	89.736	97.02506	89.764	93.74709
92.183	97.35918	92.141	97.00008	92.161	93.63465
94.545	97.28768	94.552	96.97366	94.56	93.5592
96.931	97.22327	96.956	96.95094	96.969	93.48609
99.322	97.1592	99.365	96.93638	99.37	93.41209
101.729	97.09617	101.771	96.9209	101.777	93.34234
104.138	97.0308	104.174	96.9034	104.17	93.29093
106.55	96.96628	106.574	96.89321	106.566	93.23984
108.958	96.90699	108.973	96.87854	108.964	93.19816
111.358	96.85024	111.371	96.87445	111.358	93.161
113.758	96.78996	113.77	96.86949	113.762	93.12518
116.156	96.74698	116.165	96.86826	116.154	93.09413
118.557	96.69799	118.56	96.86736	118.557	93.06182

(Continued)

120.95	96.64979	120.96	96.85999	120.956	93.03009
123.347	96.60606	123.361	96.85491	123.356	92.99853
125.745	96.56078	125.763	96.8536	125.768	92.97367
128.14799	96.50956	128.16901	96.85092	128.16901	92.96007
130.55	96.46121	130.57001	96.85233	130.567	92.9361
132.952	96.42959	132.97301	96.85545	132.961	92.915
135.354	96.39441	135.37601	96.86789	135.353	92.89676
137.759	96.35753	137.77299	96.86673	137.754	92.87451
140.162	96.32086	140.174	96.86925	140.161	92.85785
142.565	96.28247	142.57401	96.87362	142.567	92.84024
144.966	96.25087	144.97701	96.87832	144.974	92.82408
147.366	96.21722	147.383	96.88485	147.377	92.80825
149.767	96.18585	149.78799	96.89347	149.783	92.79241
152.17101	96.15694	152.188	96.90061	152.181	92.77815
154.571	96.13025	154.58701	96.91299	154.57899	92.76256
156.972	96.112	156.985	96.92046	156.978	92.75369
159.373	96.08145	159.383	96.92094	159.377	92.73827
161.772	96.05926	161.782	96.93194	161.77901	92.72834
164.16901	96.03938	164.17999	96.94127	164.17599	92.71438
166.569	96.01532	166.58099	96.95407	166.577	92.70046
168.972	95.98711	168.98199	96.9669	168.979	92.68793
171.371	95.96101	171.38699	96.97283	171.37801	92.67542
173.77299	95.93705	173.785	96.97731	173.784	92.66421
176.17101	95.91516	176.19099	96.98319	176.179	92.65171
178.573	95.89732	178.58501	96.98406	178.57899	92.63782
180.97501	95.87313	180.98599	96.99514	180.979	92.6265
183.37801	95.85105	183.38499	97.00608	183.382	92.61248
185.77299	95.82462	185.78799	97.01864	185.785	92.59708
188.17799	95.79374	188.19	97.02936	188.186	92.57634
190.57899	95.76709	190.593	97.03479	190.58501	92.55686
192.978	95.73173	192.992	97.03328	192.985	92.54113
195.37601	95.70665	195.394	97.02965	195.38499	92.52527
197.77699	95.67297	197.791	97.02422	197.789	92.50002
200.17999	95.63688	200.192	97.02024	200.19099	92.48121
202.586	95.60906	202.593	97.01966	202.59	92.45709
204.983	95.57086	204.98599	97.007	204.99001	92.43034
207.386	95.52435	207.39101	96.99429	207.38901	92.40486
209.78101	95.47994	209.789	96.98336	209.787	92.37289
212.18201	95.44379	212.192	96.95869	212.19	92.34082
214.58299	95.40356	214.59399	96.94089	214.58701	92.30493
216.98	95.34254	216.994	96.91104	216.98801	92.2676
219.381	95.28561	219.39301	96.88638	219.39	92.22642
221.782	95.21829	221.795	96.84275	221.78999	92.17605

(Continued)

224.17599	95.15943	224.19299	96.80778	224.19099	92.13095
226.57401	95.09006	226.595	96.7659	226.588	92.08057
228.976	95.01027	228.993	96.71718	228.98599	92.01178
231.37801	94.91598	231.395	96.65288	231.384	91.94169
233.78	94.82375	233.79401	96.57833	233.78101	91.86107
236.179	94.70655	236.194	96.48819	236.17999	91.77388
238.57899	94.58937	238.591	96.39814	238.57899	91.6525
240.97701	94.43471	240.991	96.29082	240.98	91.55744
243.377	94.26546	243.386	96.13182	243.38	91.43212
245.78	94.08789	245.789	96.0107	245.78	91.28709
248.17799	93.90412	248.188	95.86033	248.17999	91.14076
250.577	93.71202	250.592	95.68238	250.578	90.97863
252.976	93.47825	252.992	95.49928	252.979	90.80995
255.379	93.23618	255.392	95.28859	255.38	90.60969
257.77802	92.98164	257.79099	95.06586	257.784	90.40155
260.17599	92.69584	260.19199	94.81039	260.18201	90.16843
262.577	92.40381	262.591	94.54112	262.582	89.92479
264.97601	92.06807	264.98801	94.24774	264.98099	89.65221
267.37299	91.72192	267.39099	93.92506	267.379	89.35201
269.77499	91.35286	269.78699	93.58344	269.78	89.04261
272.17599	90.94425	272.18799	93.22286	272.17599	88.69374
274.57599	90.50649	274.58701	92.81402	274.577	88.31068
276.97601	90.03751	276.98499	92.37934	276.97601	87.9079
279.37201	89.54353	279.38	91.91018	279.375	87.46434
281.77301	89.01832	281.77899	91.42725	281.77301	86.98789
284.17099	88.44731	284.18301	90.88055	284.17099	86.48514
286.57101	87.85339	286.57999	90.32352	286.57101	85.93373
288.97198	87.21993	288.97601	89.71823	288.974	85.34285
291.371	86.53023	291.38101	89.06642	291.37701	84.71252
293.76501	85.80721	293.77802	88.38013	293.77399	84.04535
296.16501	85.0363	296.17499	87.6542	296.16699	83.3203
298.564	84.23625	298.57599	86.86969	298.564	82.565
300.96301	83.38622	300.97198	86.05413	300.95901	81.57813
303.36301	82.47156	303.371	85.17993	303.358	80.75177
305.76001	81.51727	305.772	84.25052	305.75601	79.88063
308.15799	80.51917	308.173	83.2814	308.15399	78.77525
310.55399	79.46684	310.56799	82.26398	310.55499	77.81722
312.95001	78.36449	312.96799	81.07239	312.95099	76.63416
315.34299	77.21419	315.36801	79.97042	315.35001	75.49713
317.74301	75.98677	317.772	78.60636	317.75101	74.28377
320.14801	74.73854	320.16699	77.4526	320.14899	73.00722
322.547	73.32981	322.56601	76.05747	322.54599	71.70566
324.94699	72.00026	324.97101	74.72268	324.94601	70.35674

(Continued)

327.35199	70.62491	327.36499	73.42749	327.34601	68.94333
329.759	69.03073	329.76401	71.92198	329.74301	67.49569
332.15799	67.64698	332.16199	70.46475	332.14301	66.01123
334.55801	66.00488	334.56	68.99026	334.547	64.47282
336.952	64.57528	336.95999	67.43821	336.94199	62.91596
339.34698	62.95613	339.358	65.85511	339.341	61.31177
341.745	61.14742	341.763	64.2324	341.74301	59.63391
344.13699	59.47412	344.15799	62.54931	344.142	57.9284
346.534	57.75503	346.55099	60.82658	346.53799	56.16239
348.93201	55.95472	348.94501	59.04875	348.93799	54.34248
351.33099	54.10026	351.35101	57.15375	351.336	52.42649
353.729	52.20632	353.75	55.21905	353.728	50.44475
356.129	50.20403	356.15201	53.18099	356.12701	48.37621
358.526	48.13928	358.55099	51.0274	358.53	46.17482
360.92801	45.99339	360.95099	48.79628	360.92899	43.90897
363.32501	43.76623	363.35699	46.4894	363.327	41.54974
365.72699	41.52046	365.755	44.06356	365.73099	39.07346
368.12601	39.24138	368.16199	41.64987	368.13101	36.57484
370.53101	36.9291	370.56299	39.24136	370.53201	34.0723
372.93301	34.6814	372.95999	36.8467	372.94101	31.58172
375.33701	32.56925	375.36099	34.5608	375.35001	29.21748
377.74301	30.62388	377.767	32.48704	377.758	27.03091
380.15399	29.02647	380.172	30.66849	380.16501	25.08254
382.55499	27.62495	382.58099	29.13973	382.578	23.45927
384.961	26.54029	384.98599	28.14373	384.987	22.15443
387.36301	25.63894	387.38501	27.22021	387.383	21.27858
389.75201	25.02725	389.77899	26.55024	389.78	20.55939
392.147	24.59702	392.17099	26.09413	392.17401	20.02975
394.54001	24.31063	394.55399	25.78121	394.55801	19.64487
396.92899	24.08889	396.95001	25.53917	396.944	19.37064
399.31799	23.91527	399.33899	25.36274	399.33301	19.1452
401.71399	23.77305	401.73401	25.21395	401.72699	18.95142
404.10901	23.61834	404.129	25.05835	404.12201	18.77739
406.51099	23.44292	406.52499	24.92519	406.51801	18.60606
408.909	23.32374	408.922	24.78689	408.914	18.44129
411.30301	23.18581	411.32101	24.64351	411.31299	18.27529
413.703	23.03968	413.72	24.51048	413.70901	18.11585
416.104	22.88946	416.12	24.38096	416.11301	17.9631
418.504	22.76009	418.521	24.25668	418.508	17.80635
420.89999	22.64322	420.91501	24.1375	420.90799	17.64708
423.29999	22.48062	423.311	24.02365	423.311	17.50359
425.69699	22.36392	425.70901	23.87533	425.70499	17.34956
428.09698	22.23478	428.11301	23.76164	428.10101	17.20881

(Continued)

430.491	22.10982	430.509	23.63059	430.5	17.06019
432.884	21.99326	432.90201	23.51344	432.89999	16.91421
435.28699	21.84145	435.298	23.40845	435.30801	16.77366
437.689	21.73756	437.69699	23.26555	437.70001	16.63551
440.086	21.62115	440.09601	23.16408	440.08801	16.50147
442.48401	21.51323	442.49399	23.06267	442.48499	16.38203
444.89301	21.39918	444.89001	22.96651	444.88599	16.24945
447.28201	21.29529	447.29001	22.86347	447.28299	16.1234
449.66901	21.1938	449.69101	22.76572	449.681	16.00931
452.08301	21.09897	452.08899	22.67653	452.08401	15.89659
454.508	20.99963	454.48401	22.59087	454.48199	15.79306
456.871	20.92895	456.883	22.50877	456.88501	15.68302
459.25299	20.84664	459.27701	22.43353	459.28	15.58351
461.65701	20.76229	461.677	22.36018	461.677	15.49722
464.05801	20.68613	464.07501	22.29029	464.07199	15.39125
466.45499	20.60587	466.47601	22.2239	466.47198	15.31559
468.858	20.53822	468.87299	22.16444	468.86899	15.23867
471.27899	20.47522	471.271	22.11715	471.271	15.16178
473.68399	20.41572	473.668	22.06642	473.66501	15.0862
476.05301	20.35002	476.06201	22.02777	476.065	15.01733
478.44901	20.2912	478.46301	21.98072	478.46899	14.94717
480.849	20.24476	480.85999	21.94568	480.867	14.89805
483.25	20.18588	483.26599	21.90741	483.26099	14.83582
485.64899	20.14995	485.664	21.8707	485.65799	14.77498
488.04199	20.10571	488.05499	21.83921	488.05701	14.72341
490.44101	20.06795	490.45001	21.80278	490.453	14.65872
492.841	20.03225	492.85501	21.78026	492.85101	14.61381
495.24301	19.99041	495.25299	21.75069	495.25	14.5729
497.64099	19.94445	497.642	21.72634	497.64899	14.52547
500.035	19.90891	500.035	21.7074	500.047	14.47809
502.431	19.88188	502.42899	21.68155	502.453	14.4347
504.82901	19.84656	504.82901	21.66437	504.83801	14.4004
507.22601	19.81332	507.23401	21.64214	507.229	14.36235
509.62701	19.7844	509.63501	21.62333	509.63101	14.32433
512.02502	19.7471	512.03497	21.6063	512.03003	14.28505
514.44202	19.72275	514.44098	21.5825	514.42999	14.25237
516.85999	19.6919	516.86102	21.57091	516.84198	14.21718
519.27802	19.65494	519.24799	21.55369	519.23401	14.18963
521.67499	19.62813	521.63202	21.5385	521.62097	14.15832
524.17603	19.60344	524.06702	21.52249	524.01599	14.12186
526.79602	19.58499	526.65997	21.51805	526.414	14.08935
529.18903	19.56433	529.16699	21.50766	528.81097	14.06213
531.45697	19.54072	531.51501	21.49997	531.20697	14.03756

(Continued)

533.78699	19.51875	533.85498	21.49174	533.60797	14.01047
536.12	19.49218	536.20001	21.4836	536.00598	13.98993
538.453	19.47828	538.53998	21.48241	538.40601	13.96552
540.82703	19.46707	540.90601	21.47294	540.80701	13.94509
543.21503	19.45357	543.27802	21.46687	543.20398	13.91807
545.61401	19.43398	545.64899	21.46076	545.60602	13.89383
548.01099	19.41429	548.03101	21.45661	548.00702	13.8709
550.40601	19.40087	550.42603	21.46119	550.40503	13.84925
552.784	19.38322	552.836	21.4538	552.81097	13.83184
555.18103	19.3722	555.24298	21.45148	555.53101	13.81114
557.56799	19.35265	557.64099	21.44915	558.33398	13.78659
559.97699	19.34201	560.04999	21.45054	560.54999	13.76632
562.39502	19.33334	562.46198	21.45713	562.71802	13.74308
564.81201	19.32048	564.85498	21.46688	565.06299	13.72372
567.23798	19.30158	567.24701	21.47006	567.37	13.70719
569.65198	19.2971	569.64203	21.47155	569.68597	13.69902
572.05103	19.28839	572.03601	21.46442	572.06299	13.67415
574.44397	19.27362	574.43701	21.46786	574.448	13.65433
576.854	19.26545	576.84399	21.47818	576.82703	13.63841
579.271	19.25311	579.22998	21.47972	579.211	13.6318
581.66901	19.25091	581.63501	21.48518	581.59698	13.61478
584.06201	19.24268	584.03998	21.49049	584.07501	13.60254
586.474	19.24107	586.47198	21.498	586.47302	13.59019
588.88501	19.24558	588.90198	21.50515	588.80499	13.5716
591.27301	19.24575	591.28601	21.51378	591.24799	13.55676
593.66302	19.23996	593.69501	21.5161	593.62201	13.54729
596.06702	19.23234	596.086	21.52324	595.974	13.5356
598.47198	19.23301	598.474	21.52896	598.383	13.52717
600.85901	19.22723	600.875	21.53996	600.82202	13.52001
603.245	19.23629	603.27802	21.55797	603.25403	13.51006
605.64502	19.24147	605.703	21.56753	605.67499	13.49748
608.03302	19.23811	608.09003	21.57315	608.07599	13.49405
610.422	19.24123	610.45801	21.58417	610.46503	13.48407
612.82098	19.24452	612.85699	21.59561	612.87299	13.47706
615.22803	19.2563	615.237	21.61365	615.276	13.46724
617.638	19.26593	617.62903	21.63204	617.65601	13.46132
620.03302	19.28178	620.04901	21.64382	620.05298	13.45436
622.42999	19.29366	622.46997	21.65545	622.45502	13.45275
624.82599	19.29302	624.862	21.68399	624.91901	13.45162
627.21802	19.30708	627.18903	21.70675	627.32001	13.44428
629.62299	19.3297	629.20801	21.73678	629.69598	13.44264
632.01202	19.34163	631.37	21.75205	632.12701	13.4388
634.396	19.35589	633.66998	21.76965	634.508	13.43167

(Continued)

636.82098	19.37905	636.15698	21.80237	636.94	13.43466
639.23102	19.38917	638.716	21.83105	639.33801	13.42766
641.61902	19.41187	641.271	21.84896	641.66199	13.42967
644.04401	19.4352	643.78699	21.87849	644.07898	13.42898
646.44098	19.45365	646.19702	21.9019	646.52698	13.43441
648.82397	19.47243	648.59998	21.92448	648.83801	13.43483
651.22498	19.49765	651.04797	21.94925	651.21002	13.43396
653.59802	19.52253	653.479	21.98223	653.64301	13.44625
655.995	19.54385	655.89502	22.0118	656.01898	13.45262
658.40997	19.57571	658.32098	22.04157	658.42102	13.46232
660.82202	19.60522	660.77301	22.06831	660.84698	13.46532
663.21802	19.62856	663.24701	22.10532	663.25	13.48136
665.646	19.66069	665.84601	22.13916	665.67798	13.49108
668.03601	19.69208	668.29602	22.15818	668.07898	13.50053
670.40802	19.7362	670.30902	22.19971	670.54401	13.51606
672.81403	19.76424	672.711	22.24238	672.711	13.52733
675.22198	19.79001	675.13599	22.28426	674.00098	13.54774
677.63	19.82412	677.48901	22.3224	676.30298	13.57045
680.02197	19.8685	679.922	22.35473	679.01599	13.58915
682.41699	19.90469	682.45398	22.40166	681.75598	13.60955
684.797	19.94288	684.97601	22.38924	684.72198	13.62744
687.19897	19.98154	687.39301	22.40976	686.64398	13.6483
689.61902	20.01808	689.67603	22.49038	689.08197	13.66105
691.98798	20.06233	692.08301	22.56799	691.66699	13.68622
694.37701	20.10721	694.547	22.61721	694.08197	13.71017
696.79199	20.14403	696.58801	22.65533	696.60199	13.72885
699.19299	20.18246	698.85498	22.70723	699.04498	13.74767
701.59601	20.22535	701.31	22.75755	701.43799	13.77196
703.98297	20.25756	703.73297	22.80862	703.91998	13.79582
706.38202	20.30256	706.16498	22.85634	706.47198	13.82248
708.79199	20.34147	708.59698	22.8955	708.92902	13.84798
711.19897	20.38448	711.03699	22.93642	711.32397	13.87232
713.625	20.4401	713.46301	22.98757	713.84802	13.89917
715.98297	20.48027	715.89398	23.04058	716.06598	13.92625
718.34998	20.51911	718.32001	23.09181	718.03302	13.95651
720.77502	20.56263	720.73102	23.13948	720.474	13.98582
723.15997	20.60747	723.13098	23.18719	722.92902	14.01842
725.53998	20.65673	725.54199	23.23507	725.32202	14.043
727.95398	20.70647	727.94501	23.29148	727.927	14.07593
730.354	20.75173	730.349	23.34451	730.40802	14.10023
732.79602	20.80384	732.74402	23.39233	732.78101	14.13507
735.19	20.84898	735.138	23.4385	735.216	14.1628
737.63501	20.89309	737.53198	23.48645	737.61401	14.18997

(Continued)

740.05103	20.94247	739.935	23.5345	739.95599	14.22621
742.474	20.98423	742.33899	23.58775	742.35797	14.25912
744.84802	21.03135	744.73901	23.64106	744.71698	14.28892
746.67499	21.07452	747.14099	23.69607	747.18103	14.32116
		749.539	23.74427		

Table 33. TGA data for sample 4 to sample 6.

Sample 4		Sample 5		Sample 6	
Temperature (℃)	Residue percentage (%)	Temperature (℃)	Residue percentage (%)	Temperature (℃)	Residue percentage (%)
26.207	99.99895	26.157	99.99722	27.169	99.99746
28.707	100.00306	27.341	99.98359	29.569	99.99509
31.207	100.00188	30.18	99.97348	31.969	99.99953
33.707	99.99647	33.929	99.95224	34.369	99.98747
36.207	99.99246	37.943	99.93355	36.769	99.98528
38.707	99.98502	41.688	99.90231	39.169	99.98433
41.207	99.97282	44.894	99.8249	41.569	99.97904
43.707	99.95184	47.567	99.75513	43.969	99.9742
46.207	99.92783	49.834	99.65901	46.369	99.96172
48.707	99.89625	51.888	99.55045	48.769	99.94328
51.207	99.85861	53.903	99.42124	51.169	99.91933
53.707	99.819	55.994	99.28029	53.569	99.8879
56.207	99.78387	58.222	99.12368	55.969	99.85428
58.707	99.74712	60.59	98.94979	58.369	99.82504
61.207	99.71017	63.049	98.77673	60.769	99.76901
63.707	99.67767	65.556	98.60057	63.169	99.71906
66.207	99.64229	68.101	98.40197	65.569	99.65853
68.707	99.60599	70.608	98.23582	67.969	99.58518
71.207	99.56548	73.06	98.07627	70.369	99.49958
73.707	99.51902	75.484	97.94385	72.769	99.399
76.207	99.47436	77.9	97.84591	75.169	99.28219
78.707	99.42207	80.285	97.77403	77.569	99.15621
81.207	99.37709	82.648	97.73443	79.969	99.01851
83.707	99.32344	85.002	97.70255	82.369	98.87983
86.207	99.27387	87.359	97.67881	84.769	98.76621
88.707	99.22194	89.729	97.66125	87.169	98.69751
91.207	99.16763	92.119	97.63088	89.569	98.65514
93.707	99.10992	94.52	97.61338	91.969	98.63134
96.207	99.04849	96.929	97.59602	94.369	98.61383
98.707	98.98474	99.344	97.58366	96.769	98.60267
101.207	98.91462	101.758	97.57444	99.169	98.59652

(Continued)

103.707	98.84025	104.162	97.56518	101.569	98.58977
106.207	98.76286	106.563	97.55184	103.969	98.58599
108.707	98.67603	108.962	97.54156	106.369	98.58161
111.207	98.58328	111.365	97.53559	108.769	98.58117
113.707	98.48735	113.759	97.5307	111.169	98.57915
116.207	98.38603	116.159	97.52167	113.569	98.58126
118.707	98.279	118.558	97.5163	115.969	98.58067
121.207	98.15995	120.961	97.51122	118.369	98.58004
123.707	98.03988	123.36	97.50201	120.769	98.58126
126.207	97.91482	125.763	97.50148	123.169	98.58043
128.707	97.78273	128.164	97.49834	125.569	98.58231
131.207	97.64942	130.562	97.49603	127.969	98.58207
133.707	97.5096	132.959	97.49245	130.369	98.58368
136.207	97.37265	135.36099	97.49034	132.769	98.58574
138.707	97.23026	137.763	97.48836	135.169	98.59014
141.207	97.09006	140.16701	97.4894	137.569	98.58857
143.707	96.94845	142.573	97.48697	139.969	98.58994
146.207	96.81134	144.976	97.48537	142.369	98.59109
148.707	96.68086	147.379	97.48453	144.769	98.59269
151.207	96.55159	149.78	97.48314	147.169	98.59393
153.707	96.43061	152.181	97.48037	149.569	98.59434
156.207	96.31706	154.57899	97.47414	151.969	98.59697
158.707	96.20828	156.978	97.47215	154.369	98.5971
161.207	96.10744	159.382	97.46677	156.769	98.5998
163.707	96.01258	161.774	97.46704	159.169	98.60085
166.207	95.92598	164.17101	97.46021	161.569	98.60137
168.707	95.84401	166.56799	97.4556	163.969	98.60197
171.207	95.77033	168.967	97.44743	166.369	98.6113
173.707	95.69692	171.366	97.44064	168.769	98.6024
176.207	95.6284	173.769	97.43529	171.169	98.60391
178.707	95.5649	176.16499	97.42715	173.569	98.60804
181.207	95.50516	178.56799	97.4161	175.969	98.60908
183.707	95.44231	180.964	97.40864	178.369	98.60839
186.207	95.38196	183.373	97.39813	180.769	98.6103
188.707	95.3195	185.795	97.39122	183.169	98.61091
191.207	95.25035	188.207	97.3872	185.569	98.61025
193.707	95.17426	190.60699	97.38245	187.969	98.60901
196.207	95.08441	192.995	97.37971	190.369	98.60864
198.707	94.99323	195.38	97.37472	192.769	98.60959
201.207	94.91831	197.758	97.37035	195.169	98.60789
203.707	94.85574	200.13499	97.36446	197.569	98.60686
206.207	94.78475	202.51199	97.35994	199.969	98.60538
208.707	94.71506	204.911	97.36374	202.369	98.60437

(Continued)

211.207	94.63415	207.38499	97.35255	204.769	98.603
213.707	94.53789	209.85201	97.35176	207.169	98.59942
216.207	94.43134	212.261	97.34473	209.569	98.59908
218.707	94.30081	214.64101	97.34038	211.969	98.59167
221.207	94.13634	217.013	97.33519	214.369	98.5902
223.707	93.85943	219.38901	97.32783	216.769	98.58752
226.207	93.55416	221.77299	97.32614	219.169	98.58181
228.707	93.15572	224.172	97.32305	221.569	98.57531
231.207	92.73884	226.571	97.31079	223.969	98.56936
233.707	92.384	228.968	97.2964	226.369	98.56118
236.207	92.11937	231.367	97.28557	228.769	98.55227
238.707	91.89984	233.77	97.27758	231.169	98.54051
241.207	91.72747	236.177	97.26888	233.569	98.52607
243.707	91.56212	238.576	97.25028	235.969	98.50997
246.207	91.40544	240.979	97.22671	238.369	98.49819
248.707	91.24178	243.37399	97.20173	240.769	98.4786
251.207	91.10139	245.772	97.18383	243.169	98.45985
253.707	90.97029	248.17	97.16097	245.569	98.43853
256.207	90.85125	250.567	97.13884	247.969	98.4142
258.707	90.7371	252.968	97.10111	250.369	98.38735
261.207	90.62831	255.366	97.06479	252.769	98.35052
263.707	90.51779	257.76401	97.03558	255.169	98.32329
266.207	90.41149	260.14801	96.99859	257.569	98.28705
268.707	90.31201	262.47699	96.95807	259.969	98.24587
271.207	90.21644	264.82901	96.8933	262.369	98.2038
273.707	90.10988	267.314	96.85978	264.769	98.16127
276.207	90.00498	269.83301	96.79027	267.169	98.11186
278.707	89.90896	272.29199	96.74206	269.569	98.05937
281.207	89.81267	274.69101	96.64841	271.969	97.9962
283.707	89.7249	277.05499	96.56676	274.369	97.93239
286.207	89.62746	279.41	96.49005	276.769	97.86578
288.707	89.53912	281.77701	96.40342	279.169	97.79214
291.207	89.44943	284.15701	96.30121	281.569	97.71664
293.707	89.36517	286.547	96.19547	283.969	97.62945
296.207	89.27879	288.94601	96.08903	286.369	97.53137
298.707	89.19658	291.345	95.96133	288.769	97.43667
301.207	89.12004	293.75201	95.84287	291.169	97.33087
303.707	89.04203	296.155	95.70739	293.569	97.22174
306.207	88.96758	298.556	95.56978	295.969	97.10163
308.707	88.90068	300.95401	95.38466	298.369	96.97616
311.207	88.83331	303.35501	95.20946	300.769	96.83371
313.707	88.76268	305.755	95.0158	303.169	96.67774
316.207	88.70349	308.147	94.80651	305.569	96.51775

(Continued)

318.707	88.64388	310.54999	94.58375	307.969	96.35154
321.207	88.58928	312.95499	94.35601	310.369	96.1622
323.707	88.5353	315.34799	94.10979	312.769	95.96308
326.207	88.48624	317.74701	93.83735	315.169	95.75232
328.707	88.44866	320.14301	93.57197	317.569	95.49571
331.207	88.40898	322.54501	93.29029	319.969	95.27886
333.707	88.35587	324.94299	93.01072	322.369	95.00849
336.207	88.31887	327.349	92.7255	324.769	94.77209
338.707	88.28314	329.745	92.4303	327.169	94.50251
341.207	88.24169	332.146	92.13159	329.569	94.22699
343.707	88.20777	334.54199	91.83001	331.969	93.91756
346.207	88.17538	336.94	91.5242	334.369	93.63974
348.707	88.13718	339.34399	91.20848	336.769	93.36447
351.207	88.09878	341.741	90.88281	339.169	93.07573
353.707	88.06602	344.13501	90.53161	341.569	92.73855
356.207	88.0326	346.53201	90.17831	343.969	92.42559
358.707	87.99574	348.93301	89.80515	346.369	92.08661
361.207	87.96119	351.32999	89.41356	348.769	91.70961
363.707	87.92686	353.728	89.00994	351.169	91.32486
366.207	87.894	356.13	88.60492	353.569	90.91595
368.707	87.8562	358.52899	88.21905	355.969	90.50899
371.207	87.82118	360.93399	87.76158	358.369	90.10057
373.707	87.78581	363.336	87.47719	360.769	89.72212
376.207	87.75055	365.741	87.16302	363.169	89.36956
378.707	87.71241	368.14301	86.8907	365.569	89.01793
381.207	87.68264	370.54501	86.7021	367.969	88.71513
383.707	87.64059	372.935	86.50499	370.369	88.40496
386.207	87.60214	375.33499	86.37392	372.769	88.17074
388.707	87.56479	377.73401	86.26553	375.169	87.96376
391.207	87.52962	380.12201	86.17136	377.569	87.79521
393.707	87.48882	382.51599	86.10134	379.969	87.66839
396.207	87.45067	384.91599	86.04839	382.369	87.5801
398.707	87.4141	387.311	86.00965	384.769	87.5132
401.207	87.37369	389.70499	85.97732	387.169	87.46525
403.707	87.33486	392.09799	85.90674	389.569	87.42195
406.207	87.29766	394.49301	85.86882	391.969	87.39027
408.707	87.25228	396.896	85.8416	394.369	87.35441
411.207	87.21584	399.293	85.80945	396.769	87.3145
413.707	87.17467	401.689	85.77378	399.169	87.28914
416.207	87.13512	404.09	85.74454	401.569	87.27038
418.707	87.09811	406.48901	85.71174	403.969	87.22503
421.207	87.0564	408.88199	85.68464	406.369	87.20135
423.707	87.02043	411.27399	85.63556	408.769	87.16763

(Continued)

426.207	86.97748	413.673	85.62411	411.169	87.13978
428.707	86.94281	416.069	85.59847	413.569	87.11381
431.207	86.90058	418.465	85.54732	415.969	87.09533
433.707	86.86582	420.867	85.53171	418.369	87.04794
436.207	86.83382	423.26401	85.49974	420.769	87.03369
438.707	86.79465	425.66199	85.48131	423.169	87.00364
441.207	86.75474	428.069	85.46714	425.569	86.97289
443.707	86.70489	430.45901	85.4196	427.969	86.95303
446.207	86.66711	432.85699	85.40762	430.369	86.93643
448.707	86.62427	435.25699	85.37506	432.769	86.897
451.207	86.5802	437.651	85.34037	435.169	86.87694
453.707	86.54007	440.048	85.30573	437.569	86.85375
456.207	86.4969	442.44601	85.28033	439.969	86.81646
458.707	86.44905	444.84799	85.26348	442.369	86.80312
461.207	86.40345	447.24799	85.25795	444.769	86.78727
463.707	86.35853	449.64001	85.20496	447.169	86.75371
466.207	86.30947	452.04001	85.18744	449.569	86.73937
468.707	86.26048	454.44699	85.20117	451.969	86.71853
471.207	86.22	456.827	85.11839	454.369	86.69293
473.707	86.15605	459.23401	85.10812	456.769	86.6784
476.207	86.10659	461.633	85.06158	459.169	86.65993
478.707	86.03987	464.03	85.04346	461.569	86.62849
481.207	85.99008	466.431	85.02255	463.969	86.61386
483.707	85.92692	468.82401	84.9853	466.369	86.59899
486.207	85.86281	471.229	84.95951	468.769	86.57975
488.707	85.7976	473.62701	84.92444	471.169	86.57051
491.207	85.72805	476.02301	84.90358	473.569	86.55082
493.707	85.65753	478.42099	84.87501	475.969	86.52503
496.207	85.58593	480.82199	84.85635	478.369	86.51368
498.707	85.51419	483.22101	84.83203	480.769	86.50363
501.207	85.42455	485.617	84.8042	483.169	86.48485
503.707	85.3429	488.017	84.78418	485.569	86.47087
506.207	85.25549	490.41299	84.74718	487.969	86.45433
508.707	85.16182	492.81	84.7173	490.369	86.43981
511.207	85.06692	495.20901	84.69313	492.769	86.42854
513.707	84.97339	497.61099	84.68106	495.169	86.41493
516.207	84.8634	500.01001	84.64981	497.569	86.40311
518.707	84.75416	502.40701	84.6314	499.969	86.38834
521.207	84.6419	504.80499	84.608	502.369	86.37535
523.707	84.51865	507.20099	84.58251	504.769	86.36398
526.207	84.39289	509.60101	84.55422	507.169	86.35059
528.707	84.26384	511.99399	84.51952	509.569	86.33735
531.207	84.13148	514.39398	84.48773	511.969	86.32105

(Continued)

533.707	83.98923	516.83099	84.46683	514.369	86.31178
536.207	83.83939	519.28101	84.45138	516.769	86.29501
538.707	83.68651	521.64301	84.42285	519.169	86.28345
541.207	83.52397	524.01202	84.39468	521.569	86.2668
543.707	83.35516	526.40399	84.36868	523.969	86.25812
546.207	83.18486	528.78699	84.31425	526.369	86.24498
548.707	83.00043	531.17999	84.29608	528.769	86.23732
551.207	82.80855	533.57599	84.26939	531.169	86.22052
553.707	82.61084	535.97198	84.23777	533.569	86.21343
556.207	82.40155	538.36298	84.20684	535.969	86.188
558.707	82.1868	540.763	84.16461	538.369	86.17649
561.207	81.96245	543.14502	84.1082	540.769	86.16157
563.707	81.71218	545.54797	84.07317	543.169	86.14877
566.207	81.47135	547.94598	84.03312	545.569	86.13599
568.707	81.18787	550.34198	83.9768	547.969	86.12459
571.207	80.93802	552.74597	83.95174	550.369	86.11057
573.707	80.66246	555.13898	83.86071	552.769	86.10066
576.207	80.35952	557.55603	83.80595	555.169	86.07328
578.707	80.07579	559.92499	83.72613	557.569	86.06243
581.207	79.75351	562.31097	83.64374	559.969	86.05622
583.707	79.44144	564.72601	83.55007	562.369	86.04616
586.207	79.12742	567.12097	83.45695	564.769	86.04097
588.707	78.78365	569.513	83.34693	567.169	86.01066
591.207	78.44438	571.95001	83.23865	569.569	86.00178
593.707	78.07945	574.33502	83.11063	571.969	85.99099
596.207	77.71279	576.71399	82.9964	574.369	85.97491
598.707	77.32081	579.10999	82.86595	576.769	85.96352
601.207	76.92599	581.51099	82.7355	579.169	85.94924
603.707	76.52652	583.90698	82.60148	581.569	85.93422
606.207	76.10178	586.32098	82.46834	583.969	85.92479
608.707	75.67925	588.724	82.33505	586.369	85.90077
611.207	75.25353	591.13202	82.17922	588.769	85.88851
613.707	74.79262	593.60303	82.03144	591.169	85.87778
616.207	74.34859	595.99298	81.86683	593.569	85.86266
618.707	73.87639	598.383	81.738	595.969	85.845
621.207	73.40392	600.771	81.55451	598.369	85.83377
623.707	72.91163	603.16602	81.386	600.769	85.82396
626.207	72.42159	605.55902	81.22032	603.169	85.79672
628.707	71.91235	607.95099	81.06958	605.569	85.78514
631.207	71.40498	610.35101	80.88203	607.969	85.77063
633.707	70.88411	612.74701	80.7235	610.369	85.75745
636.207	70.361	615.12799	80.52598	612.769	85.74253
638.707	69.82882	617.53802	80.34925	615.169	85.72371

(Continued)

641.207	69.28608	619.97998	80.15543	617.569	85.71107
643.707	68.75422	622.29901	79.97518	619.969	85.69744
646.207	68.18881	624.72498	79.80038	622.369	85.68303
648.707	67.65447	627.14899	79.60799	624.769	85.66604
651.207	67.08936	629.46698	79.40607	627.169	85.65019
653.707	66.52454	631.90399	79.22546	629.569	85.63521
656.207	65.97985	634.29303	78.98545	631.969	85.62114
658.707	65.43301	636.67297	78.80094	634.369	85.61414
661.207	64.87007	639.05499	78.58454	636.769	85.59039
663.707	64.30106	641.45001	78.39234	639.169	85.57831
666.207	63.75399	643.849	78.15477	641.569	85.56608
668.707	63.20632	646.26501	77.95911	643.969	85.55506
671.207	62.65219	648.66901	77.72293	646.369	85.52796
673.707	62.11163	651.05603	77.49884	648.769	85.51976
676.207	61.5717	653.46997	77.28484	651.169	85.5077
678.707	61.036	655.86298	77.05365	653.569	85.48553
681.207	60.51605	658.26001	76.82327	655.969	85.46528
683.707	60.00347	660.65698	76.59077	658.369	85.45013
686.207	59.5062	663.03497	76.35037	660.769	85.43428
688.707	58.9846	665.47302	76.13308	663.169	85.42475
691.207	58.48024	667.883	75.86442	665.569	85.40039
693.707	58.00656	670.28699	75.61498	667.969	85.38571
696.207	57.50677	672.69501	75.36984	670.369	85.36896
698.707	57.02858	675.10602	75.12685	672.769	85.35183
701.207	56.55312	677.52002	74.86901	675.169	85.32933
703.707	56.09324	681.12903	74.64147	677.569	85.30038
706.207	55.63924	682.505	74.35883	679.969	85.26915
708.707	55.18632	685.21698	74.11339	682.369	85.25261
711.207	54.76376	687.34003	73.86115	684.769	85.24694
713.707	54.31565	689.54602	73.62764	687.169	85.20258
716.207	53.88046	691.995	73.29648	689.569	85.19757
718.707	53.46174	694.27802	73.08495	691.969	85.18179
721.207	53.20737	696.70801	72.79854	694.369	85.14788
723.707	52.6782	699.104	72.50158	696.769	85.12535
726.207	52.30061	701.45398	72.25857	699.169	85.1007
728.707	51.90676	703.87	71.98466	701.569	85.06517
731.207	51.48513	706.25897	71.6495	703.969	85.03707
733.707	51.12804	708.66602	71.42447	706.369	85.0104
736.207	50.73046	711.07001	71.16175	708.769	84.98348
738.707	50.37339	713.44	70.86986	711.169	84.94166
741.207	50.01958	715.85101	70.56763	713.569	84.90975
743.707	49.65908	718.29303	70.27177	715.969	84.86789
746.207	49.30704	720.664	70.02021	718.369	84.85208

(Continued)

748.707	48.96032	723.03101	69.7285	720.769	84.80252
		725.479	69.44626	723.169	84.76676
		727.86401	69.15017	725.569	84.73074
		730.26202	68.86635	727.969	84.70282
		732.68201	68.57052	730.369	84.65834
		735.10199	68.27468	732.769	84.61021
		737.49298	67.98298	735.169	84.56702
		739.86499	67.68275	737.569	84.52458
		742.26703	67.387	739.969	84.47796
		744.65198	67.08471	742.369	84.42266
		747.03101	66.78887	744.769	84.37437
				747.169	84.33945

Table 34. TGA data for sample 7 to sample 9.

Sample 7		Sample 8		Sample 9	
Temperature (℃)	Residue percentage (%)	Temperature (℃)	Residue percentage (%)	Temperature (℃)	Residue percentage (%)
26.54	99.996	26.272	99.99843	27.252	99.99868
29.04	100.00074	28.772	100.00722	29.752	100.0027
31.54	99.99718	31.272	100.0118	32.252	100.0028
34.04	99.99309	33.772	100.00432	34.752	100.0048
36.54	99.99163	36.272	100.00238	37.252	100.00471
39.04	99.98624	38.772	99.99967	39.752	100.00224
41.54	99.97315	41.272	99.99037	42.252	99.9965
44.04	99.94494	43.772	99.97301	44.752	99.98515
46.54	99.9181	46.272	99.95446	47.252	99.97018
49.04	99.88144	48.772	99.93818	49.752	99.9543
51.54	99.84248	51.272	99.90633	52.252	99.93555
54.04	99.79287	53.772	99.87725	54.752	99.91349
56.54	99.75247	56.272	99.83866	57.252	99.89305
59.04	99.69669	58.772	99.78563	59.752	99.86881
61.54	99.64206	61.272	99.72749	62.252	99.84288
64.04	99.57626	63.772	99.66818	64.752	99.81252
66.54	99.51065	66.272	99.59806	67.252	99.78032
69.04	99.43602	68.772	99.53817	69.752	99.74641
71.54	99.36426	71.272	99.47534	72.252	99.71197
74.04	99.28876	73.772	99.41227	74.752	99.67622
76.54	99.2135	76.272	99.34987	77.252	99.64047
79.04	99.13909	78.772	99.28686	79.752	99.60292
81.54	99.0524	81.272	99.22785	82.252	99.56568
84.04	98.96914	83.772	99.1705	84.752	99.5271
86.54	98.90175	86.272	99.11061	87.252	99.48942

(Continued)

89.04	98.84209	88.772	99.05355	89.752	99.45027
91.54	98.78729	91.272	98.99435	92.252	99.40705
94.04	98.72241	93.772	98.93649	94.752	99.36175
96.54	98.65718	96.272	98.86963	97.252	99.31513
99.04	98.58856	98.772	98.79809	99.752	99.26541
101.54	98.51996	101.272	98.72466	102.252	99.21297
104.04	98.4499	103.772	98.64455	104.752	99.16012
106.54	98.38764	106.272	98.55819	107.252	99.10211
109.04	98.29862	108.772	98.46831	109.752	99.04357
111.54	98.21725	111.272	98.37434	112.252	98.98116
114.04	98.12417	113.772	98.2749	114.752	98.91715
116.54	98.03675	116.272	98.16726	117.252	98.85038
119.04	97.9402	118.772	98.05634	119.752	98.78082
121.54	97.8416	121.272	97.93893	122.252	98.70618
124.04	97.7376	123.772	97.81886	124.752	98.62863
126.54	97.62581	126.272	97.69328	127.252	98.54772
129.04	97.51409	128.772	97.56318	129.752	98.46138
131.54	97.39007	131.272	97.43182	132.252	98.37232
134.04	97.28067	133.772	97.29984	134.752	98.28017
136.54	97.17016	136.272	97.16456	137.252	98.18335
139.04	97.05788	138.772	97.02822	139.752	98.08392
141.54	96.94811	141.272	96.89534	142.252	97.98272
144.04	96.85213	143.772	96.75837	144.752	97.87679
146.54	96.73758	146.272	96.62675	147.252	97.76897
149.04	96.64336	148.772	96.50005	149.752	97.65835
151.54	96.55687	151.272	96.38215	152.252	97.54518
154.04	96.47536	153.772	96.2556	154.752	97.4336
156.54	96.39785	156.272	96.14478	157.252	97.31717
159.04	96.33325	158.772	96.04293	159.752	97.20404
161.54	96.27389	161.272	95.95089	162.252	97.09042
164.04	96.22221	163.772	95.868	164.752	96.97685
166.54	96.17197	166.272	95.79237	167.252	96.86285
169.04	96.12559	168.772	95.71967	169.752	96.75532
171.54	96.07561	171.272	95.65777	172.252	96.64593
174.04	96.01962	173.772	95.59348	174.752	96.54189
176.54	95.95582	176.272	95.53236	177.252	96.44183
179.04	95.88095	178.772	95.4691	179.752	96.34558
181.54	95.80073	181.272	95.39637	182.252	96.25421
184.04	95.73933	183.772	95.32738	184.752	96.16686
186.54	95.68575	186.272	95.24943	187.252	96.08118
189.04	95.63746	188.772	95.16568	189.752	96.00018
191.54	95.5943	191.272	95.08071	192.252	95.92401
194.04	95.5466	193.772	94.98677	194.752	95.84937

(Continued)

196.54	95.50231	196.272	94.89635	197.252	95.7767
199.04	95.46034	198.772	94.81006	199.752	95.70534
201.54	95.41229	201.272	94.72714	202.252	95.63652
204.04	95.36806	203.772	94.65438	204.752	95.57472
206.54	95.3182	206.272	94.58315	207.252	95.52349
209.04	95.28281	208.772	94.49825	209.752	95.47666
211.54	95.24559	211.272	94.41417	212.252	95.43412
214.04	95.21337	213.772	94.30921	214.752	95.38979
216.54	95.18314	216.272	94.19924	217.252	95.34038
219.04	95.15243	218.772	94.07827	219.752	95.2818
221.54	95.13038	221.272	93.93543	222.252	95.2136
224.04	95.10442	223.772	93.75496	224.752	95.12884
226.54	95.07917	226.272	93.5339	227.252	95.01917
229.04	95.05605	228.772	93.30073	229.752	94.87094
231.54	95.03477	231.272	93.07346	232.252	94.73927
234.04	95.01391	233.772	92.85653	234.752	94.61367
236.54	94.99158	236.272	92.66437	237.252	94.50124
239.04	94.9739	238.772	92.49582	239.752	94.38863
241.54	94.95107	241.272	92.35457	242.252	94.27011
244.04	94.9326	243.772	92.23207	244.752	94.16327
246.54	94.91488	246.272	92.12372	247.252	94.06129
249.04	94.8972	248.772	92.03077	249.752	93.96555
251.54	94.87858	251.272	91.9373	252.252	93.88133
254.04	94.86096	253.772	91.84564	254.752	93.8
256.54	94.84252	256.272	91.76926	257.252	93.7204
259.04	94.82574	258.772	91.69473	259.752	93.64625
261.54	94.81352	261.272	91.62616	262.252	93.57686
264.04	94.80018	263.772	91.56243	264.752	93.51223
266.54	94.78288	266.272	91.49289	267.252	93.44946
269.04	94.77148	268.772	91.43129	269.752	93.384
271.54	94.75577	271.272	91.37498	272.252	93.32023
274.04	94.74475	273.772	91.31869	274.752	93.25614
276.54	94.73385	276.272	91.26541	277.252	93.19128
279.04	94.72211	278.772	91.20848	279.752	93.12509
281.54	94.71152	281.272	91.15805	282.252	93.05819
284.04	94.70412	283.772	91.11516	284.752	92.98564
286.54	94.69394	286.272	91.05722	287.252	92.91098
289.04	94.6833	288.772	91.01273	289.752	92.83135
291.54	94.67511	291.272	90.96909	292.252	92.74433
294.04	94.66808	293.772	90.93087	294.752	92.6569
296.54	94.66068	296.272	90.88912	297.252	92.55596
299.04	94.6549	298.772	90.83986	299.752	92.44709
301.54	94.64713	301.272	90.80722	302.252	92.33291

(Continued)

304.04	94.63929	303.772	90.77479	304.752	92.17797
306.54	94.62945	306.272	90.73471	307.252	92.01275
309.04	94.62169	308.772	90.70265	309.752	91.82378
311.54	94.61305	311.272	90.67446	312.252	91.59559
314.04	94.60694	313.772	90.6429	314.752	91.3292
316.54	94.59893	316.272	90.62082	317.252	91.02267
319.04	94.59541	318.772	90.58362	319.752	90.68558
321.54	94.58812	321.272	90.56214	322.252	90.32478
324.04	94.58055	323.772	90.54113	324.752	89.96437
326.54	94.57034	326.272	90.5156	327.252	89.62066
329.04	94.56271	328.772	90.48321	329.752	89.29939
331.54	94.55328	331.272	90.46807	332.252	88.99744
334.04	94.54696	333.772	90.44803	334.752	88.71767
336.54	94.53783	336.272	90.42782	337.252	88.4519
339.04	94.53226	338.772	90.40277	339.752	88.2
341.54	94.52483	341.272	90.38692	342.252	87.96144
344.04	94.5187	343.772	90.36648	344.752	87.73399
346.54	94.51037	346.272	90.34168	347.252	87.52406
349.04	94.50279	348.772	90.32506	349.752	87.33895
351.54	94.49658	351.272	90.30664	352.252	87.20404
354.04	94.48952	353.772	90.28789	354.752	87.084
356.54	94.48208	356.272	90.26584	357.252	86.99133
359.04	94.47296	358.772	90.24803	359.752	86.91106
361.54	94.46739	361.272	90.22924	362.252	86.83769
364.04	94.45911	363.772	90.20781	364.752	86.76945
366.54	94.44954	366.272	90.19344	367.252	86.7046
369.04	94.44111	368.772	90.16424	369.752	86.64587
371.54	94.43265	371.272	90.14013	372.252	86.58519
374.04	94.42336	373.772	90.11551	374.752	86.52793
376.54	94.41645	376.272	90.09534	377.252	86.47312
379.04	94.408	378.772	90.07784	379.752	86.41834
381.54	94.39702	381.272	90.04977	382.252	86.36506
384.04	94.38704	383.772	90.03055	384.752	86.3125
386.54	94.37764	386.272	90.01314	387.252	86.26041
389.04	94.36829	388.772	89.9819	389.752	86.21007
391.54	94.35869	391.272	89.95692	392.252	86.16014
394.04	94.3476	393.772	89.93501	394.752	86.11064
396.54	94.33649	396.272	89.91851	397.252	86.06479
399.04	94.32745	398.772	89.88412	399.752	86.01755
401.54	94.31602	401.272	89.86043	402.252	85.9717
404.04	94.3046	403.772	89.83346	404.752	85.92634
406.54	94.28947	406.272	89.81073	407.252	85.88126
409.04	94.27851	408.772	89.78082	409.752	85.83812

(Continued)

411.54	94.26695	411.272	89.7592	412.252	85.79604
414.04	94.25468	413.772	89.73654	414.752	85.75165
416.54	94.23688	416.272	89.70443	417.252	85.71024
419.04	94.22507	418.772	89.67836	419.752	85.66764
421.54	94.21367	421.272	89.66459	422.252	85.6257
424.04	94.1942	423.772	89.62689	424.752	85.58417
426.54	94.17886	426.272	89.59445	427.252	85.54232
429.04	94.16426	428.772	89.57529	429.752	85.50059
431.54	94.14636	431.272	89.55251	432.252	85.45813
434.04	94.12858	433.772	89.52005	434.752	85.41557
436.54	94.10917	436.272	89.49629	437.252	85.3717
439.04	94.0944	438.772	89.46582	439.752	85.32934
441.54	94.07076	441.272	89.43111	442.252	85.28453
444.04	94.0512	443.772	89.41037	444.752	85.24084
446.54	94.02904	446.272	89.3783	447.252	85.19592
449.04	94.0031	448.772	89.34531	449.752	85.14937
451.54	93.97268	451.272	89.32216	452.252	85.10498
454.04	93.94488	453.772	89.27883	454.752	85.05696
456.54	93.91786	456.272	89.24487	457.252	85.00965
459.04	93.88752	458.772	89.21961	459.752	84.96281
461.54	93.85751	461.272	89.176	462.252	84.91293
464.04	93.81568	463.772	89.1402	464.752	84.86061
466.54	93.78405	466.272	89.10367	467.252	84.8103
469.04	93.74442	468.772	89.06252	469.752	84.75564
471.54	93.70137	471.272	89.02374	472.252	84.70386
474.04	93.65671	473.772	88.98067	474.752	84.64953
476.54	93.60572	476.272	88.9349	477.252	84.59296
479.04	93.55982	478.772	88.90234	479.752	84.53501
481.54	93.50916	481.272	88.84306	482.252	84.47557
484.04	93.44907	483.772	88.79289	484.752	84.4146
486.54	93.38261	486.272	88.74136	487.252	84.35117
489.04	93.31535	488.772	88.68666	489.752	84.28537
491.54	93.24583	491.272	88.62609	492.252	84.21842
494.04	93.16678	493.772	88.56853	494.752	84.14921
496.54	93.08427	496.272	88.50387	497.252	84.07716
499.04	92.99126	498.772	88.43718	499.752	84.00252
501.54	92.88588	501.272	88.37053	502.252	83.92501
504.04	92.77087	503.772	88.29493	504.752	83.84314
506.54	92.63831	506.272	88.22002	507.252	83.75842
509.04	92.4955	508.772	88.1368	509.752	83.67115
511.54	92.34312	511.272	88.05155	512.252	83.57997
514.04	92.17707	513.772	87.96589	514.752	83.48644
516.54	91.96704	516.272	87.87243	517.252	83.37976

(Continued)

519.04	91.7433	518.772	87.7614	519.752	83.27413
521.54	91.50395	521.272	87.66239	522.252	83.1632
524.04	91.1815	523.772	87.55245	524.752	83.04666
526.54	90.913	526.272	87.43689	527.252	82.91149
529.04	90.59563	528.772	87.31687	529.752	82.78264
531.54	90.28366	531.272	87.18519	532.252	82.65097
534.04	89.89292	533.772	87.05854	534.752	82.51543
536.54	89.51814	536.272	86.92201	537.252	82.36163
539.04	89.12086	538.772	86.77362	539.752	82.18877
541.54	88.69918	541.272	86.62413	542.252	82.0332
544.04	88.25756	543.772	86.45929	544.752	81.85226
546.54	87.78908	546.272	86.30339	547.252	81.67199
549.04	87.29462	548.772	86.13279	549.752	81.48187
551.54	86.78483	551.272	85.95818	552.252	81.28939
554.04	86.23529	553.772	85.76831	554.752	81.07935
556.54	85.66408	556.272	85.57413	557.252	80.85983
559.04	85.07362	558.772	85.37604	559.752	80.63512
561.54	84.44787	561.272	85.17868	562.252	80.39887
564.04	83.80272	563.772	84.9429	564.752	80.14946
566.54	83.14073	566.272	84.7018	567.252	79.89695
569.04	82.43227	568.772	84.46069	569.752	79.6331
571.54	81.71341	571.272	84.20273	572.252	79.36611
574.04	80.96973	573.772	83.97071	574.752	79.09299
576.54	80.19259	576.272	83.72447	577.252	78.80409
579.04	79.40015	578.772	83.47499	579.752	78.50443
581.54	78.57018	581.272	83.17878	582.252	78.20672
584.04	77.71826	583.772	82.87682	584.752	77.899
586.54	76.85714	586.272	82.58588	587.252	77.58924
589.04	75.96668	588.772	82.31732	589.752	77.27569
591.54	75.06687	591.272	81.98637	592.252	76.9486
594.04	74.15432	593.772	81.67287	594.752	76.62324
596.54	73.2118	596.272	81.34419	597.252	76.28971
599.04	72.29767	598.772	81.0121	599.752	75.95821
601.54	71.38911	601.272	80.68475	602.252	75.61259
604.04	70.50783	603.772	80.33302	604.752	75.26685
606.54	69.63769	606.272	79.98383	607.252	74.91549
609.04	68.82023	608.772	79.62408	609.752	74.5604
611.54	68.04012	611.272	79.24845	612.252	74.20149
614.04	67.32594	613.772	78.87971	614.752	73.83904
616.54	66.66484	616.272	78.50092	617.252	73.4691
619.04	66.06138	618.772	78.11443	619.752	73.09409
621.54	65.51792	621.272	77.70977	622.252	72.7146
624.04	65.01368	623.772	77.32502	624.752	72.32177

(Continued)

626.54	64.53328	626.272	76.91798	627.252	71.93728
629.04	64.08618	628.772	76.5086	629.752	71.54097
631.54	63.66139	631.272	76.10021	632.252	71.14269
634.04	63.24061	633.772	75.66084	634.752	70.73482
636.54	62.86984	636.272	75.25567	637.252	70.32839
639.04	62.49458	638.772	74.81668	639.752	69.91009
641.54	62.11016	641.272	74.37953	642.252	69.4896
644.04	61.76733	643.772	73.94366	644.752	69.07236
646.54	61.42391	646.272	73.50535	647.252	68.65167
649.04	61.10967	648.772	73.05442	649.752	68.23142
651.54	60.77255	651.272	72.61061	652.252	67.80744
654.04	60.48866	653.772	72.1611	654.752	67.37795
656.54	60.18658	656.272	71.7155	657.252	66.95186
659.04	59.87979	658.772	71.26283	659.752	66.53219
661.54	59.57198	661.272	70.80552	662.252	66.10316
664.04	59.2924	663.772	70.35794	664.752	65.68612
666.54	58.99038	666.272	69.89156	667.252	65.2689
669.04	58.71947	668.772	69.44382	669.752	64.85315
671.54	58.46354	671.272	68.97553	672.252	64.44557
674.04	58.16372	673.772	68.51818	674.752	64.03439
676.54	57.89018	676.272	68.05487	677.252	63.63151
679.04	57.63147	678.772	67.60089	679.752	63.23559
681.54	57.37093	681.272	67.15526	682.252	62.83521
684.04	57.11362	683.772	66.68034	684.752	62.44451
686.54	56.81111	686.272	66.22548	687.252	62.05521
689.04	56.55805	688.772	65.77047	689.752	61.66477
691.54	56.30797	691.272	65.30587	692.252	61.28818
694.04	56.04712	693.772	64.86195	694.752	60.91303
696.54	55.79032	696.272	64.4044	697.252	60.53833
699.04	55.53366	698.772	63.9562	699.752	60.16698
701.54	55.28517	701.272	63.49737	702.252	59.79921
704.04	55.02907	703.772	63.05728	704.752	59.43737
706.54	54.77964	706.272	62.61283	707.252	59.07925
709.04	54.53287	708.772	62.17681	709.752	58.73097
711.54	54.22969	711.272	61.73416	712.252	58.38122
714.04	54.03788	713.772	61.29948	714.752	58.03638
716.54	53.75079	716.272	60.87576	717.252	57.69781
719.04	53.55885	718.772	60.4569	719.752	57.3555
721.54	53.2801	721.272	60.03839	722.252	57.02324
724.04	53.08098	723.772	59.61464	724.752	56.69341
726.54	52.82065	726.272	59.21	727.252	56.36543
729.04	52.60378	728.772	58.81836	729.752	56.04782
731.54	52.35516	731.272	58.39667	732.252	55.72781

(Continued)

734.04	52.11504	733.772	58.01355	734.752	55.41077
736.54	51.87991	736.272	57.6234	737.252	55.0988
739.04	51.63421	738.772	57.22406	739.752	54.78689
741.54	51.40062	741.272	56.84203	742.252	54.48143
744.04	51.15434	743.772	56.46885	744.752	54.17809
746.54	50.89131	746.272	56.08442	747.252	53.87479
749.04	50.66834	748.772	55.71902		

Appendix D

Table 35. Pyrolysis of sawdust raw data.

#	flow rate (CC/min)	particle size (μm)	molten salt	molar ratio of salt	temperture (℃)	catalyst/mass (g)	bio-oil yield (%)
1	120	106-212	Zn-K-Li	40-20-40	350	-	32.4
2	135	106-212	Zn-K-Li	40-20-40	350	-	36.8
3	146	106-212	Zn-K-Li	40-20-40	350	-	40.0
4	165	106-212	Zn-K-Li	40-20-40	350	-	40.8
5	190	106-212	Zn-K-Li	40-20-40	350	-	18.0
6	165	106-212	-	-	300	-	12.9
7	165	106-212	-	-	350	-	19.1
8	165	106-212	-	-	400	-	33.2
9	165	106-212	-	-	450	-	39.6
10	165	<106	-	-	350	-	18.6
11	165	300-450	-	-	350	-	14.0
12	165	680-850	-	-	350	-	13.8
13	165	<106	Zn-K-Li	40-20-40 [a]	300	-	41.2
14	165	<106	Zn-K-Li	40-20-40 [a]	350	-	49.1
15	165	<106	Zn-K-Li	40-20-40 [a]	400	-	52.5
16	165	<106	Zn-K-Li	40-20-40 [a]	450	-	57.7
17	165	106-212	Zn-K-Li	40-20-40 [a]	300	-	37.4
18	165	106-212	Zn-K-Li	40-20-40 [a]	350	-	46.9
19	165	106-212	Zn-K-Li	40-20-40 [a]	400	-	51.5
20	165	106-212	Zn-K-Li	40-20-40 [a]	450	-	54.9
21	165	<106	Cu-K	65-35	300	-	25.4
22	165	<106	Cu-K	65-35	350	-	41.0
23	165	<106	Cu-K	65-35	400	-	48.0
24	165	<106	Cu-K	65-35	450	-	62.8
25	165	106-212	Cu-K	65-35	300	-	22.2
26	165	106-212	Cu-K	65-35	350	-	32.6
27	165	106-212	Cu-K	65-35	400	-	36.8
28	165	106-212	Cu-K	65-35	450	-	52.2
29	165	106-212	Zn-K-Li	40-20-10 [a]	400	-	54.9
30	165	106-212	Zn-K-Li	40-20-20 [a]	400	-	57.5
31	165	106-212	Zn-K-Li	40-20-30 [a]	400	-	56.6
32	165	106-212	Zn-K-Li	40-2-40 [a]	400	-	20.7
33	165	106-212	Zn-K-Li	40-5-40 [a]	400	-	56.1
34	165	106-212	Zn-K-Li	40-10-40 [a]	400	-	51.5
35	165	106-212	Zn-K-Li	40-30-40 [a]	400	-	50.1
36	165	106-212	Zn-K-Li	30-20-40 [a]	400	-	53.4
37	165	106-212	Zn-K-Li	50-20-40 [a]	400	-	66.5

(Continued)

38	165	106-212	Zn-K-Li	60-20-40 [a]	400	-	58.2
39	165	106-212	Zn-K-Li	70-20-40 [a]	400	-	58.3
40	165	106-212	Cu-K	65-35	350	PA [b]/0.5	41.0
41	165	106-212	Cu-K	65-35	350	PA/1	41.0
42	165	106-212	Cu-K	65-35	350	PA/2	41.0
43	165	106-212	Cu-K	65-35	300	PA/2	34.2
44	165	106-212	Cu-K	65-35	350	PA/2	41.0
45	165	106-212	Cu-K	65-35	400	PA/2	48.0
46	165	106-212	Cu-K	65-35	450	PA/2	58.6
47	165	106-212	Zn-K-Li	40-20-40 [a]	300	PA/1	50.6
48	165	106-212	Zn-K-Li	40-20-40 [a]	350	PA/1	55.7
49	165	106-212	Zn-K-Li	40-20-40 [a]	400	PA/1	60.4
50	165	106-212	Zn-K-Li	40-20-40 [a]	450	PA/1	63.7
51	165	106-212	Zn-Na-K	52.9-13.4-33.7	300	-	36.9
52	165	106-212	Zn-Na-K	52.9-13.4-33.7	350	-	33.8
53	165	106-212	Zn-Na-K	52.9-13.4-33.7	400	-	47.8
54	165	106-212	Zn-Na-K	52.9-13.4-33.7	450	-	51.7
55	165	106-212	Zn-Na-K	52.9-13.4-33.7	400	PA/1	51.6
56	165	106-212	Zn-Na-K	60-20-20	400	-	46.7
57	165	106-212	Zn-Na-K	60-20-20	400	PA/1	54.6
58	165	106-212	K-Li-Na	36-55-9	400	-	36.2
59	165	106-212	K-Li-Na	36-55-9	400	PA/1	43.0
60	165	106-212	K-Li-Na	24-43-33	400	-	39.5
61	165	106-212	K-Li-Na	24-43-33	400	PA/1	46.0
62	165	106-212	K-Li-Na	24-43-33	400	$ZnCl_2$/1	48.3
63	165	106-212	K-Li-Na	24-43-33	400	PA/0.5+$ZnCl_2$/0.5	48.0
64	165	106-212	K-Li-Na	24-43-33	400	$ZnCl_2$/0.5+$SnCl_2$/0.5	37.4
65	165	106-212	K-Li-Na	24-43-33	400	PA/0.5+$SnCl_2$/0.5	42.1
66	165	106-212	K-Li-Na	24-43-33	400	$Ni(OH)_2$/1	47.8
67	165	106-212	K-Li-Na	24-43-33	400	ZSM-5/1	43.5

5 g sawdust was used and the mass ratio of feed to salt was set to 1: 10 in all the experiments listed in Table 35.

a. Molar ratio is based on the molecular weight of the metal cation.

b. PA is the abbreviation of phosphomolybdic acid.